THE ROLE OF RELMα IN OSM-MEDIATED LUNG INFLAMMATION

THE ROLE OF RESISTIN-LIKE MOLECULE ALPHA IN ONCOSTATIN M-MEDIATED LUNG INFLAMMATION

By LILIAN HO, B.Sc. Honours (University of Waterloo)

A Thesis Submitted to the School of Graduate Studies in Partial Fulfillment of the Requirements for the Degree Master of Science

McMaster University MASTER OF SCIENCE (2019) Hamilton, Ontario

(Medical Sciences: Infection and Immunity)

TITLE: The Role of Resistin-like Molecule Alpha in Oncostatin M-mediated Lung Inflammation

AUTHOR: Lilian Ho, B.Sc. Hons. (University of Waterloo)

SUPERVISOR: Dr. Carl D. Richards, B.Sc., M.Sc., Ph.D.

NUMBER OF PAGES: xiv, 119

ABSTRACT

Resistin-like molecule alpha (RELMα) is a secreted protein implicated in murine models of allergen-induced asthma, bleomycin-induced pulmonary fibrosis, and helminth infection. Transient pulmonary overexpression of Oncostatin M by Adenovirus vector (AdOSM) induces lung inflammation biased toward Th2 cytokines, eosinophil and alternatively activated (AA/M2) macrophage accumulation. In AdOSM-treated C57Bl/6 and BALB/c mice, we observed RELMα mRNA and protein markedly induced. RELMα is recognized as a marker of AA/M2 macrophages, and we observed by chromogenic *in situ* hybridization that RELMα mRNA co-expresses with the macrophage marker CD68, and RELMα mRNA was also highly induced in columnar airway epithelial cells upon AdOSM treatment. Assessing IL-6 as a comparator gp130 cytokine, AdIL-6 induced RELMα at significantly lower levels, however maximal induction of RELMα by AdOSM in C57Bl/6 mice required IL-6, assessed in IL-$6^{-/-}$ mice. Maximal induction of RELMα by AdOSM also required IL-33 in C57Bl/6 mice but not in BALB/c mice, assessed in IL-$33^{-/-}$ mice.

We investigated functions of RELMα in response to OSM, in RELM$\alpha^{-/-}$ mice. Inflammatory cell infiltration and Th2-associated cytokine responses were not altered in RELM$\alpha^{-/-}$ in comparison to wildtype mice. However, RELMα-deficiency resulted in less accumulation of $CD206^{+}$ AA/M2 macrophages, $IFN\gamma^{+}$ Th1 cells in the lung, reduced induction of extracellular matrix gene mRNAs for COL1A1, COL3A1, MMP13, TIMP1, and reduced parenchymal alpha smooth muscle actin. RELM$\alpha^{-/-}$ mice also showed less

airway epithelial hyperplasia, increased epithelial cell damage/death (assessed morphologically) and increased LDH and soluble CK18 in response to AdOSM. Our findings suggest that RELMα does not modulate Th2 cytokines, but does participate in matrix deposition, airway remodelling mechanisms, and protection from inflammation-induced damage due to OSM-overexpression in lungs of C57Bl/6 mice.

ACKNOWLEDGEMENTS

With the completion of this thesis, I would like to thank those who supported and encouraged me throughout the past two years. First, I would like to express my deepest gratitude to my supervisor, Dr. Carl Richards. His patient guidance, enthusiastic encouragement, unwavering support, and passion for his research fueled my curiosity and provided me a challenging yet rewarding experience. I would also like to thank my committee members, Dr. Kjetil Ask and Dr. Zhou Xing, for their guidance and feedback throughout my project.

To all the former and current lab members of the Richards Lab, thank you for making this experience enjoyable. To Fern Botelho, thank you for all your advice and guidance and for helping with the flow cytometry experiments. To Ashley Yip, thank you for all the laughs and support, and for coming into the lab even when the school closed due to freezing rain. To Olivia Mekhael, Jane Ann Smith, Kyle MacDonald, Jewel Imani and members of McMaster Immunology Research Centre, thank you for creating a friendly learning environment to work in every day.

To my family, for their unconditional love and constant encouragement in times of uncertainty. I would not be the person I am today without all of you. Lastly, I would like to thank Michael for listening to me during both good and stressful times and reminding me to stay positive, especially on days when I doubt myself.

TABLE OF CONTENTS

LIST OF FIGURES

LIST OF ABBREVIATIONS

AA/M2	Alternatively activated/M2 macrophages
AdDel70	Adenovirus control vector, backbone only
AdIL-6	Adenovirus encoding mouse IL-6
AdOSM	Adenovirus encoding mouse OSM
AEC	Alveolar epithelial cell
Arg1	Arginase-1
αSMA	Alpha smooth muscle actin
BAL	Bronchoalveolar lavage
BSA	Bovine serum albumin
BMDM	Bone marrow-derived macrophages
CA/M1	Classically activated/M1 macrophages
CD	Cluster of differentiation
CISH	Chromogenic *in situ* hybridization
CK	Cytokeratin
COL	Collagen
COPD	Chronic obstructive pulmonary disease
DMEM	Dulbecco's Modified Eagle's Medium
DTT	Diothioretiol
ECM	Extracellular matrix
ELISA	Enzyme-linked immunosorbent assay

FBS	Fetal bovine serum
FIZZ	Found in inflammatory zone
Gp130	Glycoprotein 130
H&E	Hematoxylin & eosin
IFN	Interferon
IHC	Immunohistochemistry
IL	Interleukin
IPF	Idiopathic pulmonary fibrosis
JAK	Janus kinase
LDH	Lactate dehydrogenase
LIF	Leukemia inhibitory factor
LIFR	Leukemia inhibitory factor receptor
LPS	Lipopolysaccharide
M-CSF	Macrophage-colony stimulating factor
MAPK	Mitogen-activated protein kinase
MCP	Monocyte chemotactic factor
MMP	Matrix metalloproteinase
OSM	Oncostatin M
OSMRβ	Oncostatin M receptor beta
OVA	Ovalbumin
PAS	Periodic acid-Schiff
PBS	Phosphate buffered saline

PFU	Plaque-forming unit
PI3K	Phosphatidylinositide 3-kinase
PMA	para-Methoxyamphetamine
PMSF	Phenylmethylsulfonyl fluoride
PSR	Picrosirus red
RELM	Resistin-like molecule
RIPA	Radioimmunoprecipitation assay
RPMI	Roswell Park Memorial Institute
RT-PCR	Reverse transcription polymerase chain reaction
SDS-PAGE	Sodium dodecyl sulfate polyacrylamide gel electrophoresis
STAT	Signal transducer and activator of transcription
TBS	Tris buffered saline
Th	T helper cell
TIMP	Tissue inhibitors of metalloproteinase
TGFβ	Transforming growth factor beta

CHAPTER 1: INTRODUCTION

1.1 Chronic Respiratory Diseases

Chronic respiratory diseases such as idiopathic pulmonary fibrosis (IPF), chronic obstructive pulmonary disease (COPD), and severe asthma are conditions with reduction in lung function that involves extracellular matrix (ECM) remodelling [1]. In COPD, damaged alveolar walls and loss of shape and structure in larger airways reduces gas exchange efficiency [2], whereas IPF and severe asthma are characterized by excessive ECM deposition in the airways or around alveoli, therefore decreasing gas exchange with the capillary network and consequently impairing pulmonary function [1,3,4]. These conditions are often progressive in nature and current therapies have much room for improvement [3,5]. Animal models of lung fibrosis clearly implicate activated T cells and alternatively activated macrophages in induction of ECM [6,7]. Although cytokines such as transforming growth factor beta (TGFβ) [8] and interleukin-4 (IL-4) [9] are critical factors in fibrogenesis in many systems, studies have also shown pathways independent of TGFβ/SMAD3 and IL-4/STAT6 that can lead to fibrosis in animal models *in vivo* [10]. Overactivation of STAT3 in mouse models increases fibrotic responses in lungs, and gp130 cytokines (see below) such as Oncostatin M and IL-6 activate STAT3 in various cell types. Thus, understanding the various mechanisms of how ECM remodeling occurs and through which cells and signaling molecules will provide a better understanding to inform new potential therapeutic approaches separate from the TGFβ pathway.

1.2 GP130 Cytokines and Chronic Lung Inflammation

Gp130 cytokines, also referred to as the IL-6 family of cytokines, are secreted proteins produced by immune and nonimmune cells that have pleiotropic functions involving differentiation, hematopoiesis, cell proliferation, and inflammation [11]. Members of the gp130 family of cytokines include IL-6, leukemia inhibitory factor (LIF), IL-11, cardiotrophin-1 (CT-1), ciliary neurotrophic factor (CNTF), IL-27, oncostatin M (OSM), and IL-31. These cytokines share a common gp130 cell surface receptor subunit, with the exception of IL-31 which engages the IL-31R and OSMRβ complex rather than gp130. The gp130 cytokines bind to their specific receptor chain, then recruits the gp130 chain for cell signaling. Activation of these receptor complexes induces several signaling pathways including the Janus family of tyrosine kinases/signal transducer and activator of transcription (JAK/STAT), mitogen-activated protein kinase (MAPK), and phosphatidylinositide 3-kinase (PI3K) [11]. The STAT family of transcription factors plays a crucial role in immunity and inflammation. Upon ligand-receptor interaction, STAT proteins are phosphorylated and activated by JAKs. Phosphorylated STATs (pSTAT) dimerize and translocate to the nucleus and bind to specific DNA elements or other transcription factors to regulate gene expression. Several members of the gp130 cytokine family have been implicated in inflammatory responses of chronic respiratory diseases and ECM remodeling in the lung, including Oncostatin M and IL-6 [12–15].

1.2.1 Oncostatin M

Expressed primarily by T cells, macrophages, neutrophils and dendritic cells, OSM has been implicated in diverse physiological processes in stromal cells including bone metabolism, joint inflammation, cancer, vascularization, and inflammation [11,16]. OSMRβ and gp130 receptor chains, required for the active OSM receptor complex on cell surfaces [13], are widely expressed in stromal/connective tissue cells, including fibroblasts, osteoblasts, endothelial cells, smooth muscle cells, and epithelial cells in several organs including the heart, lungs, skin, and liver [11,16,17].

Since its discovery, OSM has been extensively studied in various homeostatic and pathological processes. It is well established that several of the gp130 cytokines can regulate bone metabolism [11,18]. Bone fracture healing is a complex process that involves the proper balance of bone resorption by osteoclasts and bone formation by osteoblasts [19]. OSM has been shown to induce osteoclast differentiation *in vitro* [20], and in a model of bone injury, OSMRβ-deficient mice had reduced osteoblast and osteoclast numbers, and thus delayed bone regeneration [21]. In joints, OSM has been found at high levels in the synovial fluid of patients with rheumatoid arthritis, and has been shown to stimulate cartilage remodeling and induce ECM remodeling components in fibroblasts including TIMPs and MMPs [11,18,22]. *In vivo*, OSM levels are elevated in mouse models of obesity and type 2 diabetes, and *in vitro* studies have shown that OSM, but not IL-6, suppresses adipogenesis while promoting dedifferentiation of mature adipocytes [23,24]. In the cardiovascular system, while OSM can have pathological consequences in promoting

atherosclerosis and cardiomyopathy, if appropriately regulated OSM signaling can promote wound healing and revascularization through increasing endothelial and smooth muscle cell proliferation and cardiomyocyte dedifferentiation [25,26]. While OSM signaling can elicit different pathophysiological responses depending on the organ or cell type, in general OSM-induced effects include the induction of inflammatory cytokines and chemokines, modulating the expression of ECM components, and altering cell proliferation and differentiation.

Although receptors for other gp130 cytokines, such as IL-6Rα, may also be expressed on connective tissue cells, their expression are relatively lower than OSMRβ [27]. In addition, we have previously shown that OSM is able to activate such cells more robustly than other cytokines in this family [14,28]. Furthermore, OSM has been detected at elevated levels in the bronchoalveolar lavage (BAL) fluid of IPF patients, sputum of asthma and COPD patients, as well as in allergic rhinitis tissue suggesting that OSM may be participating in the pathogenesis in these chronic diseases [12,29–31]. We have previously shown that overexpression of OSM induces ECM accumulation and accumulation of arginase-1^+ (Arg1) alternatively activated (AA/M2-like) macrophages, which was associated with eosinophilia and a T helper 2 (Th2)-skewed cytokine profile in lungs of C57Bl/6 mice [14,32–34]. In preliminary work for the present study, we observed marked induction of the gene for resistin-like molecule alpha (RELMα), a typical AA/M2 macrophage product. Regulation of RELMα by OSM has not been previously described, and whether RELMα participates in OSM-induced inflammation and pathology is examined here.

1.2.2 Interleukin-6

IL-6 is a cytokine with pleiotropic functions in inflammation, immune response, and hematopoiesis. It signals through two pathways, classical and *trans*-signaling, where IL-6 interacts with membrane-bound IL-6Rα or a soluble IL-6Rα respectively [35]. Unlike OSMRβ which is widely expressed on stromal cells, membrane-bound IL-6Rα is found predominantly on leukocytes and forms a receptor complex with gp130 in classical IL-6 signaling [36]. Upon binding of soluble IL-6 with soluble IL-6Rα, the complex can then interact with two gp130 receptor subunits to initiate *trans*-signaling in cells that possess gp130 but not membrane-bound IL-6Rα.

IL-6 is a pleotropic cytokine with both pro-inflammatory and anti-inflammatory properties. For example, in a model of colon cancer, signaling through the membrane-bound IL-6Rα initiates anti-inflammatory responses and activates STAT3, resulting in epithelial cell proliferation while inhibiting epithelial cell apoptosis. In contrast, *trans*-signaling through the soluble IL-6Rα initiates pro-inflammatory responses and activates the immune system. IL-6 is known to play significant roles in recruiting mononuclear cells to the site of infection, as well as stimulate B cell and T cell differentiation [37]. Although a limited number of cells express membrane-bound IL-6Rα, *trans*-signaling through the soluble IL-6Rα greatly increases target cells of IL-6. This has been demonstrated in several studies showing that hematopoietic stem cells, liver progenitor cells and neural cells, for example, respond to IL-6 and is dependent on soluble IL-6Rα [37].

Engagement of IL-6 with IL-6Rα/gp130 activates the JAK/STAT pathway. *In vivo* studies have shown that hyperactivation of STAT3 can lead to excessive ECM deposition and consequently pulmonary fibrosis [15]. Similar to OSM, IL-6 has also been detected at elevated levels in patients with COPD and IPF [38]. In bleomycin-induced pulmonary fibrosis models, ablation of systemic IL-6 attenuated fibrosis, whereas overexpression of IL-6 in mouse lung amplified fibrotic responses [15,39]. Previous work have shown that IL-6 can hyperpolarize macrophages into the AA/M2 macrophage phenotype and induce the expression of Arg1 in AA/M2-polarized macrophages [39,40]. Recent studies have also suggested that AA/M2 macrophages can enhance the anti-inflammatory response by recruiting Th2 and group 2 innate lymphoid cells (ILC2) to the site of injury, which enhances myofibroblast differentiation and consequently tissue fibrosis [7,39,41]. However, whether IL-6 can also induce RELMα in AA/M2 macrophages has not been characterized yet.

1.2.3 Interleukin-33

The alarmin IL-33 is a member of the IL-1 family of cytokines that is expressed predominantly by stromal cells including endothelial and epithelial cells. It signals through the ST2 and IL-1 receptor accessory protein (IL-1RAP) receptor complex which is expressed on group 2 innate lymphoid cells (ILC2s) and Th2 cells, and thus plays an important role in Th2 inflammation [42,43]. IL-33 is constitutively expressed and localized in the nucleus. It is known as an ‘alarmin’ because for biologically active full-length IL-33 to be released, the cell must undergo cell death by necrosis or necroptosis. If the cell

undergoes apoptosis, activated caspase-3 and -7 will cleave IL-33, making it inactive [44,45]. Once released, full-length IL-33 can be processed by serine proteases to enhance its activity [43]. Engagement with the ST2/IL-1RAP receptor complex on target cells activates the NFκB or MAPK signaling pathways.

IL-33 has been detected at elevated levels in lung epithelial cells of patients with asthma and COPD in comparison to healthy individuals [46,47]. Studies using ST2-deficient mice in a model of OVA-induced airway inflammation showed that in comparison to wildtype mice, $ST2^{-/-}$ mice have impaired type 2 inflammatory responses [46]. IL-33 has also been implicated in inflammation models through eosinophil accumulation and AA/M2 macrophage polarization in mouse lungs, which resulted in exacerbated airway inflammation [46,48]. Recently, IL-33 was shown to induce RELMα in eosinophils through an IL-4/IL-13-dependent manner [49]. Bouffi *et al.* proposed that IL-33 could directly stimulate eosinophils to produce IL-4, which then acts on eosinophils in an autocrine fashion to activate the STAT6 signaling pathway and induce RELMα [50]. This was demonstrated using eosinophils derived from $IL\text{-}4^{-/-}$ mice and stimulating with IL-4 or IL-33 [50]. Thus, induction of RELMα mRNA expression in OSM-induced lung inflammation *in vivo* may originate from a number of cell sources including macrophages and eosinophils.

1.3 Family of Resistin-like Molecules

The RELM/FIZZ (found in inflammatory zone) family is a class of cysteine-rich secreted proteins that consists of four known members – RELMα (FIZZ1), RELMβ (FIZZ2), resistin

(FIZZ3), and RELMγ [51]. These proteins are characterized based on their highly conserved 10-cysteine residue motif at the C-terminal domain but have unique tissue-specific expression patterns [52]. Their conserved signature region suggests that there may be a related family of receptors that remains to be discovered. All four members exist in mice, however in humans only RELMβ and resistin have been identified.

1.3.1 Resistin

Resistin or FIZZ3, also known as adipocyte-specific secreted factor (ADSF), is predominantly expressed in white adipose tissue in mice [53]. It has been implicated in adipogenesis and insulin resistance [54,55]. Kim *et al.* showed that resistin was able to inhibit adipocyte differentiation *in vitro* using 3T3-L1 preadipocytes [54]. Interestingly, another group showed that RELMα could also inhibit adipocyte differentiation in the same cell line [56], suggesting some degree of functional overlap between members of the RELM family, at least in certain cell types. Receptors for resistin are better characterized than for RELMα or RELMβ. In mouse adipose stromal cells, resistin can bind to an isoform of decorin, a proteoglycan, and lead to adipocyte proliferation and migration [57]. However in humans, resistin binds to TLR4 thereby inhibiting binding of LPS and preventing endotoxic shock in a model of sepsis [58].

1.3.2 RELMα

RELMα or FIZZ1 (9.4 kDa) can be secreted by several different cell types including AA/M2 macrophages, eosinophils, B lymphocytes, adipocytes, and alveolar epithelial cells

(AEC) [59–63]. In both AA/M2 macrophages and type II AECs, RELMα could be upregulated by IL-4 or IL-13 *in vitro*, and its dependence on STAT6 was confirmed using STAT6 knockout mice [64,65]. Unlike other members of the RELM family, RELMα lacks a cysteine residue at the N-terminus, at position Cys26, and thus cannot homodimerize [66]. However, co-immunoprecipitation experiments have shown that RELMα could form heterooligomeric structures with resistin or RELMβ [56,67].

RELMα has been implicated in murine models of experimental asthma, parasitic infection, pulmonary fibrosis, and wound healing [52,60,63,68–71]. Liu *et al.* showed that RELMα-deficient mice challenged with bleomycin were protected from the fibrotic phenotype, suggesting a profibrotic role for RELMα [52]. In a different model, Nair *et al.* demonstrated that RELMα-deficient mice challenged with the parasite *Schistosoma mansoni* developed exacerbated lung inflammation associated with elevated Th2 cytokine expression, presenting a healing phenotype [60]. Similarly, Sutherland *et al.* showed that RELMα-deficient mice infected with the nematode *Nippostrongylus brasiliensis* presented with greater lung tissue damage, and that RELMα was required for tissue repair following parasitic infection [72]. Given the proposed functions of RELMα in mouse lung inflammation, in this study we evaluate the regulation of RELMα by gp130 cytokines OSM and IL-6 *in vivo* and examine the roles of RELMα in OSM-induced lung inflammation and ECM gene expression *in vivo* using RELMα-deficient mice.

1.3.3 RELMβ

Similar to RELMα, RELMβ or FIZZ2 is also a secreted protein but was originally found to be only expressed in the gastrointestinal tract in both mouse and human [73]. It is implicated in allergen-induced airway inflammation in animal models, and was later reported to induce fibrosis through lung collagen deposition following intratracheal administration of RELMβ [74,75]. In human asthmatic patients, RELMβ is produced in excess in the bronchial mucosal tissue [76]. It is believed to play a significant role in airway remodeling through myofibroblast differentiation and induction of ECM proteins including type I collagen and αSMA [77,78]. Although the human RELMβ gene is the closest homolog to murine RELMα, whether they play similar roles in human and mouse lung inflammation remains unclear.

1.3.4 RELMγ

RELMγ is the least studied among the RELM family of proteins. RELMγ is most closely related to RELMα since the two genes share the highest homology within this gene family [79]. Like RELMα, there is no human ortholog of RELMγ. Despite the highly conserved genetic sequences, the expression pattern of RELMγ is clearly distinct from that of RELMα. In mice, RELMγ is highly expressed in cells and organs of the hematopoietic system including bone marrow, white blood cells, the spleen and thymus [79,80]. Although RELMγ can also be expressed in lung and adipose tissue, its expression is significantly lower than RELMα [79].

1.4 Adenoviral Vectors for Assessing Cytokine Function

Currently, adenoviral vectors are being used for gene therapy, as vaccine delivery vehicles, and in cancer immunotherapy studies. In this study, we use replication-deficient adenoviral vectors to examine effects of cytokine function expressed in the mouse lung. The adenoviral vectors used here have deletions in the E1 genomic region, rendering the virus replication-incompetent, and in the E3 genomic region, which is not essential for replication of viral DNA [81,82]. By using this system, adenoviruses can infect a variety of non-replicating cell types, with natural tropism for epithelial cells, which can express the inserted cytokines of interest, OSM or IL-6. The virus can be administered endotracheally to ensure it infects cells locally in the lung, and at a controlled dosage. To some degree, the transient overexpression of cytokine by the adenoviral vector mimics cytokine expression in inflammatory diseases [82]. Previous work have shown that intra-articular administration of adenoviral vectors expressing mouse OSM (AdOSM) but not mouse IL-6 (AdIL-6) induced joint inflammation and cartilage damage [83]. Intramuscular injection of AdOSM also induced IL-6 and acute-phase protein levels in serum, and endotracheal treatment of AdOSM induced accumulation of ECM and immune cells in mouse lungs, demonstrating that adenovirus-encoded mouse OSM can induce local and systemic effects *in vivo* [82,84].

1.5 Hypothesis and Aims

Preliminary data showed high induction of RELMα mRNA expression in lung tissue upon AdOSM treatment in wildtype mice. This was associated with a Th2-skewed cytokine

profile and accumulation of AA/M2 macrophages, conditions which are known to regulate RELMα. Thus, we hypothesize that OSM induces the expression of RELMα in mouse lung epithelial cells and macrophages, and that lung inflammation and ECM remodeling induced by OSM *in vivo* is elevated in part through the increase of RELMα (**Figure 1a**).

1.5.1 Aim 1: In vivo regulation of RELMα

The first aim is to assess the *in vivo* regulation of RELMα by OSM, IL-6, and IL-33 in both C57Bl/6 and BALB/c mice. Wildtype C57Bl/6 and BALB/c mice will be endotracheally administered with adenoviral vectors expressing mouse OSM (AdOSM) or IL-6 (AdIL-6) to induce transient overexpression of these cytokines over various time points. Empty adenoviral vectors (AdDel70) will be used as controls. To further assess the role of IL-33 and IL-6 in OSM-induced inflammation, IL-33$^{-/-}$ mice on both C57Bl/6 and BALB/c backgrounds or IL-6$^{-/-}$ C57Bl/6 mice will also be treated with AdDel70 or AdOSM. Following adenovirus administration, mice will be culled at various time points (day 2, 7, or 14) and assessed for RELMα expression, lung inflammation and ECM accumulation.

1.5.2 Aim 2: In vitro regulation of RELMα

The second aim is to assess the *in vitro* regulation of RELMα by OSM and other cytokines to determine potential sources of RELMα. Mouse C10 type 2 AEC and LA4 epithelial cells will be stimulated for 24 h with recombinant mouse OSM as well as other gp130 cytokines as comparators. Cells will also be co-stimulated with IL-4 and IL-13 to characterize

synergistic responses with OSM. After 24 h, cell culture supernatants will be analyzed for pro-inflammatory cytokines, such as MCP-1, by ELISA.

To assess macrophage expression of RELMα, bone marrow cells will be extracted from femurs of wildtype mice and differentiated *ex vivo* into macrophages. Bone marrow-derived macrophages (BMDM) will then be stimulated with LPS/IFNγ for classically activated (CA)/M1 macrophage polarization, or with IL-4/IL-13 for AA/M2 macrophage polarization. BMDMs will also be co-stimulated with IL-6 or IL-33. Cell culture supernatants will be analyzed for RELMα by ELISA.

1.5.3 Aim 3: OSM-induced inflammation in RELMα-deficient mice

The third aim is to examine the role of RELMα using RELMα$^{-/-}$ mice following administration of AdOSM. RELMα$^{-/-}$ mice will be endotracheally administered with AdDel70, AdOSM, or PBS as a negative control. At day 7 following adenovirus administration, mice will be culled and lung tissue assessed for mRNA and protein expression of RELMα and other molecules by NanoString analysis and Western blot, as well as ECM accumulation in the lung by histology. Sources of RELMα mRNA and colocalization with CD68 or IL-33 will be determined by chromogenic *in situ* hybridization (CISH). BAL fluid will also be examined for cellular infiltration, inflammatory mediators by ELISA, and measures of cell damage/death (cytocentrifuge smears), including LDH and CK18 in BAL by Western blot.

CHAPTER 2: MATERIALS AND METHODS

2.1 Animals

Female wildtype C57Bl/6 and BALB/c mice (6-8 or 8-10 weeks old) were purchased from The Jackson Laboratory (Bar Harbor, ME, USA) or Charles River Laboratories (Wilmington, MA, USA). Female IL-6$^{-/-}$ mice (C57Bl/6 background; 6-8 weeks old) were purchased from The Jackson Laboratories. Female IL-33$^{-/-}$ mice (C57Bl/6 and BALB/c background; 6-8 weeks old) were obtained from MedImmune, LLC (Gaithersburg, MD, USA). Female RELMα$^{-/-}$ mice (C57Bl/6 background; 8-10 weeks old) were purchased from The Jackson Laboratory (Bar Harbor, ME, USA). Mice were acclimatized one week prior to experimental procedures and housed under specific pathogen-free conditions within the McMaster University Central Animal Facility. All experimental procedures were approved by the McMaster University Animal Research Ethics Board.

2.2 Administration of Adenoviruses

Mice were anaesthetized and endotracheally administered 50 µL of sterile phosphate buffered saline (PBS) as naïve controls, empty adenoviral vectors AdDel70 (5×10^7 PFU/mouse), or those expressing mouse OSM (AdOSM, 5×10^7 PFU/mouse) or mouse IL-6 (AdIL-6, 3×10^7 PFU/mouse). Mice were culled 2, 7, or 14 days following adenovirus administration.

2.3 Sample Collection

Mice were anaesthetized by isoflurane and serum was collected from the hepatic vein. After exsanguination, bronchoalveolar lavage (BAL) fluid and cells were collected from lungs by perfusing twice with 500 µL of cold sterile PBS. The lobes of the right lung were excised and flash frozen in liquid nitrogen, which were then stored at –80 °C for further protein and RNA extraction. The left lung was perfused and fixed with 10% formalin for 48 h then transferred and stored in 70% ethanol prior to embedding in paraffin for histological analyses.

2.4 Bronchoalveolar Lavage Cytospin Preparation

BAL fluid cells were enumerated by manual counting using a haemocytometer and stained by Trypan Blue (Life Technologies, Carlsbad, CA, USA) to assess cell viability. Samples were centrifuged and the supernatants were stored at –80 °C for further cytokine analysis. Cell pellets were resuspended in PBS and cytocentrifuged at 1000 rpm for 3 min. Cytospin slides were stained with Hema-3 fixative solutions (Thermo Fisher Scientific, Waltham, MA, USA) for differential cell analysis of 500 leukocytes, and classified as macrophages, eosinophils, neutrophils, or lymphocytes.

2.5 Protein Extraction from Lung Tissues

Flash frozen lung tissues were transferred back into liquid nitrogen, then crushed into a fine powder. Each sample was divided into two and placed in either 1 mL of TRIzol (Invitrogen, Carlsbad, CA, USA) for RNA extraction or 1mL of RIPA buffer (1X PBS, 1% IGEPAL

CA-130, 0.5% Na-deoxycholate, 0.1% SDS) containing protease inhibitors (1 mM Na-orthovanadate, 5 μg/mL aprotinin, 1 mM phenylmethylsulphonylfluoride, 1 mM dithiothreitol) for protein extraction. Protein samples were processed using a homogenizer and stored at –80 °C until further analysis.

2.6 RNA Extraction from Lung Tissues

RNA from lung tissue samples in TRIzol were purified by phenol-chloroform extraction. One volume of chloroform was added to homogenized tissue and inverted. After mixing, the sample was centrifuged and the upper aqueous phase was transferred to a new Eppendorf. One volume of RNase-free isopropanol was added to the sample and inverted. After mixing, the sample was centrifuged to pellet the RNA, and the isopropanol was decanted. The RNA pellet was washed with 70% RNase-free ethanol, centrifuged, and the supernatant was removed. The pellet was dried at room temperature, resuspended with RNase-free water, and stored at –80 °C for further analysis.

2.7 Cell Culture

2.7.1 Isolation and Culture of Mouse Bone Marrow-derived Macrophages

Bone marrow cells were isolated from femurs of naïve female C57Bl/6 mice following euthanization. Bone marrow cells were cultured in Dulbecco's Modified Eagle Medium/Nutrient Mixture F12 (DMEM/F12) medium containing 10% fetal bovine serum (FBS) and 20 ng/mL of macrophage colony-stimulating factor (M-CSF) for 7 days. Non-adherent cells were washed off and adherent cells constituting the macrophage population,

known as bone marrow-derived macrophages (BMDM), were plated in 6-well plates at a cell density of 1 000 000 cells/well. Cells were then treated with various exogenous stimuli for 24 or 48 h. To polarize macrophages into the classically activated/M1 phenotype, BMDMs were treated with 100 ng/mL of LPS and 10 ng/mL of IFNγ. To polarize macrophages into the alternatively activated/M2 phenotype, BMDMs were treated with 20 ng/mL of IL-4 and 50 ng/mL of IL-13. Macrophages were co-stimulated with IL-6 or IL-33 and the CA/M1 or AA/M2 polarization cocktails to test the effect of IL-6 and IL-33 on macrophage RELMα production.

2.7.2 Mouse Lung Epithelial Cells (LA4)

LA4 cells (ATCC, Manassas, VA, USA) were thawed from previously frozen vials and cultured in 150 mm^2 tissue culture flasks under standard conditions (37 °C, 5% CO_2) in DMEM/F12 media containing 10% FBS and supplemented with 1% L-glutamine and 1% penicillin/streptomycin. Cells were passaged 1:4 or 1:6 when they reached 80-90% confluency.

2.7.3 Mouse Type II Alveolar Epithelial cells (C10)

C10 cells (gift from Dr. Christopher Migliaccio, University of Montana) were thawed from previously frozen vials and culture in 150 mm^2 tissue culture flasks under standard conditions (37 °C, 5% CO_2) in Roswell Park Memorial Institute (RPMI) media containing 10% FBS and supplemented with 1% L-glutamine and 1% penicillin/streptomycin. Cells were passaged 1:4 or 1:6 when they reached 80-90% confluency.

2.7.4 Cytokine Stimulations

LA4 or C10 cells were seeded at a cell density of 100 000 cells/well in 96-well plates and incubated overnight at 37 °C, 5% CO_2 prior to cytokine stimulations. The following day, cells were washed with 1X PBS to remove residual serum and stimulated with 5 ng/mL of IL-6, 100 ng/mL of LPS, 10 ng/mL of IFNγ, 20 ng/mL of IL-4, 50 ng/mL of IL-13, or 10 ng/mL of OSM in media containing 0.5% FBS, or in various of combinations of cytokines as indicated. After 24 h, supernatants were collected and stored at –80 °C for further analysis by ELISA.

2.7.5 Preparation of Cell Lysates and RNA Extracts

To extract protein, cells were lysed in RIPA buffer (1X PBS, 1% IGEPAL CA-130, 0.5% Na-deoxycholate, 0.1% SDS) containing protease inhibitors (1 mM Na_3VO_4, 5 μg/mL aprotinin, 1 mM PMSF, 1 mM DTT), and homogenized by passing the lysate through 23 gauge needles. RNA was extracted from cells using PureLink™ RNA Mini Kit (Thermo Fisher Scientific, Waltham, MA, USA). Protein and RNA extracts were stored in -80 °C.

2.8 Chromogenic *In Situ* Hybridization

Chromogenic *in situ* hybridization (CISH) for mouse CD68, IL-33, and RELMα mRNA was performed using the RNAscope® 2.5 Duplex Assay Kit (Advanced Cell Diagnostics, Newark, CA, USA). Formalin-fixed, paraffin-embedded lung tissue sections were pretreated with heat and protease prior to hybridization with the target oligo probes.

Specific RNA staining signal was identified as punctate dots unless at very high levels in which signals converge.

2.9 Histology and Immunohistochemistry

Following formalin fixation, the left lobe of lungs was dissected into three sections per lung, embedded in paraffin and stored at rt for further analysis. Sections of 3 μm were cut and stained with hematoxylin and eosin (H&E) to assess lung pathology, Periodic acid-Schiff (PAS) to assess mucous-producing goblet cells, and Picrosirius red (PSR) to assess collagen fibrils. Immunohistochemistry for Ki67 to assess cell proliferation and alpha smooth muscle actin (αSMA) was also performed. Slide images were captured using Zeiss Axio Imager 2 (ZEISS, Oberkochen, Germany), or scanned using Aperio ImageScope (Leica Biosystems, Wetzlar, Germany).

2.9.1 Quantification of Ki67 and αSMA Staining

Images from Ki67-stained slides were captured using Zeiss Axio Imager 2 (ZEISS, Oberkochen, Germany). Ki67 staining was quantified using ImageJ v1.51k ImmunoRatio plugin (National Institutes of Health, USA). Images from αSMA-stained slides were scanned using Aperio ImageScope (Leica Biosystems, Wetzlar, Germany). αSMA staining in the lung parenchyma was quantified using QuPath v0.1.2 (https://qupath.github.io/). Three sections were analyzed per mouse, excluding major airways and blood vessels.

2.10 Western Blot

Cell lysates, whole lung homogenates, or BAL fluid were loaded onto 12-15% SDS-PAGE gels (20 μg of protein/well) and separated by electrophoresis at 120 V for 1 h, then transferred to nitrocellulose membranes at 400 mA for 2 h. Blots were blocked using Odyssey Blocking Buffer (LI-COR Biosciences, Lincoln, NE, USA) for 1 h at rt, then probed for using rabbit anti-RELMα pAb (PeproTech, Rocky Hill, NJ, USA), rabbit anti-pSTAT3 (Tyr705) mAb (Cell Signaling Technology, Danvers, MA, USA), mouse anti-Arg1 mAb (BD Biosciences, San Jose, CA, USA), goat anti-IL-33 pAb (R&D Systems, Minneapolis, MN, USA), rabbit anti-CK18 pAb (Abcam, Cambridge, MA, USA), or mouse anti-β-actin mAb (Santa Cruz Biotechnology, Dallas, TX, USA) overnight at 4 °C. The following day blots were washed with TBS + 0.15% Tween20, and IRDye® donkey anti-rabbit, goat anti-mouse, or donkey anti-goat secondary antibodies (LI-COR Biosciences, Lincoln, NE, USA) was added to the blots for 45 min at rt. After subsequent washes with TBS + 0.15% Tween20, blots were imaged on Odyssey LI-COR Imaging System (Lincoln, NE, USA). Protein bands of interest were quantified by densitometry using Image Studio Lite (LI-COR Biosciences, Lincoln, NE, USA).

2.11 NanoString Analysis

Gene expression using a custom probe set was measured by NanoString Technologies (Seattle, WA, USA). Analysis of raw mRNA counts was performed using nSolver™ Analysis Software v4.0 (NanoString Technologies, Seattle, WA, USA). Gene expression levels were normalized to housekeeping genes *Actb* and *Pgk1*.

2.12 Reverse Transcription Polymerase Chain Reaction (RT-PCR)

Lung RNA purified by phenol-chloroform extraction were reverse transcribed into cDNA and stored at –80 °C. cDNA was analyzed by TaqMan® Gene Expression Assay (Applied Biosystems, Foster City, CA, USA) using pre-determined assay reagents and specific probes for 18S, RELMα, endogenous OSM and viral OSM (Thermo Fisher Scientific, Waltham, MA, USA).

2.13 Enzyme-linked Immunosorbent Assay (ELISA)

BAL fluid and serum from mice were analyzed using commercially available DuoSet ELISA kits from R&D Systems (Minneapolis, MN, USA). For measuring RELMα by ELISA, an in-house sandwich ELISA was developed using rabbit anti-mouse RELMα polyclonal antibody (PeproTech, Rocky Hill, NJ, USA) and biotinylated anti-mouse RELMα antibody (PeproTech, Rocky Hill, NJ, USA).

2.14 Flow Cytometry

Whole lung mononuclear cell suspensions were generated from a section of the right lobe by mechanical mincing and collagenase digestion. Tissues were degraded with Collagenase I and DNase I for 2 h on an incubated shaker at 37 °C. Debris were removed by passage through 45 μm mesh filter and cells were resuspended in 1X PBS/0.3% bovine serum albumin (BSA). Cells were stimulated with para-methoxyamphetamine (PMA) and ionomycin for 4 h prior to flow cytometric analysis. Forward scatter and side scatter parameters and Zombie-Aqua dye (BioLegend, San Diego, CA, USA) were used to define

the live cell gate. Cells were stained with Zombie-Aqua dye for 20 min at rt prior to surface staining with fluorophore-conjugated antibodies. Cells were surface-stained for 30 min at 4 °C with antibodies for CD3, CD4, CD38, and CD45 (BD Biosciences, San Jose, CA, USA). Following surface staining, cells were fixed with BD Cytofix/CytoPerm (BD Biosciences, San Jose, CA, USA) for 20 min at 4 °C and then washed with BD 1X Perm/Wash (BD Biosciences, San Jose, CA, USA) prior to intracellular staining for 30 min at 4 °C with antibodies for CD206 and IFNγ (BD Biosciences, San Jose, CA, USA). Cells were then washed and resuspended in 1X PBS/0.3% BSA for analysis on the BD LSR II flow cytometer (BD Biosciences, San Jose, CA, USA).

2.15 Lactate Dehydrogenase Assay

Lactate dehydrogenase in BAL fluid was measured using Pierce LDH Cytotoxicity Assay Kit (Thermo Fisher Scientific, Waltham, MA, USA) according to manufacturer's protocol.

2.16 Statistical Analysis

Statistical analyses were carried out using GraphPad Prism 7. The Student's t test, one-way or two-way analysis or variance was used to determine significant differences between sample groups, where $^{*}P < 0.05$, $^{**}P < 0.01$, $^{***}P < 0.001$, $^{****}P < 0.0001$, and $^{\#}P < 0.05$ relative to controls groups.

CHAPTER 3: *IN VIVO* REGULATION OF RELMA BY OSM, IL-6, AND IL-33 IN C57BL/6 AND BALB/C MICE

3.1 Induction of RELMα by OSM

To examine the *in vivo* regulation of RELMα, wildtype C57Bl/6 and BALB/c mice were endotracheally administered PBS as naïve controls, AdDel70, or AdOSM to induce transient overexpression of mouse OSM in the lungs for 7 or 14 days as previous [14,32,33,40], as outlined in **Figure 1b**. Whole lung tissues were assessed for RELMα mRNA expression by RT-PCR, and BAL fluid and serum were analyzed for RELMα protein by ELISA. In AdDel70-treated C57Bl/6 mice, RELMα mRNA was detectable at low levels, which was significantly upregulated upon treatment with AdOSM at day 7 (**Figure 3a, left panel**). At the protein expression levels, RELMα was detectable at basal levels of approximately 100 ng/mL in BAL fluid of naïve and AdDel70-treated C57Bl/6 mice. Following overexpression of OSM, RELMα protein detected was markedly induced 180-fold to up to approximately 12 μg/mL at day 7, and afterwards decreased to approximately 4 μg/mL by day 14 (**Figure 3b, left panel**). RELMα was present at 150-200 ng/mL in serum of naïve and AdDel70-treated animals, and elevated 2-fold upon AdOSM infection both at days 7 and 14 in C57Bl/6 mice (Figure 3c, left panel). Similar trends were observed in BALB/c mice at the mRNA expression level and in BAL fluid (**Figure 3a, b, right panels**), however, RELMα levels in serum of BALB/c mice were similar across all treatments (**Figure 3c, right panel**).

Given that previous studies in other models have shown that RELMα could be expressed in other cell types in addition to AA/M2 macrophages [60,85], we sought to determine the cell sources of RELMα following AdOSM treatment. Lung tissue sections from wildtype C57Bl/6 and BALB/c mice treated with AdOSM were analyzed for RELMα mRNA expression by CISH using custom probes for RELMα. Upon overexpression of OSM for 7 days, RELMα mRNA is highly expressed in columnar airway epithelial cells in both strains of mice (**Figure 4**). In C57Bl/6 mice, RELMα is also expressed in mononuclear cells throughout the lung parenchyma, whereas the RELMα mRNA signal in BALB/c lung parenchyma was much lower than in C57Bl/6 lung parenchyma. This is associated with lower total RELMα mRNA levels in BALB/c mice (**Figure 3a**). This is consistent with unpublished observations, where less accumulation of $Arg1^+$ AA/M2 macrophages is observed in the lung parenchyma of BALB/c mice in this model. The specificity of the custom RELMα CISH probe is demonstrated using CISH negative control probe of serial sections of the same lung tissue sample.

3.2 Induction of RELMα by IL-6

As a comparator of OSM to another typical gp130 cytokine IL-6, AdIL-6 was endotracheally administrated to both C57Bl/6 and BALB/c strains of mice to induce transient overexpression of mouse IL-6 for 2 and 7 days and compared to mice treated in parallel with AdOSM. RELMα protein in BAL fluid was quantified by ELISA (**Figure 5a**) and Western blot (**Figure 5b, c**). In C57Bl/6 mice, AdOSM induced RELMα in BAL fluid 2 days following treatment, and levels were further elevated by day 7 (**Figure 5a, left**

panel). A similar trend was observed with AdIL-6, where RELMα levels at day 2 were elevated but not statistically different from controls, whereas AdIL-6 was also able to induce RELMα by day 7 albeit to markedly lower levels than AdOSM (2 vs 6 μg/mL). Similar trends were observed in BAL fluid of BALB/c mice (**Figure 5a, right panel**). Analysis of day 7 BAL fluid samples by Western blot showed that AdOSM treatment resulted in high levels of RELMα protein detected as a single full-length band at the expected molecular weight (~10 kDa), and that AdIL-6 induced some but significantly lower levels of signal at the expected molecular size (**Figure 5b**, signals in left panel quantified by densitometry in right panel).

To determine if IL-6 is required for AdOSM-induced RELMα expression, wildtype C57Bl/6 and IL-6$^{-/-}$ mice were administered AdDel70 or AdOSM, and BAL fluid was assessed for RELMα by Western blot. In this assay (less sensitive than ELISA), RELMα could not be detected in BAL fluid of AdDel70-treated mice (**Figure 5c**). RELMα was highly expressed in BAL fluid of AdOSM-treated wildtype mice, but was significantly reduced in IL-6$^{-/-}$ mice (signals quantified by densitometry in **Figure 5c, right panel**), suggesting that IL-6 is required for maximal induction of RELMα by OSM.

3.3 Regulation of RELMα in the Absence of IL-33

In our model of lung inflammation, OSM is known to upregulate IL-33 which enhances the Th2 inflammatory response in the mouse lung [28]. This raised questions as to whether RELMα also participates in such activity in the lung, and whether RELMα is regulated

downstream of IL-33 or directly induced by OSM. To address this, wildtype and IL-33$^{-/-}$ C57Bl/6 mice were endotracheally administered with AdDel70 or AdOSM. Mice were culled 7 or 14 days following adenovirus administration. At day 7, whole lung homogenates were analyzed by RT-PCR for mRNA expression of RELMα. Both wildtype and IL-33$^{-/-}$ mice treated with AdDel70 expressed minimal levels of RELMα mRNA in C57Bl/6 mice at day 7 (**Figure 6a**). After 7 days, AdOSM markedly upregulated RELMα mRNA expression in whole lung, but in the absence of IL-33, RELMα expression was significantly reduced more than 2-fold.

To assess if similar trends were reflected at the protein level, RELMα in BAL fluid of wildtype and IL-33$^{-/-}$ C57Bl/6 mice collected at days 7 and 14 were analyzed by Western blot (**Figure 6b**) and ELISA (**Figure 6c**). Both assays showed similar trends where basal levels of RELMα were detected in control animals at both time points. At day 7 in wildtype C57Bl/6 mice treated with AdOSM, RELMα protein could be detected, and at significantly higher levels than in IL-33$^{-/-}$ mice, consistent with mRNA expression levels at day 7 (**Figure 6c, left panel**). By day 14 although RELMα protein levels were lower than at day 7, it remained elevated in AdOSM-treated mice, with significantly lower levels in IL-33$^{-/-}$ mice than in wildtype mice (**Figure 6c, right panel**). Similar trends were also observed in day 7 and day 14 serum, where RELMα protein was found at elevated levels in AdOSM-treated wildtype mice, but not in IL-33$^{-/-}$ mice (**Figure 6d**).

To examine possible differences in another strain of mouse, wildtype and IL-33$^{-/-}$ BALB/c mice were endotracheally administered with AdDel70 or AdOSM, and mice were culled 7 or 14 days following adenovirus administration, similar to experiments in the C57Bl/6 model. At day 7, very low levels of RELMα mRNA were detected by RT-PCR in AdDel70-treated mice, and upon AdOSM infection RELMα expression was significantly upregulated in whole lung of both wildtype and IL-33$^{-/-}$ BALB/c mice (**Figure 7a**). BAL fluid collected at day 7 and day 14 post adenovirus infection were analyzed by Western blot (**Figure 7b**) and ELISA (**Figure 7c**). In both assays, RELMα was detected at basal levels in naïve and AdDel70-treated mice at day 7. Upon AdOSM treatment, RELMα in BAL fluid at day 7 were markedly elevated in both wildtype and IL-33$^{-/-}$ mice, however there was no effect of IL-33-deficiency on RELMα protein expression (**Figure 7c, left panel**). By day 14, RELMα protein levels in BAL fluid of AdOSM-treated mice remained elevated but at lower levels than at day 7 (**Figure 7c, right panel**). RELMα protein in serum was measured by ELISA, however the levels were similar across all treatments in both wildtype and IL-33$^{-/-}$ BALB/c mice (**Figure 7d**).

Day 7 lung tissue sections from AdDel70- and AdOSM-treated wildtype and IL-33$^{-/-}$ C57Bl/6 mice were analyzed by CISH and stained for RELMα and IL-33 mRNA (**Figure 8**). In AdDel70-treated mouse lung sections, RELMα mRNA expression could be seen in some cells in the airway epithelium, and very few IL-33^{+} cells in the lung parenchyma. Upon AdOSM treatment, RELMα mRNA is highly expressed in columnar airway epithelial cells, and consistent with mRNA levels measured by RT-PCR (**Figure 6a**) there is less

RELMα staining in AdOSM-treated IL-33$^{-/-}$ mice. IL-33^{+} cells could be observed in cells throughout the lung parenchyma and in the basement membrane of the airway epithelium. A number of cells in the lung parenchyma were also RELMα^{+} IL-33^{+}, as demonstrated by colocalization of the two stains.

Figure 1. Schematic of RELMα regulation by OSM and IL-6, and *in vivo* experimental design. (a) Proposed mechanism by which RELMα is regulated. Classically activated/M1 macrophages produce gp130 cytokines OSM and IL-6. We speculate that OSM acts on connective tissue/stromal cells whereas IL-6 acts on alternatively activated/M2 macrophages to induce expression of RELMα. Regulation of RELMα by OSM or IL-6 has not been previously described, and whether RELMα participates in OSM-induced inflammation and pathology is examined here. **(b)** As a model of chronic pulmonary inflammation, we use adenovirus vectors to transiently overexpress mouse OSM (AdOSM) or IL-6 (AdIL-6) in the lung through endotracheal administration, or the empty vector AdDel70 as negative controls. 7 and 14 days after infection, mice are culled and lung cells and tissue are harvested for analysis of inflammation and ECM accumulation. Yellow shaded region shows the level of adenovirus vector expression of cytokines OSM or IL-6 over time.

Figure 1

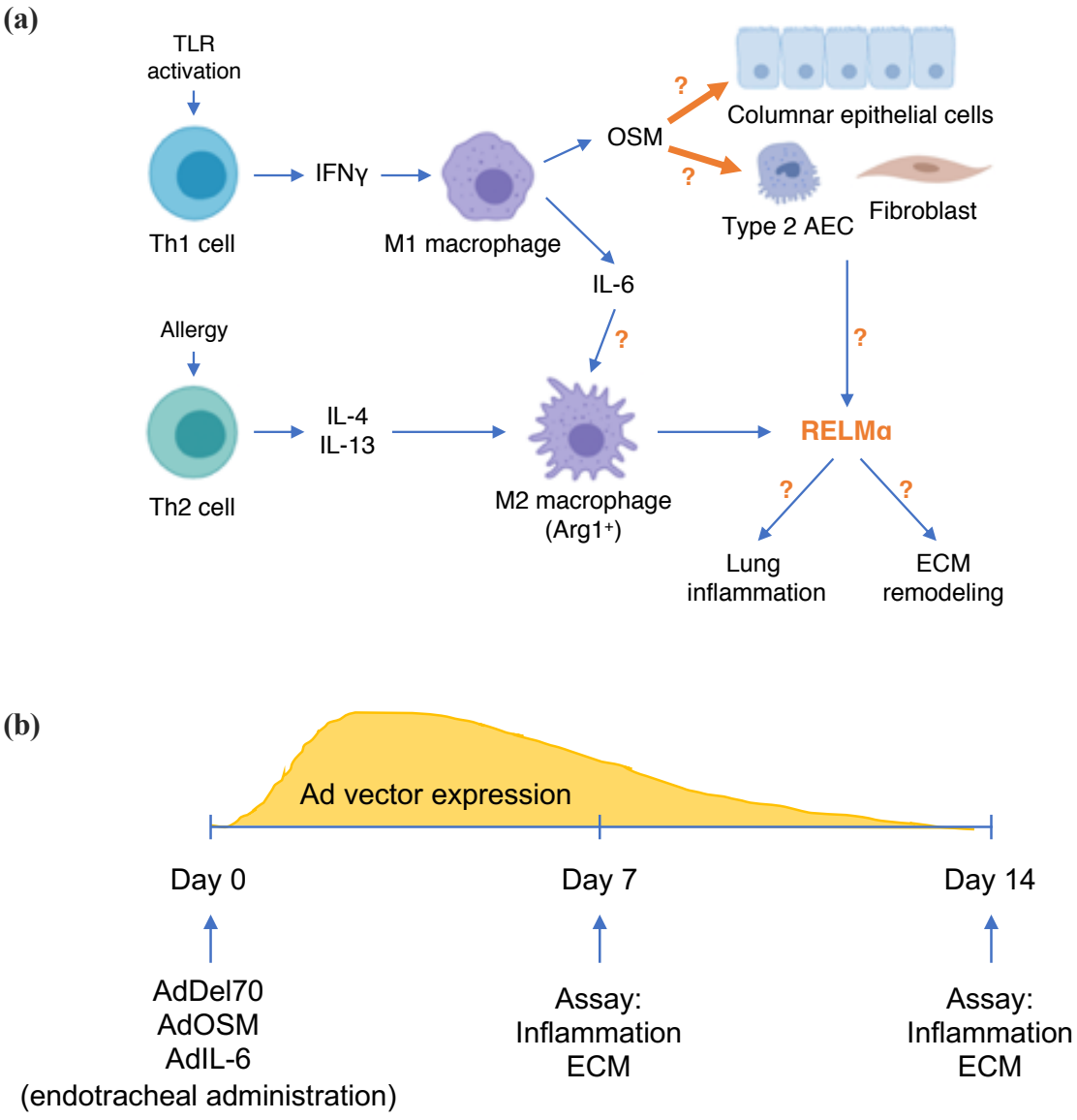
(a)
TLR activation
Th1 cell
IFNγ
M1 macrophage
OSM
?
?
Columnar epithelial cells
Type 2 AEC
Fibroblast
IL-6
?
?
Allergy
Th2 cell
IL-4
IL-13
M2 macrophage (Arg1+)
RELMα
?
?
Lung inflammation
ECM remodeling
(b)
Ad vector expression
Day 0
Day 7
Day 14
AdDel70
AdOSM
AdIL-6
(endotracheal administration)
Assay:
Inflammation
ECM
Assay:
Inflammation
ECM

Figure 2. Specificity of anti-murine RELMα polyclonal antibody by Western blot. Whole lung homogenates and BAL fluid from AdDel70- and AdOSM-treated C57Bl/6 mice were analyzed by Western blot. Known amounts of recombinant RELMα (0-2 ng) were loaded on the same gel as a positive control and to generate a standard curve for semi-quantitative densitometric analysis. **(a)** Immunoblot was probed with rabbit anti-murine RELMα polyclonal antibody and donkey anti-rabbit secondary antibody. **(b)** Immunoblot was probed with donkey anti-rabbit secondary antibody alone, showing that bands detected in **(a)** are not due to non-specific binding of the secondary antibody. Each lane indicates sample extracts from separate mouse lungs. (n = 3 mice/group). *(Submitted to Journal of Leukocyte Biology in the manuscript entitled "RELMα is induced by Oncostatin M in vivo and modulates extracellular matrix and cytoprotection in mouse lung inflammation.")*

Figure 2

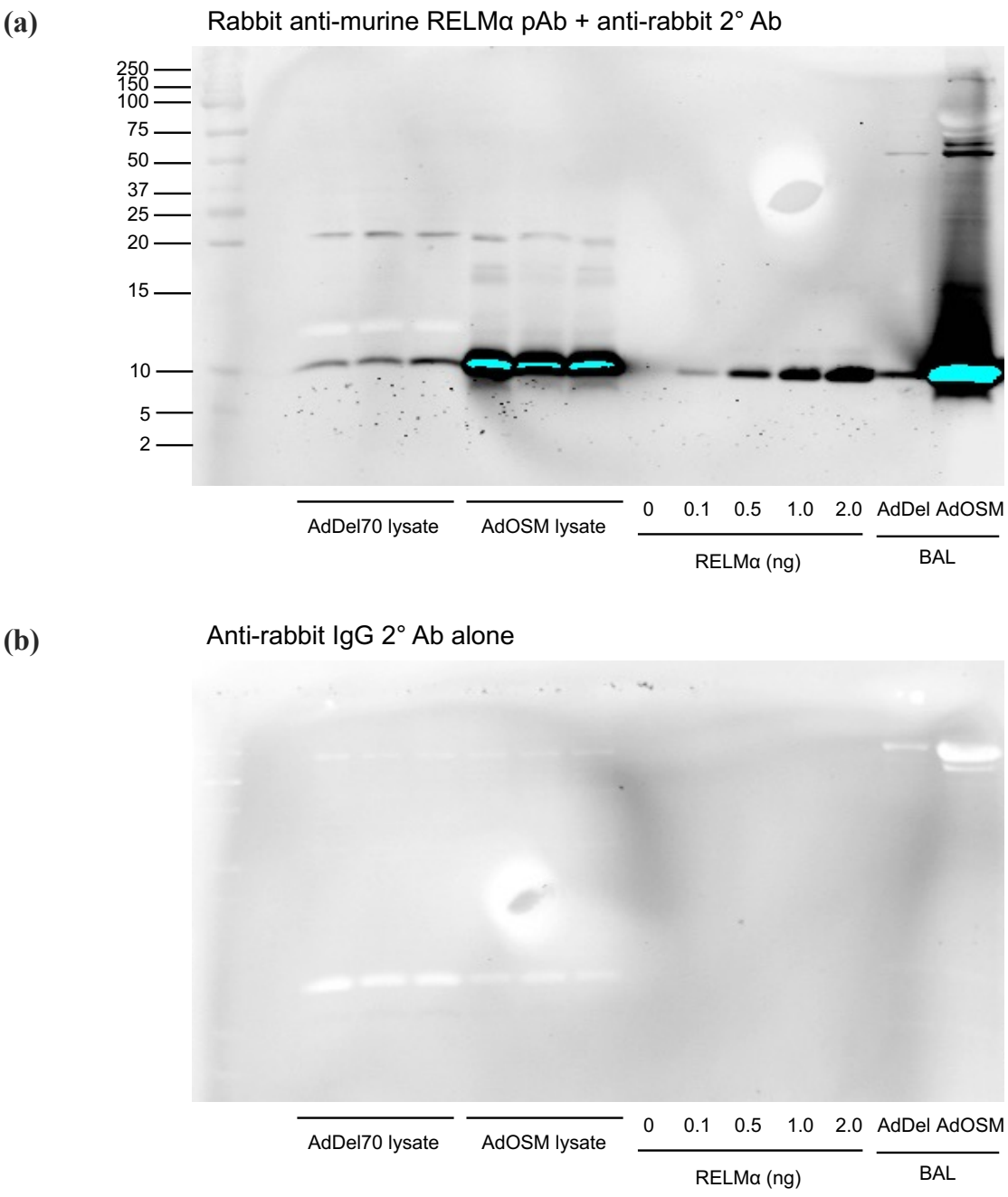
(a)
Rabbit anti-murine RELMα pAb + anti-rabbit 2° Ab
250
150
100
75
50
37
25
20
15
10
5
2
AdDel70 lysate
AdOSM lysate
0 0.1 0.5 1.0 2.0
RELMα (ng)
AdDel AdOSM
BAL
(b)
Anti-rabbit IgG 2° Ab alone
AdDel70 lysate
AdOSM lysate
0 0.1 0.5 1.0 2.0
RELMα (ng)
AdDel AdOSM
BAL

Figure 3. Transient overexpression of OSM induces RELMα mRNA and protein expression in lungs of C57Bl/6 and BALB/c mice. (a) RELMα mRNA expression in total lung homogenates 7 days following administration of AdDel70 or AdOSM to wildtype C57Bl/6 (left panels) and BALB/c mice (right panels). RELMα mRNA levels are expressed relative to 18S ribosomal RNA. RELMα protein levels in **(b)** BAL fluid and **(c)** serum in naïve animals or 7 and 14 days post adenovirus infection, assessed by ELISA. Data are expressed as mean ± SEM (n = 4-6 mice/group). Statistical significance determined by one-way ANOVA with Tukey's post hoc test ($^{\#}P < 0.05$ relative to controls at the indicated time point; $^{*}P < 0.05$, $^{**}P < 0.01$, $^{****}P < 0.0001$ between indicated groups). *(RT-PCR performed by Rex Park; ELISAs performed by Ashley Yip. Submitted to Journal of Leukocyte Biology in the manuscript entitled "RELMα is induced by Oncostatin M in vivo and modulates extracellular matrix and cytoprotection in mouse lung inflammation.")*

Figure 3

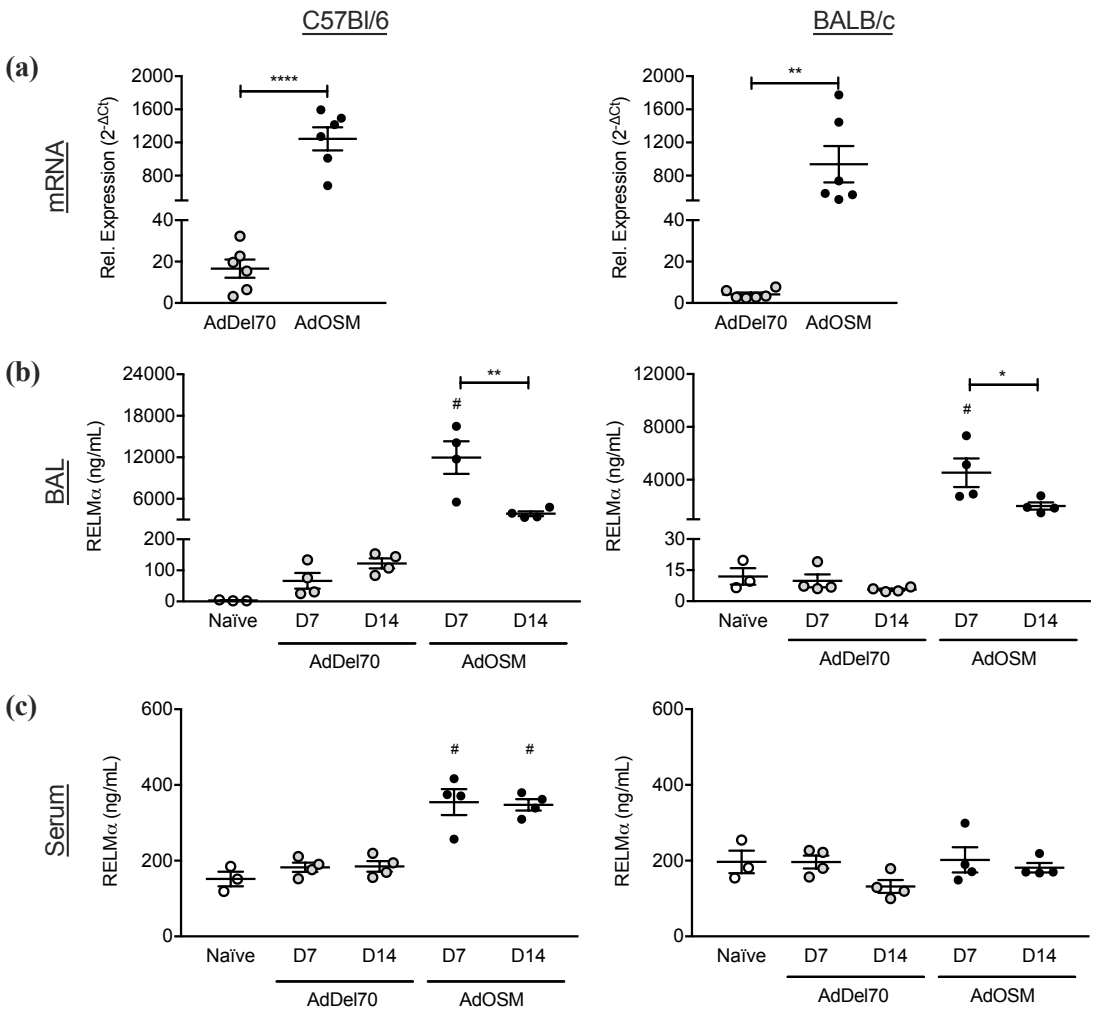
C57Bl/6
BALB/c
(a)
mRNA
Rel. Expression (2-ΔCt)
2000
1600
1200
800
40
20
0
****
**
AdDel70
AdOSM
(b)
BAL
RELMα (ng/mL)
24000
18000
12000
6000
200
100
0
12000
8000
4000
30
15
**
*
#
Naïve
D7
D14
AdDel70
AdOSM
(c)
Serum
600
400
200
0

Figure 4. RELMα mRNA is highly induced in columnar airway epithelial cells. Representative images are shown of CISH for RELMα in formalin-fixed, paraffin-embedded lung tissue sections from AdOSM-treated wildtype C57Bl/6 and BALB/c mice at day 7. RELMα mRNA (red) in AdOSM-treated mouse lung sections (top panels). Negative controls for serial sections of the same lung sample are shown (bottom panels). Scale bars, 50 μm. (n = 5 mice/group). *(Submitted to Journal of Leukocyte Biology in the manuscript entitled "RELMα is induced by Oncostatin M in vivo and modulates extracellular matrix and cytoprotection in mouse lung inflammation.")*

Figure 4

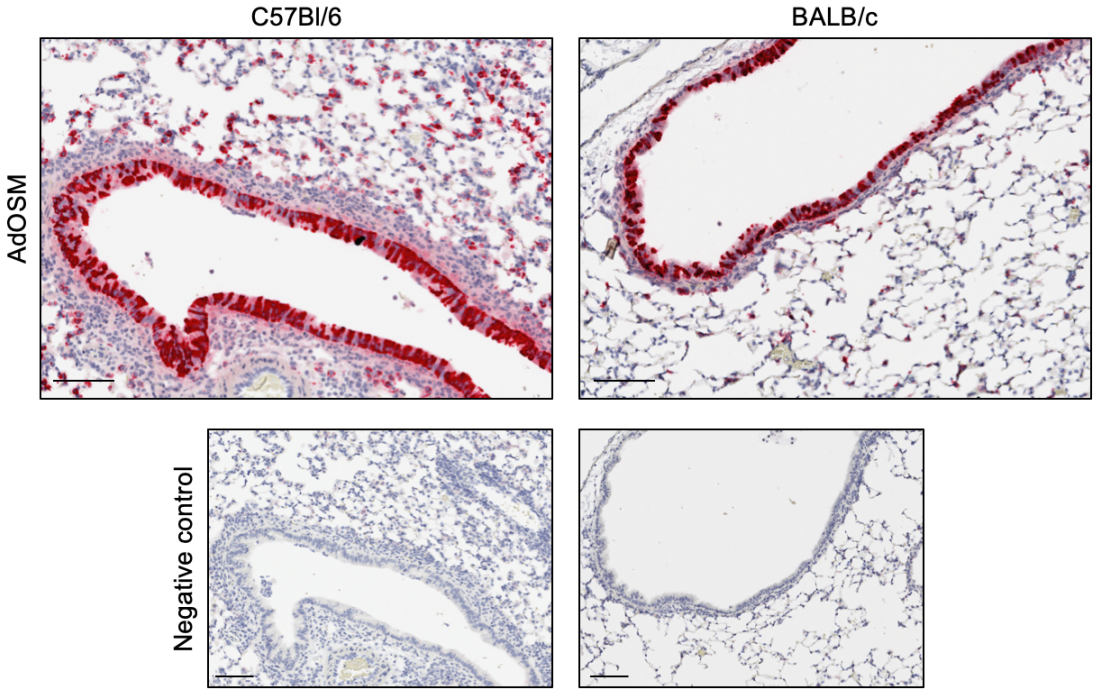

Figure 5. IL-6 is required for maximal induction of RELMα by OSM. (a) RELMα protein levels in BAL fluid from C57Bl/6 (left panel) and BALB/c mice (right panel) at day 2 or day 7 after AdDel70, AdOSM or AdIL-6 treatment, as assessed by ELISA. **(b)** BAL fluid from wildtype C57Bl/6 mice 7 days post-infection with AdDel70, AdOSM or AdIL-6 were analyzed by Western blot for RELMα (detecting a single band, left panel) and densitometry signals were quantified (right panel). **(c)** BAL fluid from wildtype and IL-6$^{-/-}$ C57Bl/6 mice 7 days post-infection with AdDel70 or AdOSM were analyzed by Western blot (left panel), and densitometry signals were quantified (right panel). Each lane indicates sample extracts from separate mouse lungs. Data are expressed as mean ± SEM (n = 4-5 mice/group). Statistical significance determined by one-way ANOVA with Tukey's post hoc test ($^{\#}P < 0.05$ relative to controls at the indicated time point; $^{**}P < 0.01$, $^{****}P < 0.0001$ between indicated groups). *(ELISAs performed by Ashley Yip. Submitted to Journal of Leukocyte Biology in the manuscript entitled "RELMα is induced by Oncostatin M in vivo and modulates extracellular matrix and cytoprotection in mouse lung inflammation.")*

Figure 5

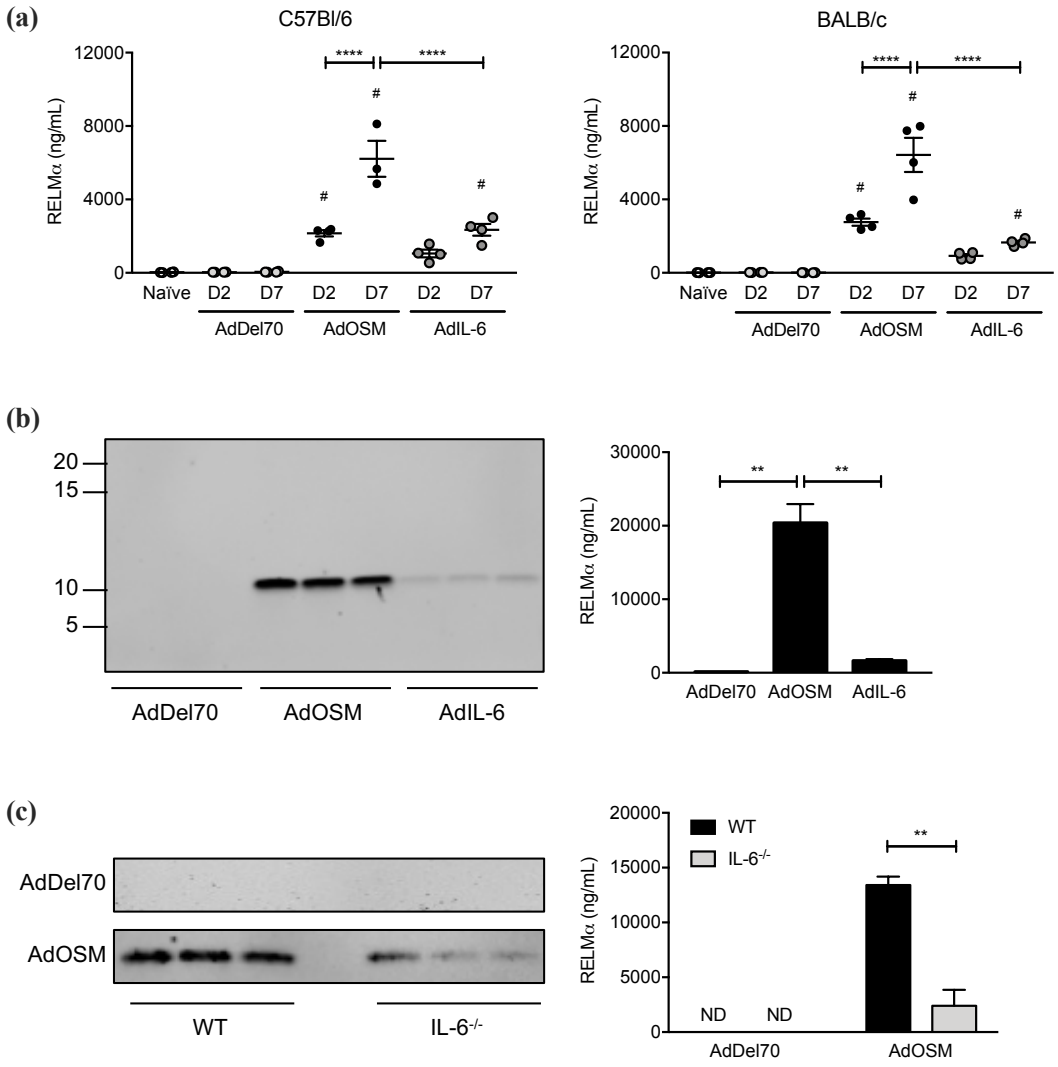
(a)
C57Bl/6
BALB/c
RELMα (ng/mL)
12000
8000
4000
0
****
#
Naïve
D2
D7
AdDel70
AdOSM
AdIL-6
(b)
20
15
10
5
AdDel70
AdOSM
AdIL-6
30000
20000
10000
**
(c)
WT
IL-6-/-
15000
5000
ND

Figure 6. Regulation of RELMα by IL-33 in C57Bl/6 mice. Wildtype and IL-33$^{-/-}$ C57Bl/6 mice were endotracheally administered AdDel70 or AdOSM. **(a)** RELMα mRNA expression in total lung homogenates 7 days post-infection. mRNA levels are expressed relative to 18S ribosomal RNA. RELMα protein levels 7 days (left panels) and 14 days (right panels) post-infection in BAL fluid assessed by **(b)** Western blot and **(c)** ELISA, and in **(d)** serum, assessed by ELISA. Each lane indicates sample extracts from separate mouse lungs. Data are expressed as mean ± SEM (n = 4-6 mice/group). Statistical significance determined by two-way ANOVA with Tukey's post hoc test ($^{*}P < 0.05$, $^{**}P < 0.01$, $^{***}P < 0.001$, $^{****}P < 0.0001$ between indicated groups). *(RT-PCR performed by Rex Park; ELISAs performed by Ashley Yip.)*

Figure 6

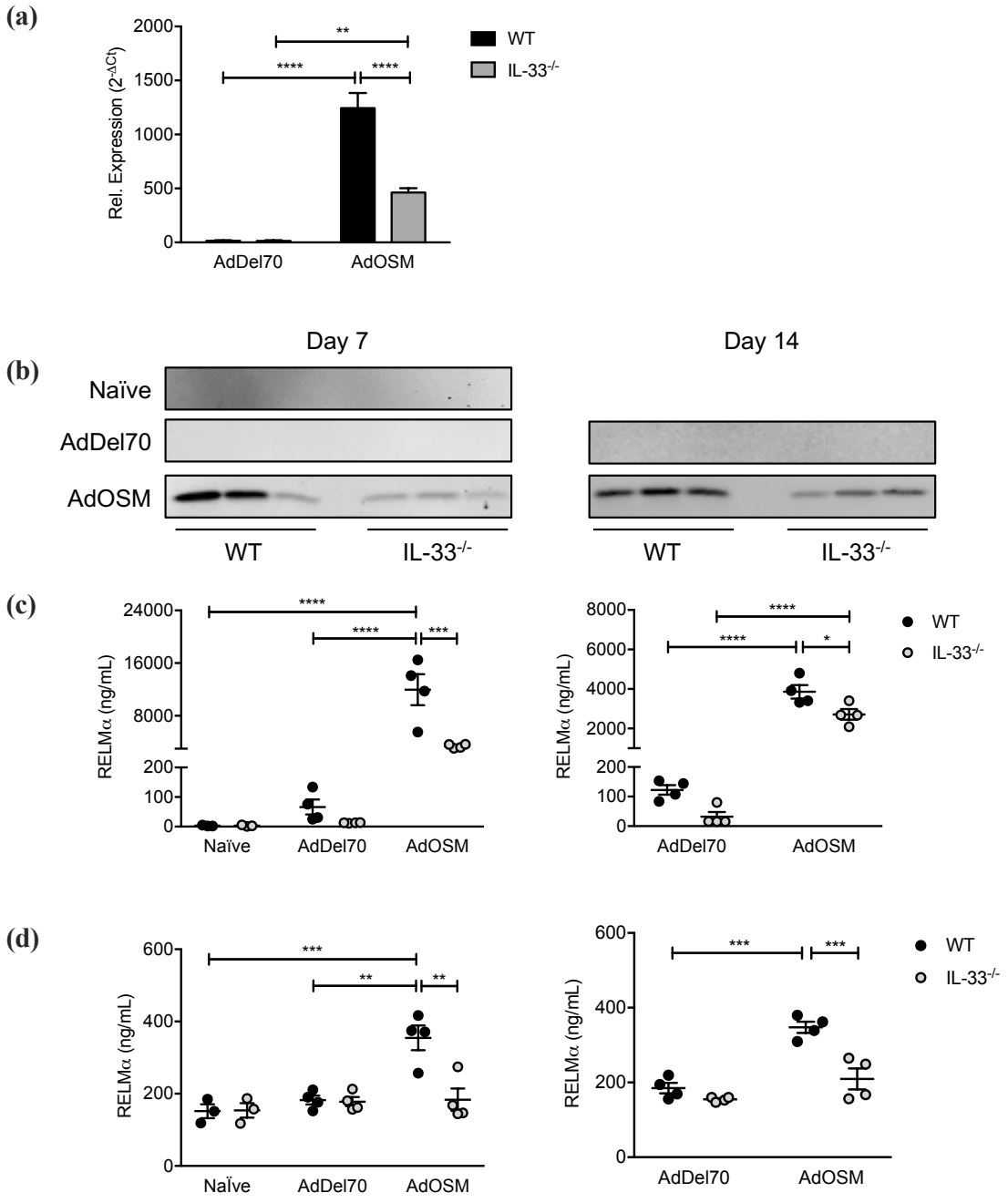
(a)
Rel. Expression ($2^{-\Delta Ct}$)
2000
1500
1000
500
0
**
****
****
WT
IL-33-/-
AdDel70
AdOSM
(b)
Day 7
Day 14
Naïve
AdDel70
AdOSM
WT
IL-33-/-
WT
IL-33-/-
(c)
RELMα (ng/mL)
24000
16000
8000
200
100
0
****
****
***
Naïve
AdDel70
AdOSM
8000
6000
4000
2000
200
100
0
****
****
*
AdDel70
AdOSM
WT
IL-33-/-
(d)
RELMα (ng/mL)
600
400
200
0
***
**
**
Naïve
AdDel70
AdOSM
600
400
200
0
***
***
AdDel70
AdOSM
WT
IL-33-/-

Figure 7. Regulation of RELMα by IL-33 in BALB/c mice. Wildtype and IL-33$^{-/-}$ BALB/c mice were endotracheally administered AdDel70 or AdOSM. **(a)** RELMα mRNA expression in total lung homogenates 7 days post-infection. mRNA levels are expressed relative to 18S ribosomal RNA. RELMα protein levels 7 days (left panels) and 14 days (right panels) post-infection in BAL fluid assessed by **(b)** Western blot and **(c)** ELISA, and in **(d)** serum, assessed by ELISA. Each lane indicates sample extracts from separate mouse lungs. Data are expressed as mean ± SEM (n = 4-6 mice/group). Statistical significance determined by two-way ANOVA with Tukey's post hoc test ($^{**}P < 0.01$, $^{****}P < 0.0001$ between indicated groups). *(RT-PCR performed by Rex Park; ELISAs performed by Ashley Yip.)*

Figure 7

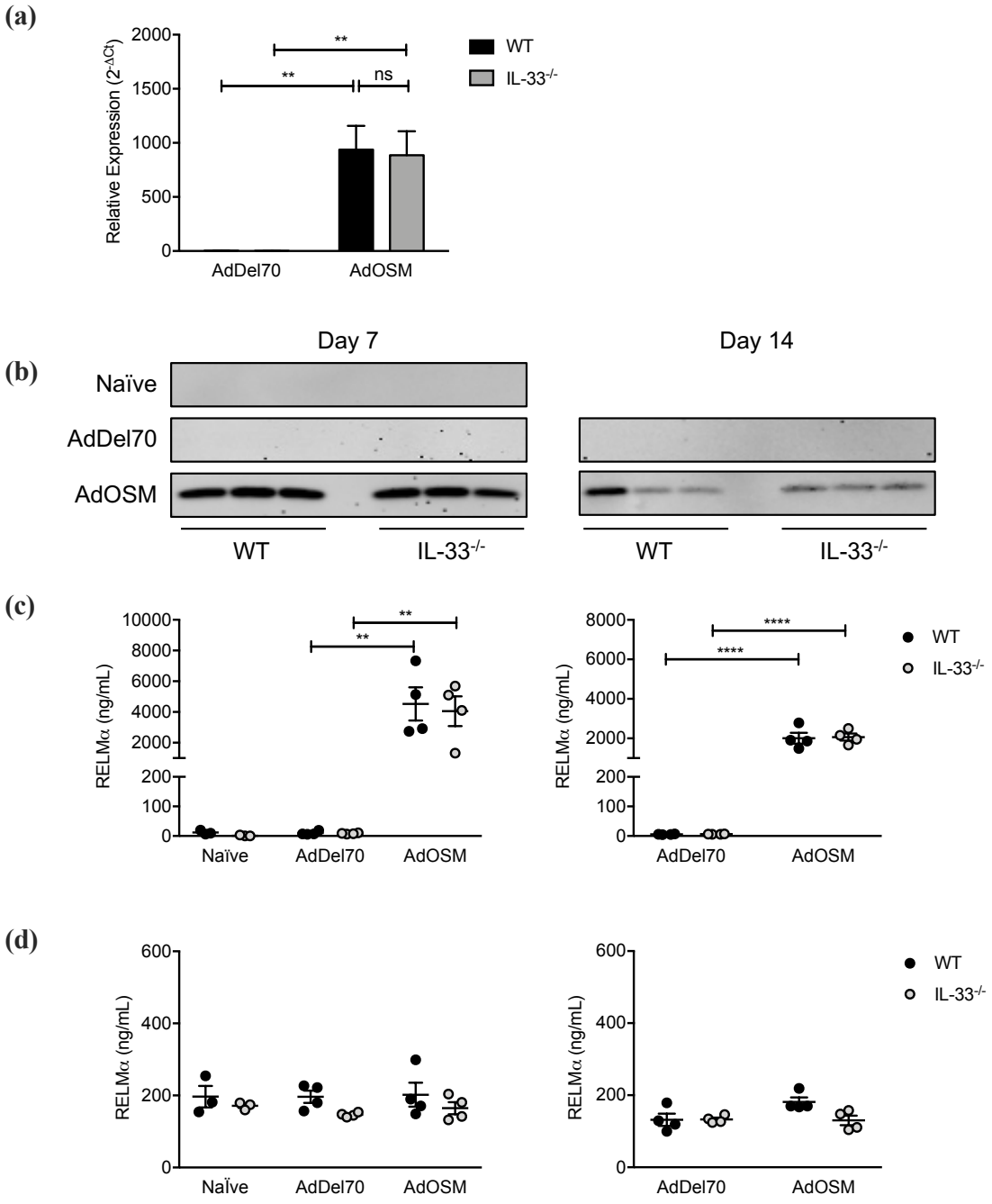
(a)
Relative Expression (2^-ΔCt)
2000
1500
1000
500
0
**
**
ns
WT
IL-33-/-
AdDel70
AdOSM
(b)
Day 7
Day 14
Naïve
AdDel70
AdOSM
WT
IL-33-/-
WT
IL-33-/-
(c)
RELMα (ng/mL)
10000
8000
6000
4000
2000
200
100
0
**
**
Naïve
AdDel70
AdOSM
8000
6000
4000
2000
200
100
0
****
****
AdDel70
AdOSM
WT
IL-33-/-
(d)
RELMα (ng/mL)
600
400
200
0
Naïve
AdDel70
AdOSM
600
400
200
0
AdDel70
AdOSM
WT
IL-33-/-

Figure 8. Chromogenic *in situ* hybridization of RELMα and IL-33 in AdDel70- and AdOSM-treated wildtype and IL-33$^{-/-}$ C57Bl/6 mice. Representative images of CISH for RELMα (turquoise) and IL-33 (red) in formalin-fixed, paraffin-embedded lung tissue sections from AdDel70- and AdOSM-treated wildtype and IL-33$^{-/-}$ C57Bl/6 mice 7 days post adenovirus infection. Colocalization of both signals is shown in AdOSM-treated wildtype sections (yellow arrowheads). Scale bars, 50 μm. (n = 5 mice/group).

Figure 8

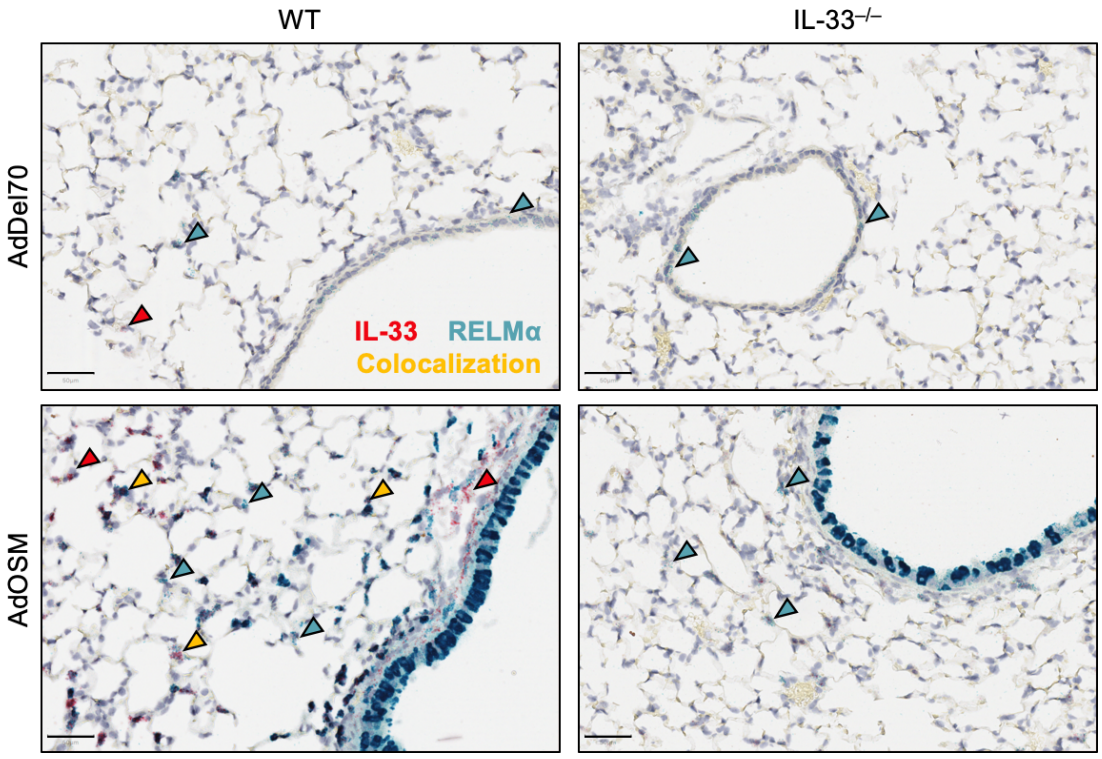

CHAPTER 4: *IN VITRO* REGULATION OF RELMA

4.1 Expression of RELMα in Bone Marrow-derived Macrophages

Given that RELMα is widely recognized as a marker of AA/M2 macrophages, we examined the *in vitro* regulation of RELMα in bone marrow-derived macrophages (BMDM). Bone marrow cells were extracted from femurs of naïve C57Bl/6 mice and differentiated into macrophages by treating with M-CSF for 7 days. BMDMs were then stimulated with either LPS/IFNγ (CA/M1 stimulus) or IL-4/IL-13 (AA/M2 stimulus) and in the presence or absence of IL-6 or IL-33 for 24 and 48 hours, as outlined in **Figure 9a**. RELMα in culture supernatants were measured by Western blot and ELISA (**Figure 9b**), and in both assays RELMα was not detectable in unstimulated cells or those stimulated with IL-6 alone or with CA/M1 cytokines. AA/M2-polarized BMDMs secreted significant amounts of RELMα, and when co-stimulated with IL-6, RELMα expression was further enhanced.

Since *in vivo* experiments using IL-33$^{-/-}$ C57Bl/6 mice demonstrated that RELMα mRNA and protein expression were reduced upon overexpression of AdOSM in the absence of IL-33, suggesting that IL-33 is an upstream regulator of RELMα, we tested whether IL-33 could also regulated RELMα expression in BMDMs *in vitro*. BMDMs derived from C57Bl/6 mice were polarized into CA/M1 or AA/M2 macrophage phenotypes and co-stimulated with IL-33 for 24 or 48 hours. After 24 and 48 hours, RELMα protein was not detectable in culture supernatants of unstimulated or CA/M1-polarized BMDMs. IL-33 alone also did not stimulate the production of RELMα, demonstrating that IL-33 cannot

directly induce RELMα in this cell type under these conditions (**Figure 9c**). AA/M2-polarized macrophages produced RELMα after 24 and 48 hours, but this was not further enhanced when cells were co-stimulated with IL-33. Thus, *in vivo*, IL-33 may be acting on a different cell population other than macrophages to regulate RELMα through an indirect pathway.

4.2 Stimulation of Alveolar Epithelial Cell Lines

Another possible source of RELMα is alveolar epithelial cells [63]. To address this, C10 type 2 alveolar epithelial and LA4 lung epithelial cell lines were stimulated for 24 hours with a number of cytokines including OSM, IL-6, LPS/IFNγ (CA/M1 stimulus) and IL-4/IL-13 (AA/M2 stimulus), alone or in combinations. However, RELMα protein in culture supernatants could not be detected by ELISA in any of the conditions (**Figure 10a**). To test if these cells were responsive to stimuli, culture supernatants were also analyzed by ELISA for MCP-1 and eotaxin-2. C10 alveolar epithelial cells responded to CA/M1 and AA/M2 stimuli with induced MCP-1 production after 24 hours, whereas LA4 epithelial cells responded to CA/M1 stimuli with significant induction of MCP-1 in comparison to unstimulated cells (**Figure 10b**). Co-stimulation of OSM with AA/M2 stimuli also induced MCP-1 production in LA4 epithelial cells. Both C10 and LA4 cells also produced eotaxin-2, but the levels were not statistically different across the treatments (**Figure 10c**).

Figure 9. Secretion of RELMα by M2-polarized bone marrow-derived macrophages. **(a)** Experimental design for stimulation of BMDMs. Bone marrow cells are harvested from femurs of wildtype C57Bl/6 mice. Cells are differentiated into macrophages by stimulating with M-CSF for 7 days, and non-adherent cells were washed off. At day 7, BMDMs were stimulated with LPS/IFNγ (classically activated/M1 stimulus) or IL-4/IL-13 (alternatively activated/M2 stimulus) and in the presence or absence of IL-6 and IL-33. 24 or 48 h after, cell culture supernatants were analyzed by ELISA for secretion of RELMα. **(b)** Secretion of RELMα in culture supernatants by CA/M1- and AA/M2-polarized BMDMs in the presence or absence of IL-6 after 24 h was measured by Western blot (left panel) and ELISA (right panel). **(c)** RELMα protein in culture supernatants by CA/M1- and AA/M2-polarized BMDMs in the presence or absence of IL-33 after 24 h (left panel) and 48 h (right panel) was measured by ELISA. Data are expressed as mean ± SEM (n = 4-6/group). Statistical significance determined by one-way ANOVA with Tukey's post hoc test ($^{****}P < 0.0001$ between indicated groups). *(Figure 9b submitted to Journal of Leukocyte Biology in the manuscript entitled "RELMα is induced by Oncostatin M in vivo and modulates extracellular matrix and cytoprotection in mouse lung inflammation.")*

Figure 9

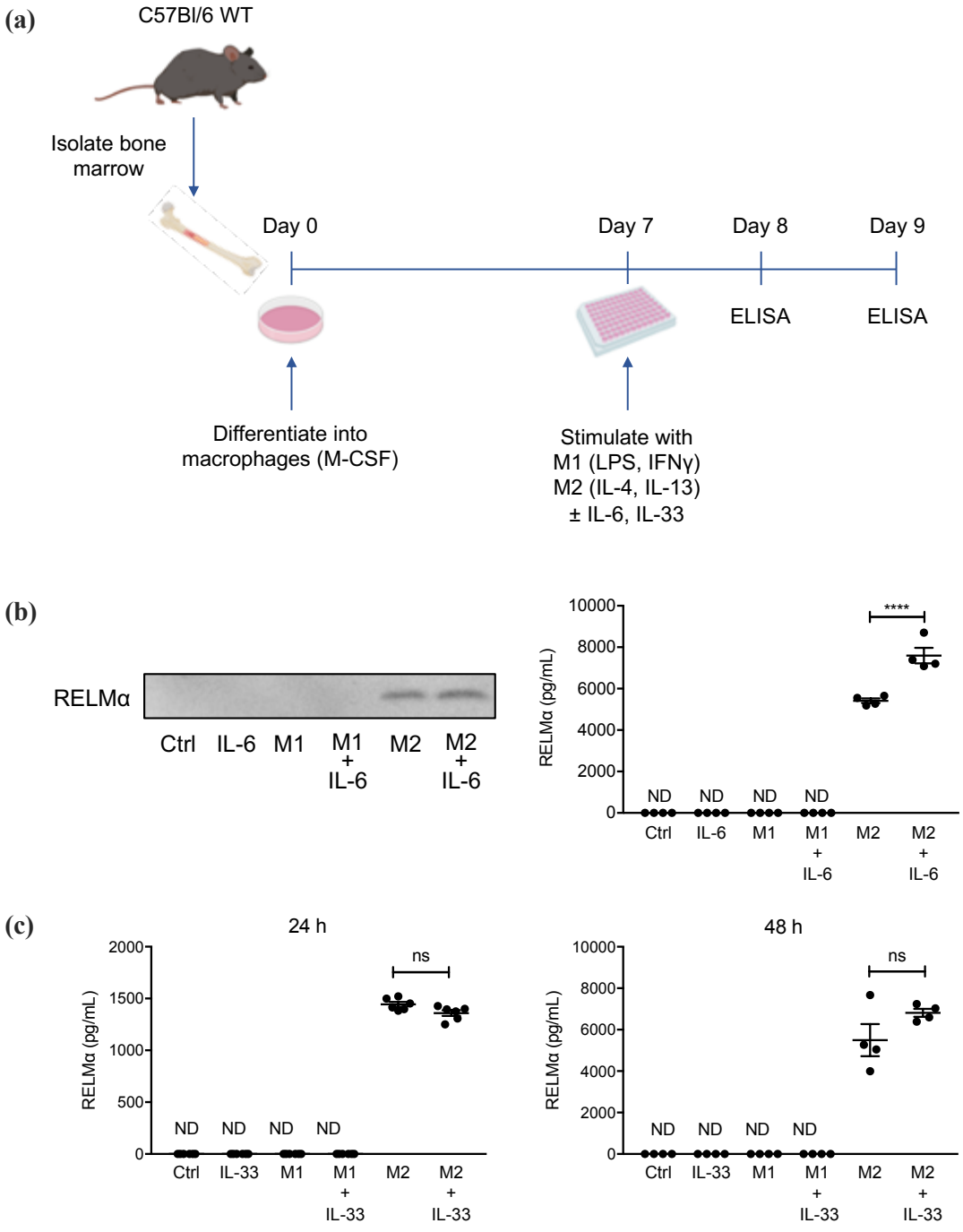
(a)
C57Bl/6 WT
Isolate bone marrow
Day 0
Day 7
Day 8
Day 9
ELISA
ELISA
Differentiate into macrophages (M-CSF)
Stimulate with M1 (LPS, IFNγ) M2 (IL-4, IL-13) ± IL-6, IL-33
(b)
RELMα
Ctrl
IL-6
M1
M1 + IL-6
M2
M2 + IL-6
RELMα (pg/mL)
10000
8000
6000
4000
2000
0
****
ND
ND
ND
ND
Ctrl
IL-6
M1
M1 + IL-6
M2
M2 + IL-6
(c)
24 h
48 h
RELMα (pg/mL)
2000
1500
1000
500
0
ns
ND
ND
ND
ND
Ctrl
IL-33
M1
M1 + IL-33
M2
M2 + IL-33

Figure 10. Stimulation of C10 and LA4 alveolar epithelial cell lines. C10 alveolar epithelial cells (left panels) and LA4 epithelial cells (right panels) were stimulated with LPS/IFNγ (CA/M1 stimulus) or IL-4/IL-13 (AA/M2 stimulus), alone or in combination with IL-6 and OSM (as indicated) for 24 h. **(a)** RELMα protein in culture supernatants were assessed by ELISA but were not detectable. **(b)** MCP-1 and **(c)** eotaxin-2 in culture supernatants were also measured by ELISA as an assessment of cell responsiveness. Data are expressed as mean ± SEM (n = 4/group). Statistical significance determined by one-way ANOVA with Tukey's post hoc test ($^{*}P < 0.01$, $^{**}P < 0.01$, $^{****}P < 0.0001$ relative to control).

Figure 10

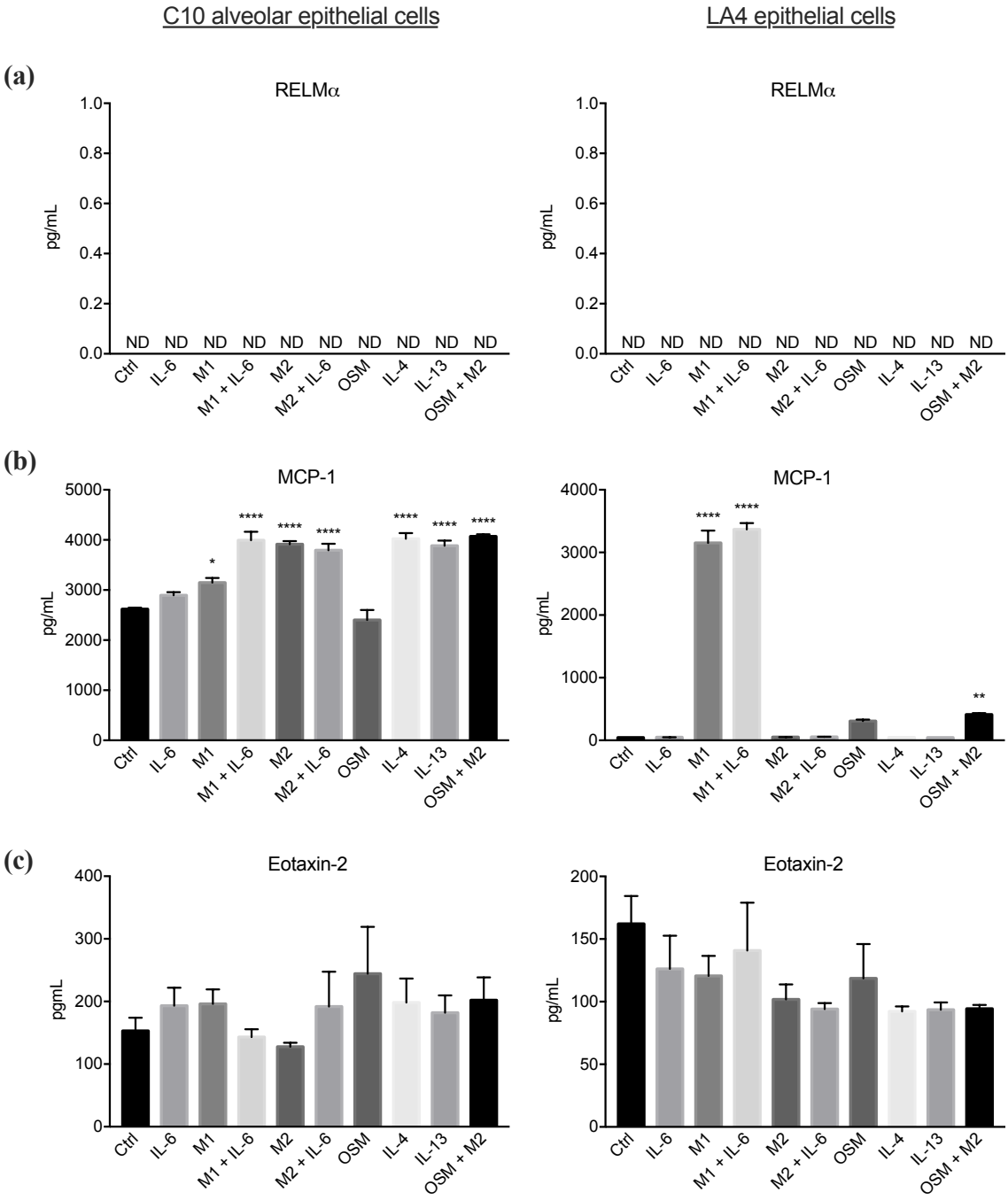
C10 alveolar epithelial cells
LA4 epithelial cells
(a)
RELMα
pg/mL
ND
Ctrl
IL-6
M1
M1 + IL-6
M2
M2 + IL-6
OSM
IL-4
IL-13
OSM + M2
(b)
MCP-1
pg/mL
(c)
Eotaxin-2
pgmL
pg/mL

CHAPTER 5: EFFECT OF RELMA IN OSM-INDUCED LUNG INFLAMMATION

Although RELMα has been implicated in mouse models of allergic airway inflammation, pulmonary fibrosis, and parasitic infection, its biological function remains unclear [52,60,69]. To address the role of RELMα in our model of lung inflammation, wildtype and RELMα$^{-/-}$ C57Bl/6 mice were endotracheally administered PBS, AdDel70, or AdOSM. Mice were culled 7 days later, at which the OSM-induced effects reached its peak. RELMα mRNA expression in whole lung homogenates was measured by NanoString analysis (**Figure 11a**), RELMα levels in BAL fluid (**Figure 11b**) and serum (**Figure 11c**) were measured by ELISA, and RELMα protein in whole lung homogenates were measured by Western blot (**Figure 11d**). In all three assay systems, RELMα mRNA and protein were not present at detectable levels in naïve, AdDel70-treated or AdOSM-treated RELMα$^{-/-}$ mice, but markedly upregulated by AdOSM in wildtype animals in comparison to control animals.

Total OSM mRNA in whole lung and protein in BAL fluid were also measured to confirm overexpression of the cytokine in AdOSM-treated animals. The absence of RELMα did not affect overexpression of adenovirus-encoded OSM mRNA or protein in whole lung (**Figure 12a, left panel**) or BAL fluid (**Figure 12c**) as assessed by NanoString or ELISA, respectively. In addition, the absence of RELMα did not alter mRNA expression of OSMRβ (**Figure 12a, right panel**) as assessed by NanoString analysis. Viral and endogenous OSM

in whole lung were also measured by RT-PCR (**Figure 12b**), and mRNA expression of viral OSM showed similar trends as total OSM expression assessed by NanoString analysis. Of note, viral and endogenous OSM mRNA expression were measured on separate PCR plates and cannot be compared directly. Serum OSM levels were also measured by ELISA but were not detectable in any of the treatments (**Figure 12d**).

Cells were recovered from BAL fluid, cytocentrifuged and stained for differential cell analysis. Macrophage, eosinophil, neutrophil, and lymphocyte populations were counted as an indication of immune cell infiltration upon adenovirus infection. Consistent with previous findings [40], AdOSM-treated wildtype mice demonstrated accumulation of eosinophils, lymphocytes, and neutrophils in BAL fluid in comparison to naïve or AdDel70-treated animals (**Figure 13**). However, RELMα-deficiency did not affect the accumulation of these immune cell populations detected at day 7. Interestingly, differential cell counts in BAL fluid revealed an additional population of cells that morphologically appeared to be dead cells (**Figure 14a**). This population was enumerated and designated as "dead cells" (**Figure 14b**). These cells were observed at significantly higher counts in RELMα$^{-/-}$ mice treated with AdOSM in comparison to wildtype controls. To examine possible indicators of cell death, a lactate dehydrogenase (LDH) assay was performed on BAL fluid. This assay measures the release of the enzyme LDH as an indication of necrosis since necrotic cells are characterized by membrane permeabilization. In naïve and AdDel70-treated wildtype and RELMα$^{-/-}$ mice, LDH levels were similar to the background signal (PBS alone) (**Figure 14c**). The levels of LDH in BAL fluid were significantly

increased in wildtype animals treated with AdOSM, and was further enhanced in RELMα$^{-/-}$ mice.

Based on *in vitro* experiments, we show that RELMα can be expressed by BMDMs (**Figure 9**). Next, we examined whether RELMα could be expressed by macrophages in the lung. Lung tissues harvested at day 7 post-infection were analyzed by CISH and stained for RELMα and CD68, a marker of macrophages. As expected, RELMα mRNA was not detected in knockout mouse sections (**Figure 15a, lower panels**). CD68^{+} RELMα^{-} cells were found throughout the parenchyma across all treatments. RELMα^{+} CD68^{-} cells were found in the airway epithelium of naïve and AdDel70-treated wildtype lung sections, and upon AdOSM infection, cells in the lung parenchyma and airway epithelium highly expressed RELMα mRNA (**Figure 15a, upper panels**). In the lung parenchyma of AdOSM-treated wildtype mice, CD68^{+} RELMα^{+} macrophages were also observed, as demonstrated by colocalization of both stains (**Figure 15b, left panel**).

Lung tissue sections were also stained for RELMα and IL-33 by CISH. In AdDel70-treated wildtype lungs, RELMα mRNA expression was observed in some cells of the airway epithelium, whereas IL-33 mRNA was localized to cells of the lung parenchyma (**Figure 16, upper panel**). After AdOSM treatment, columnar airway epithelial cells highly expressed RELMα mRNA, as well as cells in the lung parenchyma (**Figure 16, lower panel**). IL-33^{+} cells were observed in the basement membrane of the airway epithelium and

also throughout the lung parenchyma. RELMα^{+} IL-33^{+} cells could also be seen distributed throughout the lung parenchyma, as demonstrated by colocalized of both stains.

We next examined whether RELMα would affect the accumulation of AA/M2 macrophages in lungs treated with AdOSM by flow cytometry. Macrophages were classified as CD45^{+} (hematopoietic cell marker), F4/80^{+} (macrophage marker), and either CD206^{+} (AA/M2 macrophage marker) or CD38^{+} (CA/M1 macrophage marker). Similar to previous observations [40], AdOSM induced the accumulation of CD206^{+} CD38^{-} AA/M2 macrophages in the lung at day 7 (**Figure 17b**), and CD38^{+} CD206^{-} CA/M1 macrophages also accumulated in the lung following AdOSM treatment (**Figure 17c**). In the absence of RELMα, there was approximately 60% reduction in total numbers of CD206^{+} AA/M2 macrophages in the AdOSM group in comparison to wildtype counterparts, whereas there was no significant effect of RELMα-deficiency on CD38^{+} CA/M1 macrophage accumulation.

Th1 cells were identified through flow cytometry as CD45^{+}, CD3^{+} (T cell marker), CD4^{+} (T helper cell marker), and IFNγ^{+} (Th1 cell marker). At day 7, AdOSM markedly induced the accumulation of IFNγ-producing Th1 cells in the lungs of both wildtype and RELMα$^{-/-}$ mice, with 40% fewer total IFNγ^{+} Th1 cells in knockout animals in comparison to wildtypes (**Figure 18b, right panel**). In correlation with the IFNγ^{+} Th1 cell population as assessed by flow cytometry, IFNγ mRNA in total lung was upregulated, albeit to a low extent (2-fold), by AdOSM treatment in wildtype animals, but in RELMα$^{-/-}$ mice its gene

expression was similar across all treatment groups (**Supplementary Figure 1**). Other genes associated with Th1 inflammation (IFNβ, IFNAR, and IFIT1) were not differentially expressed between wildtype and RELMα$^{-/-}$ mice in whole lung, as assessed by NanoString analysis (**Supplementary Figure 1**).

We did not observe significant changes of Th2-associated inflammatory cytokine mRNA expression as a result of RELMα-deficiency (**Figure 19**). AdOSM upregulated similar levels of MCP-1, IL-4, IL-5, IL-6, and IL-33 mRNA after 7 days in both wildtype and RELMα$^{-/-}$ mice. mRNA expression of IL-4Rα were similar across all treatments (**Supplementary Figure 1**). Consistent with our previous findings [40], AdOSM induced Arg1 mRNA, but its expression was significantly reduced in the absence of RELMα. Together with flow cytometry of CD206^{+} macrophages (**Figure 17**), this suggests a potential role for RELMα in maximizing the accumulation of AA/M2 macrophages.

We have previously demonstrated that pulmonary overexpression of OSM can induce ECM deposition in C57Bl/6 mice. We therefore examined the role of RELMα in OSM-induced ECM accumulation by analysis of gene expression. Consistent with our previous findings [14], genes implicated in ECM remodeling COL1A1, COL3A1, MMP13, and TIMP1 were upregulated in lungs of AdOSM-treated wildtype mice at day 7 (**Figure 20**). Similar trends were observed in RELMα$^{-/-}$ mice; however, expression of these genes was significantly reduced in the absence of RELMα, suggesting that ECM accumulation induced by OSM may be regulated in part through RELMα.

Protein expression of cell signaling molecules and cytokines were analyzed by Western blot. Whole lung homogenates from wildtype and RELMα$^{-/-}$ mice treated with AdOSM or AdDel70 were probed for pSTAT3, Arg1, IL-33, cytokeratin 18 (CK18), and actin as the loading control (**Figure 21a**). Densitometric analysis of signals (**Figure 21b**) showed that pSTAT3, IL-33, and CK18 were induced in AdOSM treatments relative to AdDel70-treated controls, but were not differentially detected between wildtype and RELMα$^{-/-}$ mice, consistent with IL-33 mRNA expression (**Figure 19**). Arg1 protein expression in AdOSM-treated RELMα$^{-/-}$ mice were lower than in wildtype mice, however this was not statistically significant due to variability within treatment groups, but similar to trends detected at the mRNA level by NanoString analysis (**Figure 19**). CK18 in BAL fluid was analyzed by Western blot and signals were quantified by densitometry (**Figure 21c, d**) and normalized to Ym1 levels in BAL fluid since levels were consistent in both AdOSM-treated wildtype and RELMα$^{-/-}$ mice (**Figure 22**). CK18 levels in BAL fluid of RELMα$^{-/-}$ mice were markedly elevated in comparison to wildtype mice treated with AdOSM.

BAL fluid was assessed by ELISA for proteins elevated in Th2 inflammation including Ym1, eotaxin-2, and IL-5 (**Figure 22**). In addition to RELMα , Ym1 is another protein that is widely recognized as a marker of AA/M2 macrophages [65]. In naïve and AdDel70-treated wildtype and RELMα$^{-/-}$ mice, Ym1 was detected at basal levels of ~500 ng/mL. Upon AdOSM treatment, Ym1 was significantly induced to as high as ~6000 ng/mL, however the absence of RELMα did not alter OSM-induced Ym1. Similar trends were observed with eotaxin-2, where low levels were detected by ELISA in naïve and AdDel70-

treated mice, and AdOSM induced similar levels of eotaxin-2 in both wildtype and RELMα$^{-/-}$ mice. IL-5 protein levels in BAL fluid were not statistically different across treatments.

Lung tissue sections from AdDel70- and AdOSM-treated wildtype and RELMα$^{-/-}$ mice were examined by histological analyses to determine the effects of RELMα on cell proliferation, goblet cell hyperplasia, and accumulation of αSMA. Formalin-fixed, paraffin-embedded lung tissue sections stained with H&E showed thickening of the airway epithelium in AdOSM-treated wildtype mouse lungs, which was reduced in RELMα-deficient animals (**Figure 23a**, high magnification images of AdOSM-treated lung sections shown in **Figure 24a**). These sections were stained with the cell proliferation marker Ki67 to determine whether airway thickness was due to increased proliferating epithelial cells, however, there did not appear to be obvious differences in Ki67^{+} cells in the epithelium between wildtype and RELMα$^{-/-}$ mice at day 7 (**Figure 23b**). Quantification of Ki67^{+} cells in these sections did show that AdOSM-treated lungs had a greater proportion of Ki67^{+} cells around the airways and throughout the lung parenchyma, whereas in the absence of RELMα there was a significant reduction in proliferating cells (**Figure 23e**). PAS staining, an indicator of mucous-producing goblet cells, indicated increased numbers of goblet cells in the epithelium of AdOSM-treated mouse lungs, however we did not observe striking differences between wildtype and RELMα$^{-/-}$ animals (**Figure 23c**). Lung tissues were stained for αSMA (**Figure 23d**), and analysis of parenchymal cells in entire lung sections, excluding major airways and blood vessels, revealed that AdOSM induced the

accumulation of αSMA$^+$ cells in the lung parenchyma of wildtype mice (**Figure 23f**, entire lung tissue sections of AdOSM-treated lungs shown in **Figure 24b**). In RELMα$^{-/-}$ mice treated with AdOSM there were significantly less αSMA$^+$ staining. These sections were also stained for PSR as an assessment of collagen accumulation (**Figure 24c**), however at day 7 in preliminary examination, not quantified, we did not observe striking differences in PSR staining between wildtype and RELMα$^{-/-}$ mouse lungs.

Other studies have shown that among the RELM family of proteins, RELMα lacks a cysteine residue in the N-terminus which is responsible for forming disulfide bonds and higher order (hexamer) complex formations by resistin and RELMβ [66,86]. Day 7 BAL fluid from AdDel70-treated wildtype and AdOSM-treated wildtype and RELMα$^{-/-}$ mice were analyzed by Western blot under reducing and non-reducing conditions to examine structural properties of RELMα. Under reducing conditions, a single band for RELMα was detected at the expected size (~9.4 kDa) in BAL fluid from AdOSM-treated wildtype mice, but under non-reducing conditions RELMα signal was detected as multiple bands ranging from 10-70 kDa, which were absent in BAL fluid of AdOSM-treated RELMα$^{-/-}$ mice (**Figure 25**).

Since RELMα has not been identified in humans yet, and RELMβ is the closest human homolog for murine RELMα, we examined whether mouse RELMβ was regulated in our model of OSM-mediated lung inflammation. Similar to RELMα mRNA expression in whole lung, RELMβ was expressed at low levels in AdDel70-treated wildtype and IL-33$^-$

$^{/-}$ mice, assessed by RT-PCR. In wildtype C57Bl/6 mice, AdOSM upregulated RELMβ expression at day 7 and in the absence of IL-33, its expression was reduced (**Supplementary Figure 2a, left panel**). A similar trend was observed in AdOSM-treated wildtype BALB/c mice, but RELMβ expression was not altered in IL-33$^{-/-}$ BALB/c mice (**Supplementary Figure 2a, right panel**).

In the experiment assessing wildtype vs RELMα$^{-/-}$ mice, RELMβ mRNA expression was markedly upregulated in whole lung extracts of AdOSM-treated wildtype C57Bl/6 mice, assessed by NanoString analysis, consistent with **Supplementary Figure 2a, left panel** assessed by TaqMan® assay. In RELMα$^{-/-}$ mice treated with AdOSM, RELMβ was induced to a much lower extent than in wildtype counterparts at day 7 (**Supplementary Figure 2b**). Lung tissue sections from AdDel70- and AdOSM-treated wildtype and RELMα$^{-/-}$ mice at day 7 were analyzed by CISH and stained for OSM and RELMβ mRNA. OSM^{+} cells could be observed in some cells of the airway epithelium and throughout the lung parenchyma in AdOSM-treated mouse lung sections (**Supplementary Figure 2c, lower panels**). RELMβ^{+} cells were localized in the airway epithelium, and unlike RELMα, parenchymal cells did not express RELMβ. We could not detect OSM and RELMβ mRNA colocalization.

Figure 11. RELMα expression in wildtype and RELMα$^{-/-}$ mice. Wildtype and RELMα$^{-/-}$ mice were endotracheally administered PBS, AdDel70 or AdOSM. **(a)** Total lung mRNA expression of RELMα 7 days post-infection analyzed by NanoString Technologies. Gene expression levels are normalized to housekeeping genes ACTB and PGK1. RELMα protein in **(b)** BAL fluid and **(c)** serum were quantified by ELISA. Data are expressed as mean ± SEM (n = 5 mice/group). Statistical significance was determined by two-way ANOVA with Tukey's post hoc test ($^{****}P < 0.0001$ between indicated groups). **(d)** Total lung homogenates were probed by Western blot for RELMα protein. Each lane (dot) indicates sample extracts from separate mouse lungs. (n = 3-4 mice/group). *(ELISAs performed by Ashley Yip. Submitted to Journal of Leukocyte Biology in the manuscript entitled "RELMα is induced by Oncostatin M in vivo and modulates extracellular matrix and cytoprotection in mouse lung inflammation.")*

Figure 11

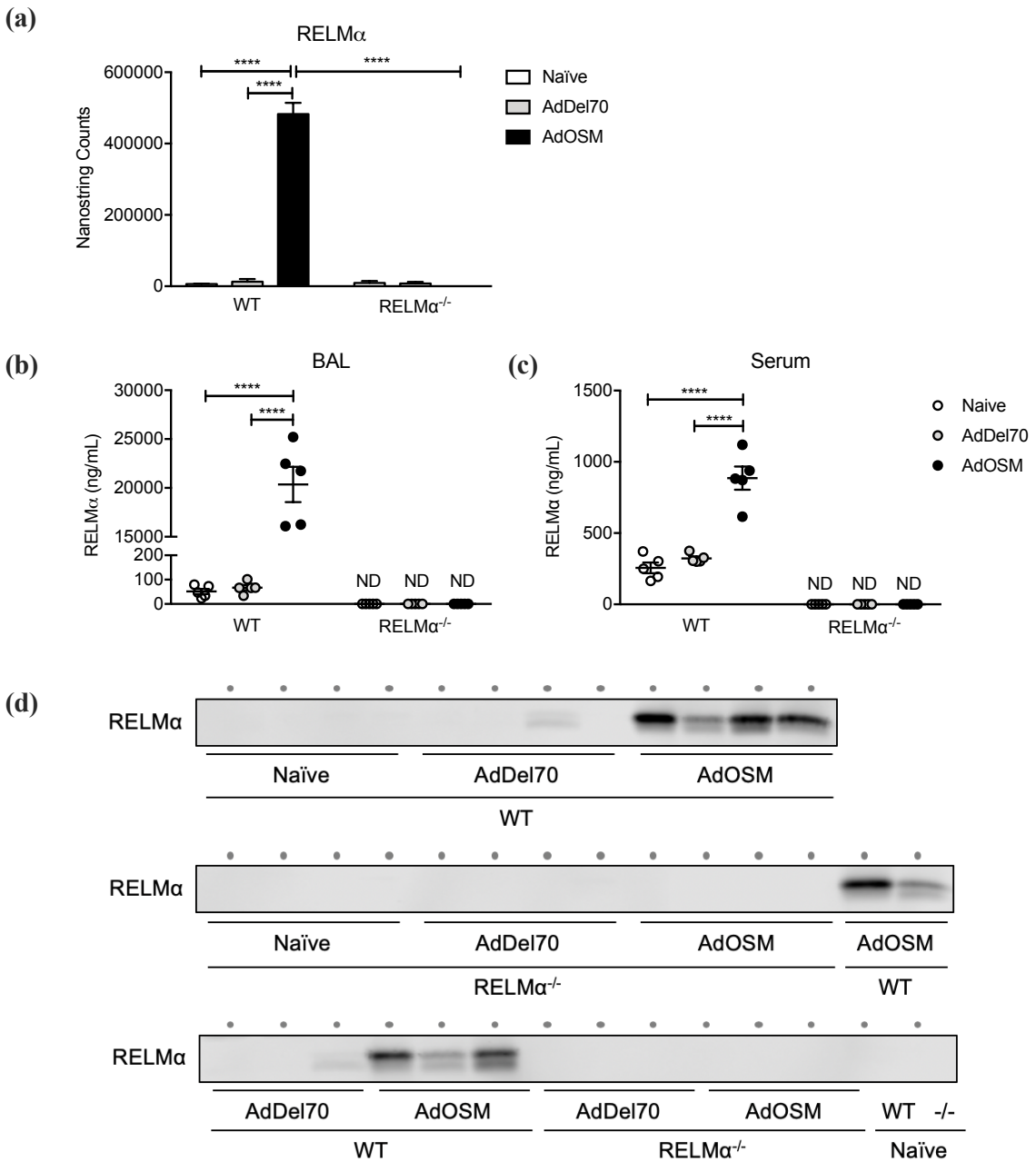
(a)
RELMα
Nanostring Counts
600000
400000
200000
0
****
****
****
Naïve
AdDel70
AdOSM
WT
RELMα-/-
(b)
BAL
RELMα (ng/mL)
30000
25000
20000
15000
200
100
0
ND ND ND
WT
RELMα-/-
(c)
Serum
RELMα (ng/mL)
1500
1000
500
0
Naive
AdDel70
AdOSM
(d)
RELMα
Naïve
AdDel70
AdOSM
WT
RELMα
Naïve
AdDel70
AdOSM
AdOSM
RELMα-/-
WT
RELMα
AdDel70
AdOSM
AdDel70
AdOSM
WT
-/-
WT
RELMα-/-
Naïve

Figure 12. RELMα-deficiency does not alter OSM overexpression by AdOSM vector. **(a)** Total lung mRNA expression of OSM and OSMRβ 7 days post adenovirus infection, analyzed by NanoString Technologies. Gene expression levels are normalized to housekeeping genes ACTB and PGK1. **(b)** Viral and endogenous OSM mRNA expression analyzed by RT-PCR. mRNA levels are expressed relative to 18S ribosomal RNA. **(c)** OSM protein in BAL fluid were quantified by ELISA, and was not detectable in naïve or AdDel70-treated animals. **(d)** OSM protein could not be detected in serum by ELISA. Data are expressed as mean ± SEM (n = 5 mice/group). Statistical significance was determined by two-way ANOVA with Tukey's post hoc test ($^{*}P < 0.05$, $^{****}P < 0.0001$ between indicated groups; $^{\S}P < 0.05$ relative to the limit of detection of the assay). *(ELISAs performed by Ashley Yip. Submitted to Journal of Leukocyte Biology in the manuscript entitled "RELMα is induced by Oncostatin M in vivo and modulates extracellular matrix and cytoprotection in mouse lung inflammation.")*

Figure 12

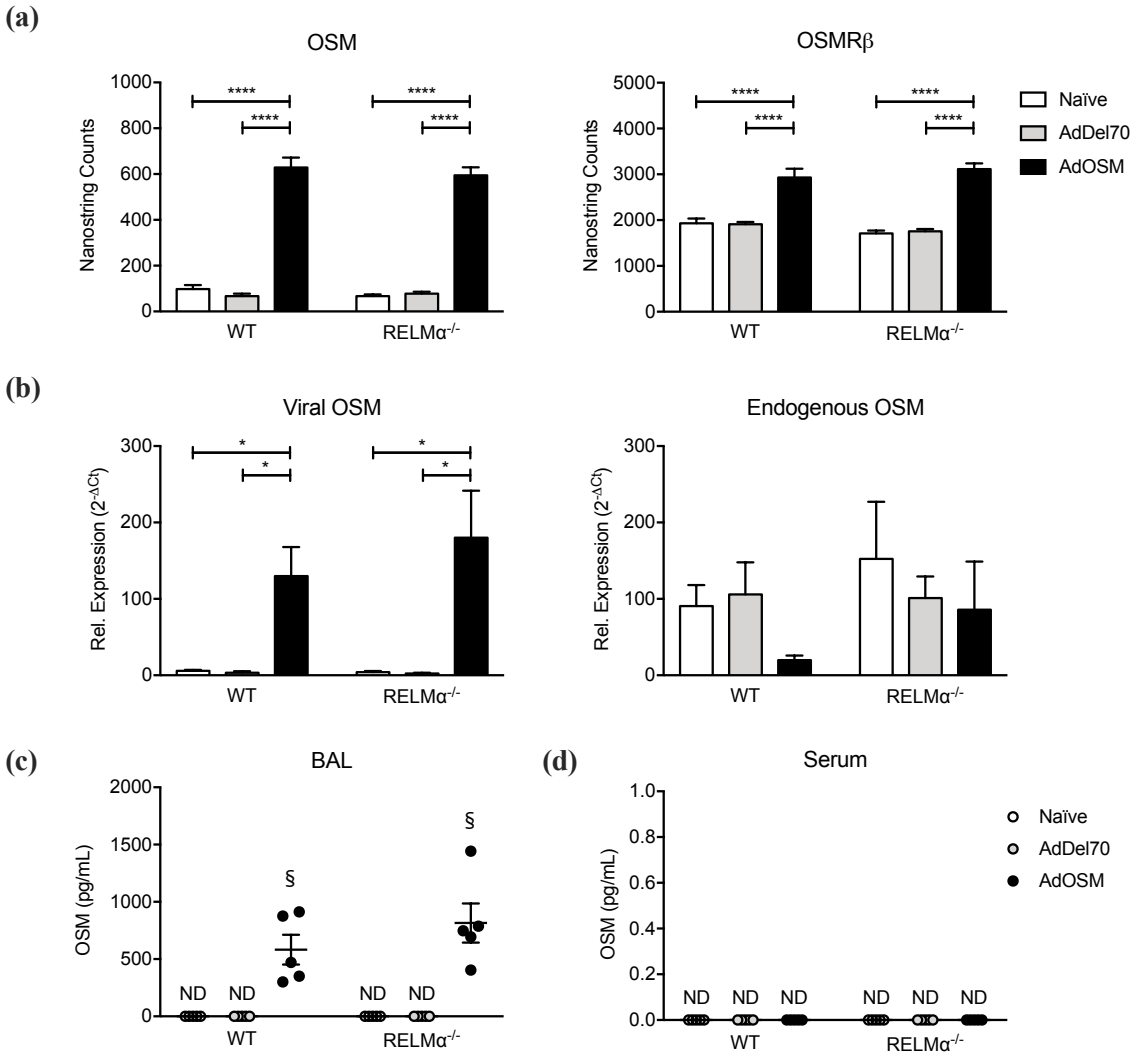
(a)
OSM
OSMRβ
Nanostring Counts
1000
800
600
400
200
0
5000
4000
3000
2000
1000
****
WT
RELMα-/-
Naïve
AdDel70
AdOSM
(b)
Viral OSM
Endogenous OSM
Rel. Expression (2-ΔCt)
300
200
100
0
*
(c)
BAL
OSM (pg/mL)
2000
1500
1000
500
§
ND
(d)
Serum
1.0
0.8
0.6
0.4
0.2
0.0

Figure 13. BAL fluid differential cell counts in naïve, AdDel70- and AdOSM-treated wildtype and RELMα$^{-/-}$ mice. 7 days post adenovirus infection with AdDel70 or AdOSM, cells recovered from BAL fluid were cytocentrifuged and stained with Hema-3 fixative. Macrophages, eosinophils, neutrophils and lymphocytes were enumerated in cytocentrifuge smears and shown as **(a)** total cells and **(b)** percentage of total BAL fluid cells. Data are expressed as mean ± SEM (n = 5 mice/group). Statistical significance was determined by two-way ANOVA with Tukey's post hoc test ($^{*}P < 0.05$, $^{**}P < 0.01$, $^{****}P <$ 0.0001 between indicated groups). *(Figure 13a submitted to Journal of Leukocyte Biology in the manuscript entitled "RELMα is induced by Oncostatin M in vivo and modulates extracellular matrix and cytoprotection in mouse lung inflammation.")*

Figure 13

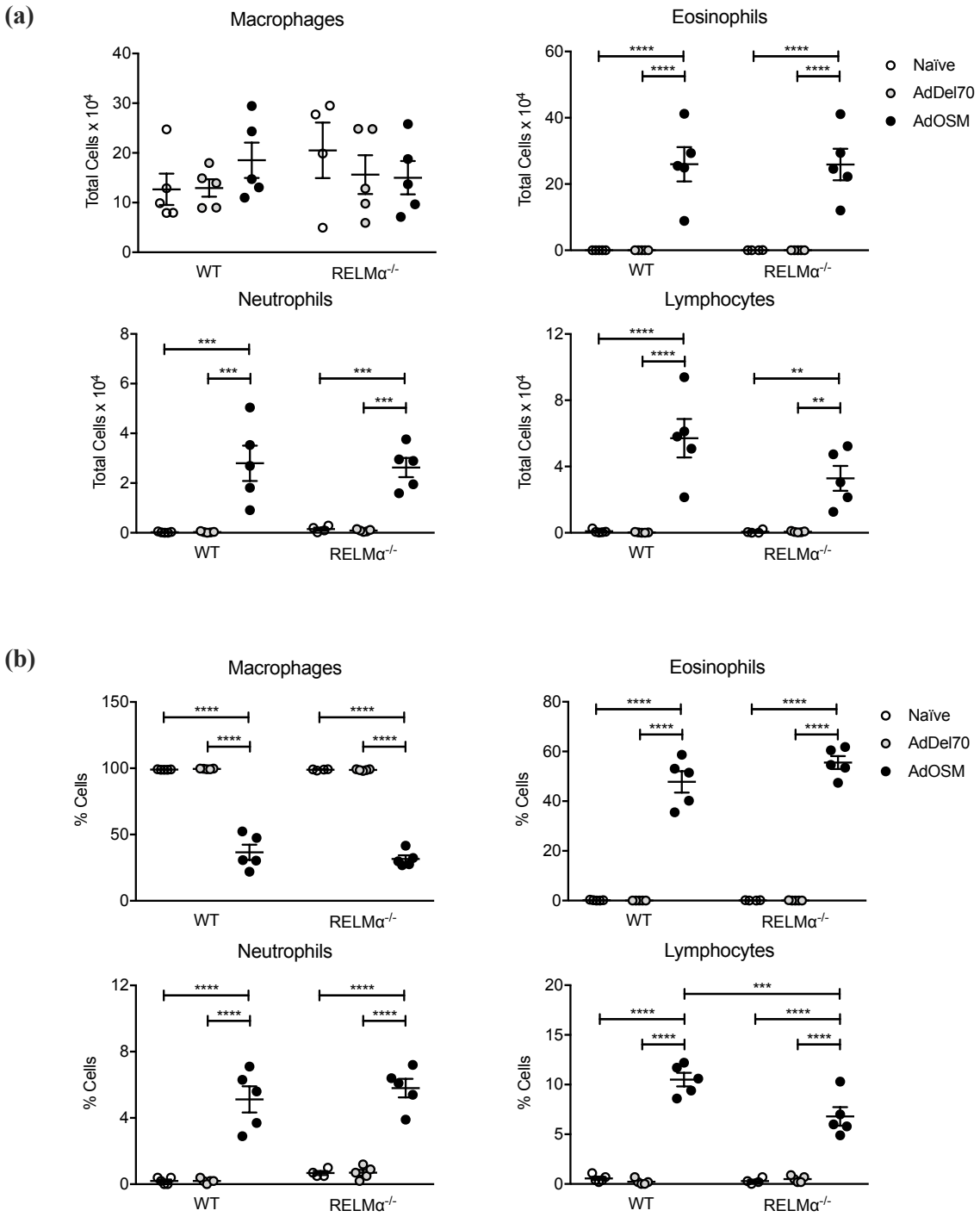
(a)
Macrophages
Eosinophils
Neutrophils
Lymphocytes
Total Cells x 10^4
WT
RELMα-/-
Naïve
AdDel70
AdOSM
(b)
% Cells

Figure 14. RELMα$^{-/-}$ mice may be more susceptible to cell death upon AdOSM treatment. Cells recovered from BAL fluid 7 days post adenovirus infection were cytocentrifuged and stained with Hema-3 fixative solutions. **(a)** Representative images of cytospin slides from AdDel70- and AdOSM-treated wildtype and RELMα$^{-/-}$ mice. In the BAL fluid of AdOSM-treated RELMα$^{-/-}$ mice, we observed a subset of cells that morphologically appeared to be dead cells (red arrowheads). These cells were designated as "Dead cells" and quantified in **(b)**. **(c)** An LDH assay was performed on BAL fluid as a measure of cell death. Data are expressed as mean ± SEM (n = 5 mice/group). Statistical significance was determined by two-way ANOVA with Tukey's post hoc test ($^{****}P <$ 0.0001 between indicated groups). *(LDH assay performed by Preksha Rathod. Submitted to Journal of Leukocyte Biology in the manuscript entitled "RELMα is induced by Oncostatin M in vivo and modulates extracellular matrix and cytoprotection in mouse lung inflammation.")*

Figure 14

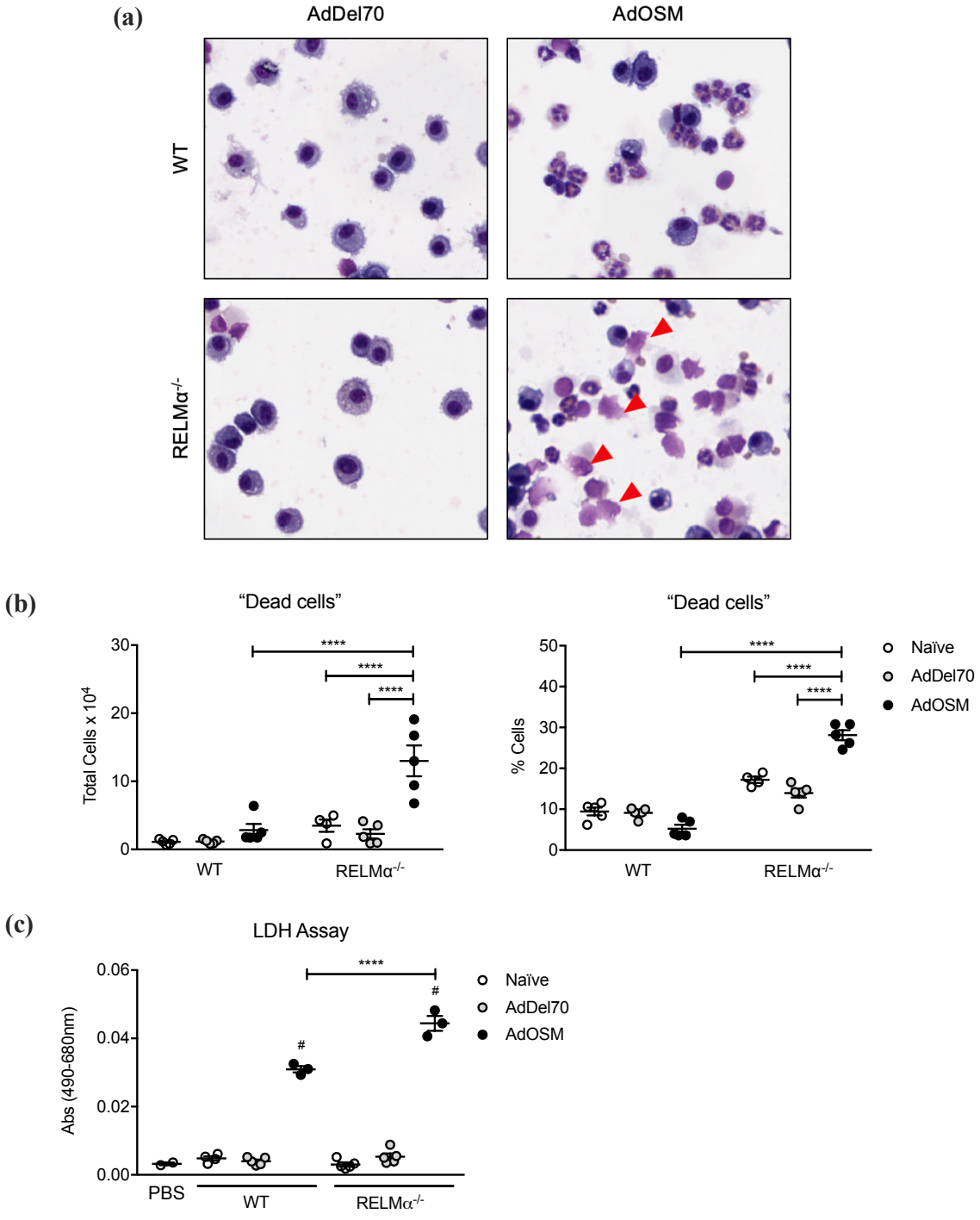
(a)
AdDel70
AdOSM
WT
RELMα-/-
(b)
"Dead cells"
Total Cells x 10^4
WT
RELMα-/-
"Dead cells"
% Cells
Naïve
AdDel70
AdOSM
(c)
LDH Assay
Abs (490-680nm)
PBS
WT
RELMα-/-

Figure 15. Colocalization of RELMα and CD68, a macrophage marker, in AdOSM-treated wildtype lung tissue. Representative images are shown of CISH for RELMα and CD68 in formalin-fixed, paraffin-embedded lung tissue sections from naïve, AdDel70- or AdOSM-treated wildtype or RELMα$^{-/-}$ mice (as indicated) at day 7. **(a)** RELMα (turquoise) and CD68 (red) mRNA signals shown as punctate dots unless at very high levels in which signals converge. **(b)** High magnification images of indicated regions from AdOSM-treated mouse lungs from **(a)**, and colocalization of both signals (yellow arrowheads) in wildtype mice. Scale bars, 50 μm. (n = 5 mice/group). *(Submitted to Journal of Leukocyte Biology in the manuscript entitled "RELMα is induced by Oncostatin M in vivo and modulates extracellular matrix and cytoprotection in mouse lung inflammation.")*

Figure 15

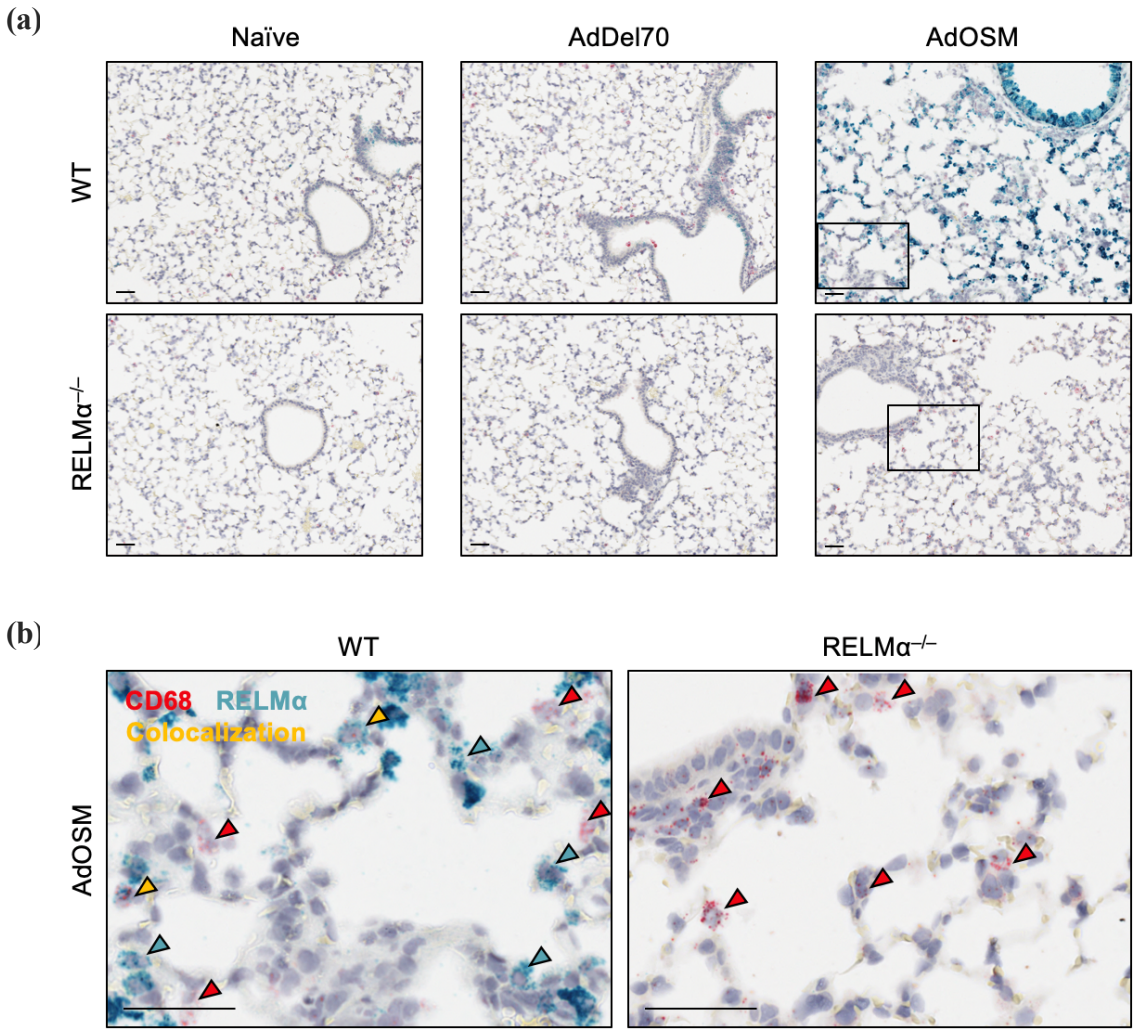
(a)
Naïve
AdDel70
AdOSM
WT
RELMα−/−
(b)
WT
RELMα−/−
AdOSM
CD68
RELMα
Colocalization

Figure 16. Colocalization of RELMα and IL-33 in AdOSM-treated wildtype lung tissue. Representative images of CISH for RELMα (turquoise) and IL-33 (red) in formalin-fixed, paraffin-embedded lung tissue sections from AdDel70- and AdOSM-treated wildtype and RELMα$^{-/-}$ C57Bl/6 mice 7 days post adenovirus infection. Colocalization of both signals is shown in AdOSM-treated wildtype lung sections (yellow arrowheads). Scale bars, 50 μm. (n = 5 mice/group).

Figure 16

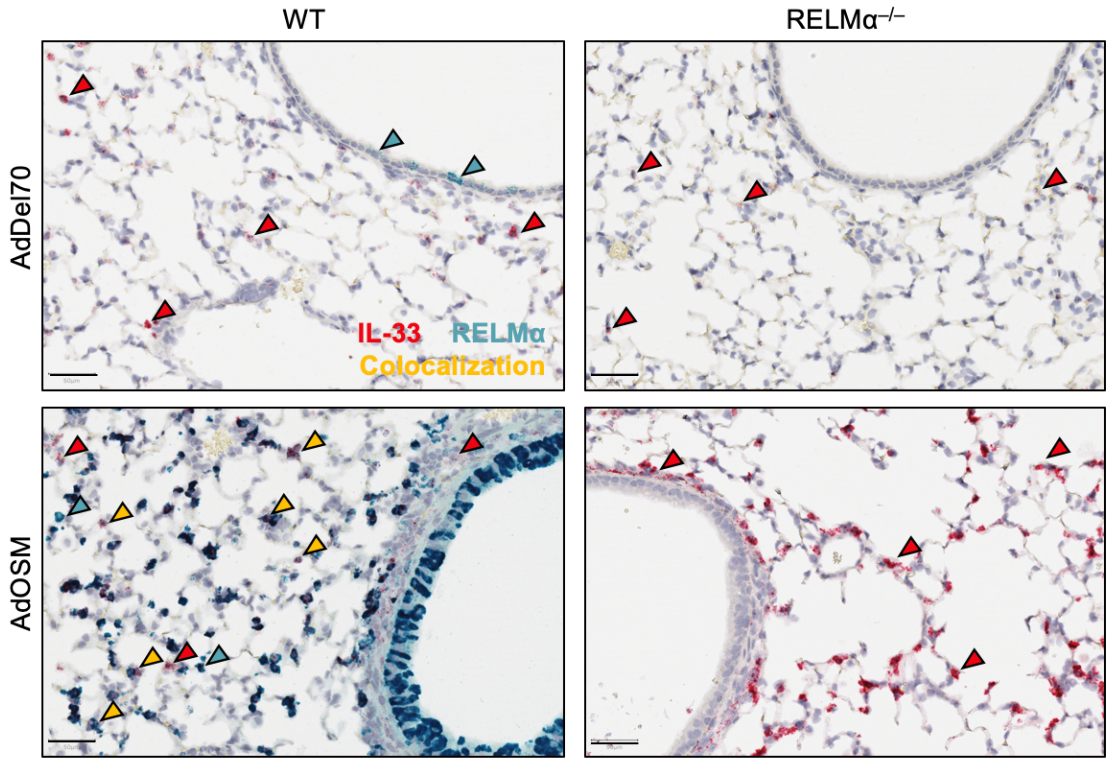

Figure 17. Reduced CD206^{+} alternatively activated macrophage numbers in total lung of AdOSM-treated RELMα$^{-/-}$ mice. Lung tissue cells were harvested 7 days post-infection and analyzed for macrophage accumulation by flow cytometry. Macrophages were identified as CD45^{+} F4/80^{+}. **(a)** Representative FACS plots showing gating strategy of F4/80^{+} macrophages and percent and total **(b)** CD206^{+} AA/M2 macrophages or **(c)** CD38^{+} CA/M1 macrophages. Data are represented as mean ± SEM (n = 5 mice/group). Statistical significance was determined by two-way ANOVA with Tukey's post hoc test ($^{*}P < 0.05$, $^{***}P < 0.001$ between indicated groups). *(Submitted to Journal of Leukocyte Biology in the manuscript entitled "RELMα is induced by Oncostatin M in vivo and modulates extracellular matrix and cytoprotection in mouse lung inflammation.")*

Figure 17

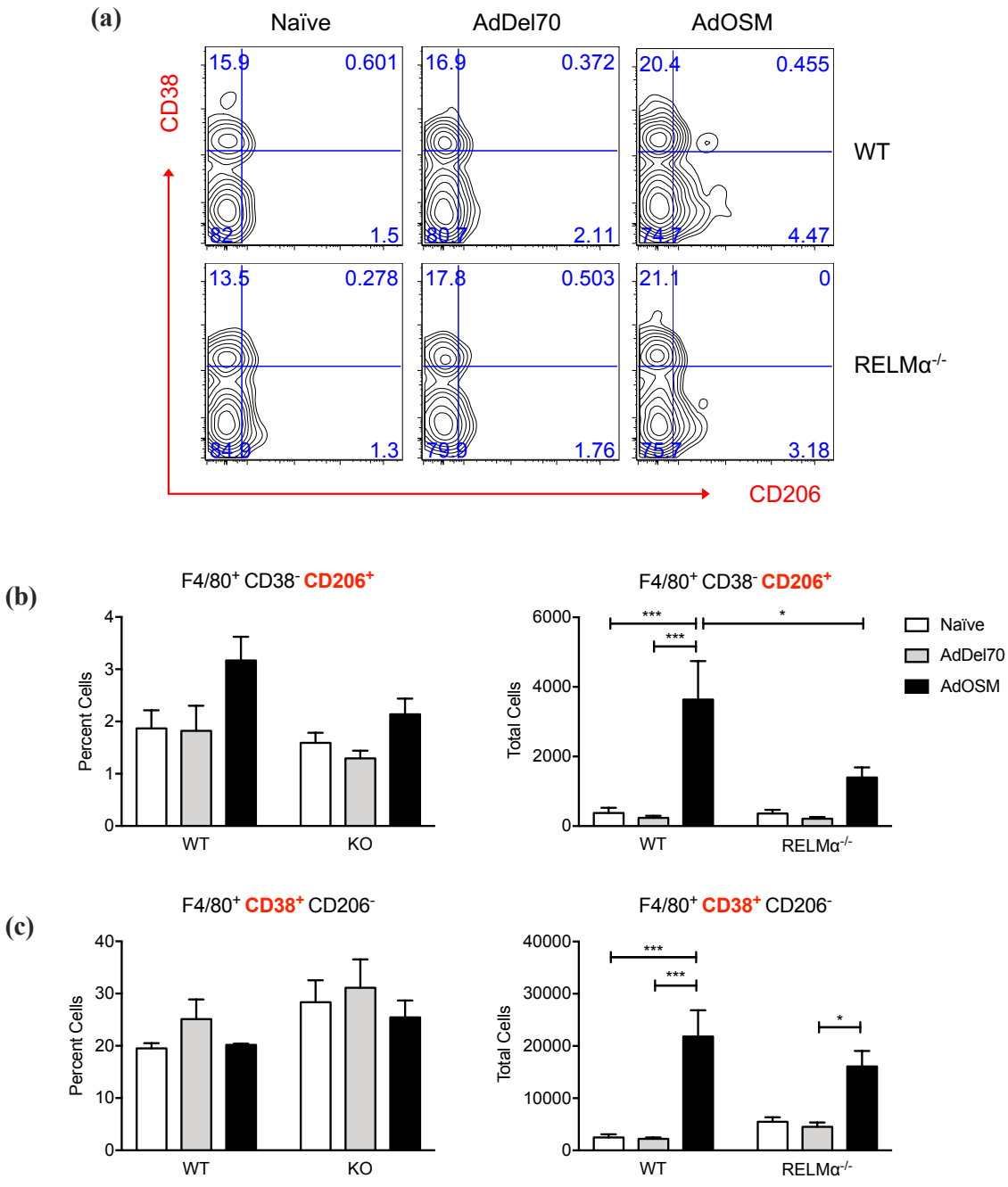
(a)
Naïve
AdDel70
AdOSM
CD38
CD206
WT
RELMα-/-
15.9
0.601
82.1
1.5
16.9
0.372
80.7
2.11
20.4
0.455
74.7
4.47
13.5
0.278
84.9
1.3
17.8
0.503
79.9
1.76
21.1
0
75.7
3.18
(b)
F4/80+ CD38- CD206+
Percent Cells
WT
KO
Total Cells
RELMα-/-
Naïve
AdDel70
AdOSM
(c)
F4/80+ CD38+ CD206-

Figure 18. Reduced IFNγ-producing $CD4^+$ Th1 cells in total lung of AdOSM-treated RELMα$^{-/-}$ mice. Lung tissue cells harvested 7 days post-infection were analyzed for T cell accumulation by flow cytometry. Cells were stimulated with PMA and ionomycin for 4 hours prior to flow cytometric analysis. Th cells were identified as $CD45^+$ $CD3^+$ $CD19^-$ $CD4^+$. **(a)** Representative FACS plots showing gating strategy and **(b)** percent and total IFNγ-producing $CD4^+$ Th1 cells. Data are represented as mean ± SEM (n = 5 mice/group). Statistical significance was determined by two-way ANOVA with Tukey's post hoc test ($^*P < 0.05$, $^{**}P < 0.01$, $^{***}P < 0.001$, $^{****}P < 0.0001$ between indicated groups). *(Submitted to Journal of Leukocyte Biology in the manuscript entitled "RELMα is induced by Oncostatin M in vivo and modulates extracellular matrix and cytoprotection in mouse lung inflammation.")*

Figure 18

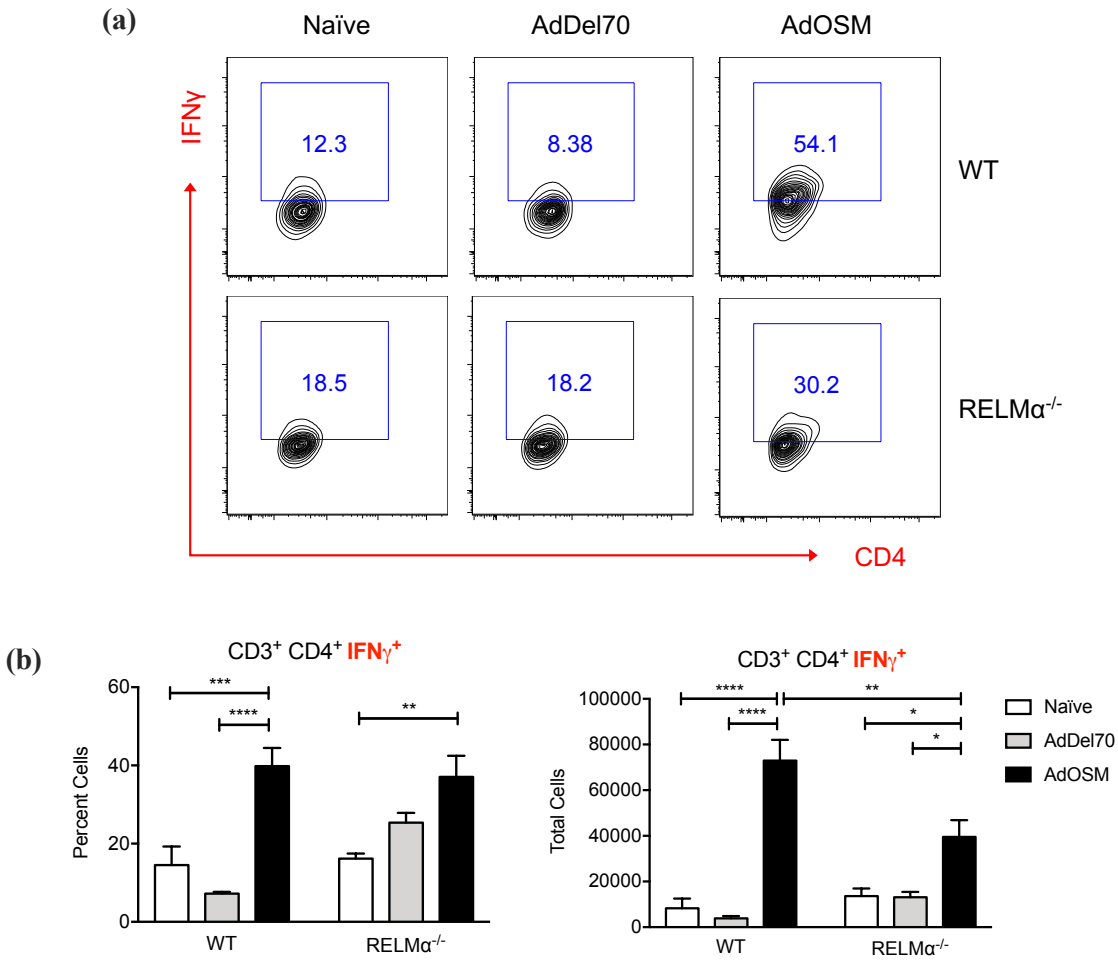
(a)
Naïve
AdDel70
AdOSM
IFNγ
12.3
8.38
54.1
WT
18.5
18.2
30.2
RELMα-/-
CD4
(b)
CD3+ CD4+ IFNγ+
Percent Cells
60
40
20
0
***
****
**
WT
RELMα-/-
CD3+ CD4+ IFNγ+
Total Cells
100000
80000
60000
40000
20000
0
****
****
**
*
*
WT
RELMα-/-
Naïve
AdDel70
AdOSM

Figure 19. RELMα modulates gene expression of Arg1, but not of Th2-associated inflammatory cytokines. Total lung mRNA expression of inflammatory cytokines MCP-1, IL-4, IL-5, and IL-6, and Arg1 and IL-33, analyzed by NanoString Technologies 7 days post adenovirus infection. Gene expression levels are represented as NanoString counts and are normalized to housekeeping genes ACTB and PGK1. Data are expressed as mean ± SEM ($n = 5$ mice/group). Statistical significance was determined by two-way ANOVA with Tukey's post hoc test ($^{*}P < 0.05$, $^{**}P < 0.01$, $^{****}P < 0.0001$ between indicated groups). *(Submitted to Journal of Leukocyte Biology in the manuscript entitled "RELMα is induced by Oncostatin M in vivo and modulates extracellular matrix and cytoprotection in mouse lung inflammation.")*

Figure 19

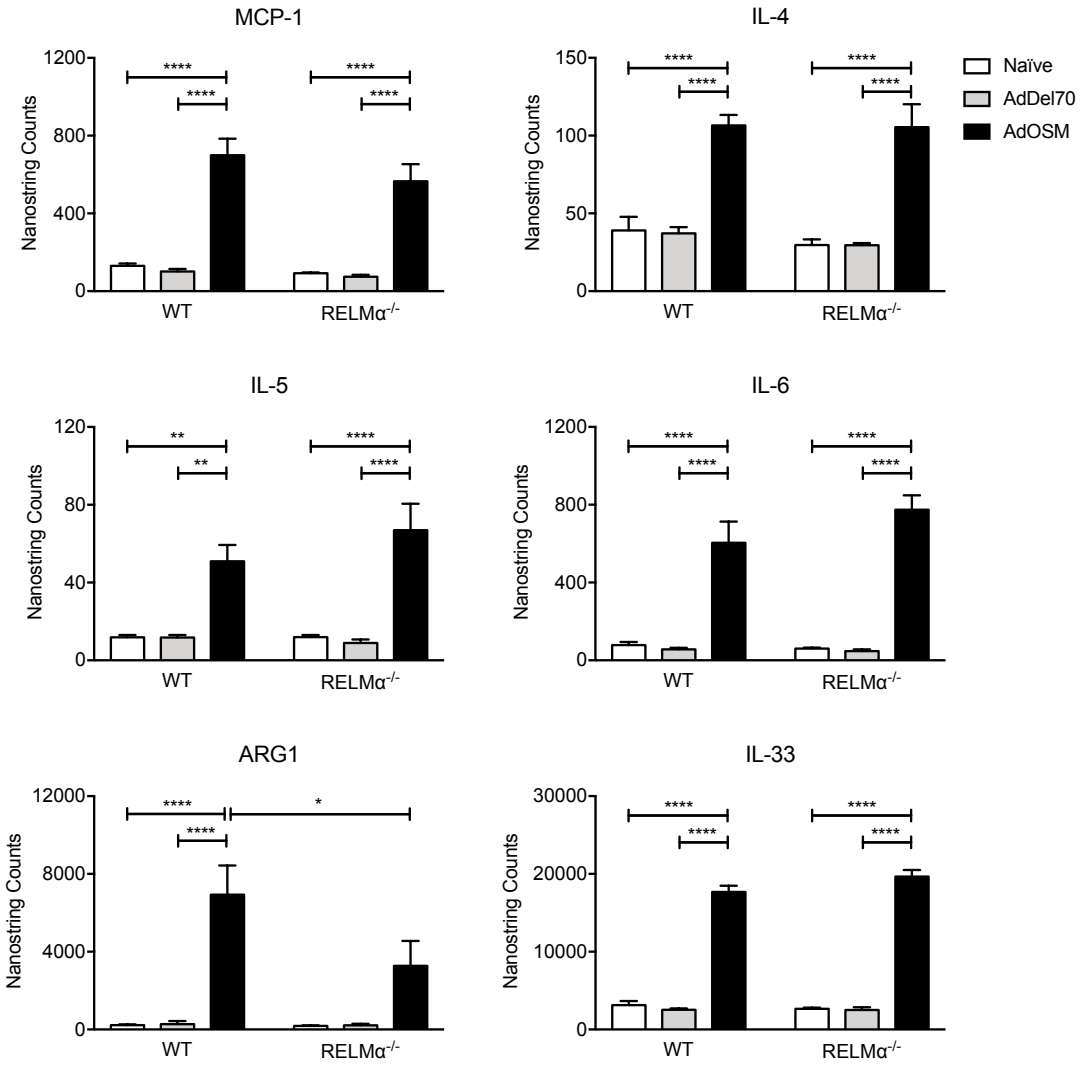
MCP-1
IL-4
IL-5
IL-6
ARG1
IL-33
Nanostring Counts
WT
RELMα-/-
Naïve
AdDel70
AdOSM

Figure 20. RELMα modulates gene expression of ECM proteins. Total lung mRNA expression of ECM genes analyzed by NanoString Technologies 7 days post-infection. Gene expression levels are represented as NanoString counts and are normalized to housekeeping genes ACTB and PGK1. Data are expressed as mean ± SEM (n = 5 mice/group). Statistical significance was determined by two-way ANOVA with Tukey's post hoc test ($^{*}P < 0.05$, $^{**}P < 0.01$, $^{***}P < 0.001$, $^{****}P < 0.0001$ between indicated groups). *(Submitted to Journal of Leukocyte Biology in the manuscript entitled "RELMα is induced by Oncostatin M in vivo and modulates extracellular matrix and cytoprotection in mouse lung inflammation.")*

Figure 20

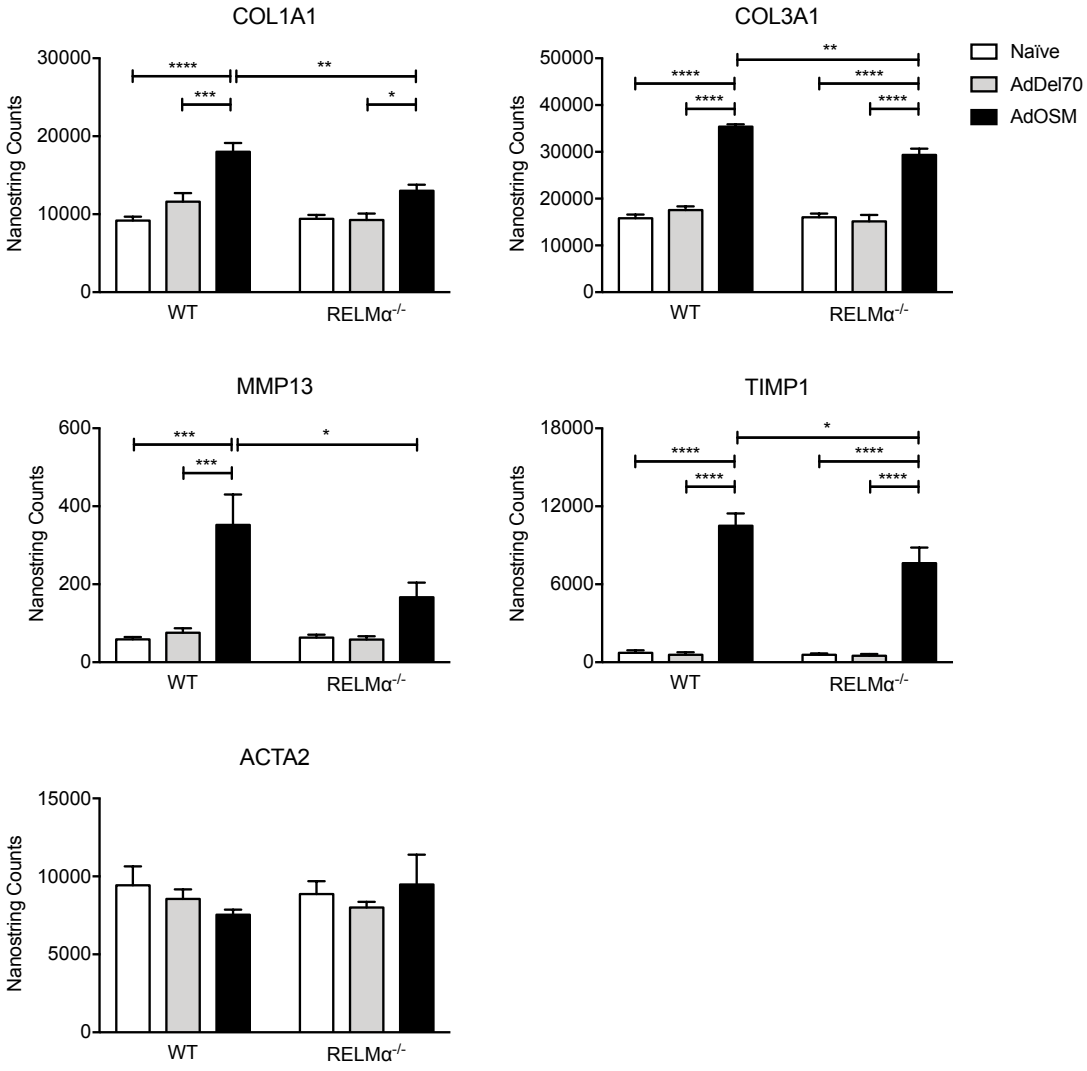
COL1A1
COL3A1
MMP13
TIMP1
ACTA2
Nanostring Counts
Naïve
AdDel70
AdOSM
WT
RELMα-/-
****
***
**
*

Figure 21. Protein expression in whole lung extracts and BAL fluid of AdOSM-treated wildtype and RELMα$^{-/-}$ mice. (a) Day 7 whole lung homogenates were analyzed by Western blot and probed for pSTAT3, Arg1, IL-33, and cytokeratin-18 (CK18), and actin as a loading control. **(b)** Signals in **(a)** were quantified by densitometry and corrected to actin. **(c)** Day 7 BAL fluid was analyzed by Western blot and probed for CK18. **(d)** Signals in **(c)** were quantified by densitometry and corrected to Ym1 levels in BAL fluid (Figure 22), and expressed as arbitrary units. Each lane (dot) indicates sample extracts from separate mouse lungs. (n = 5 mice/group). *(Submitted to Journal of Leukocyte Biology in the manuscript entitled "RELMα is induced by Oncostatin M in vivo and modulates extracellular matrix and cytoprotection in mouse lung inflammation.")*

Figure 21

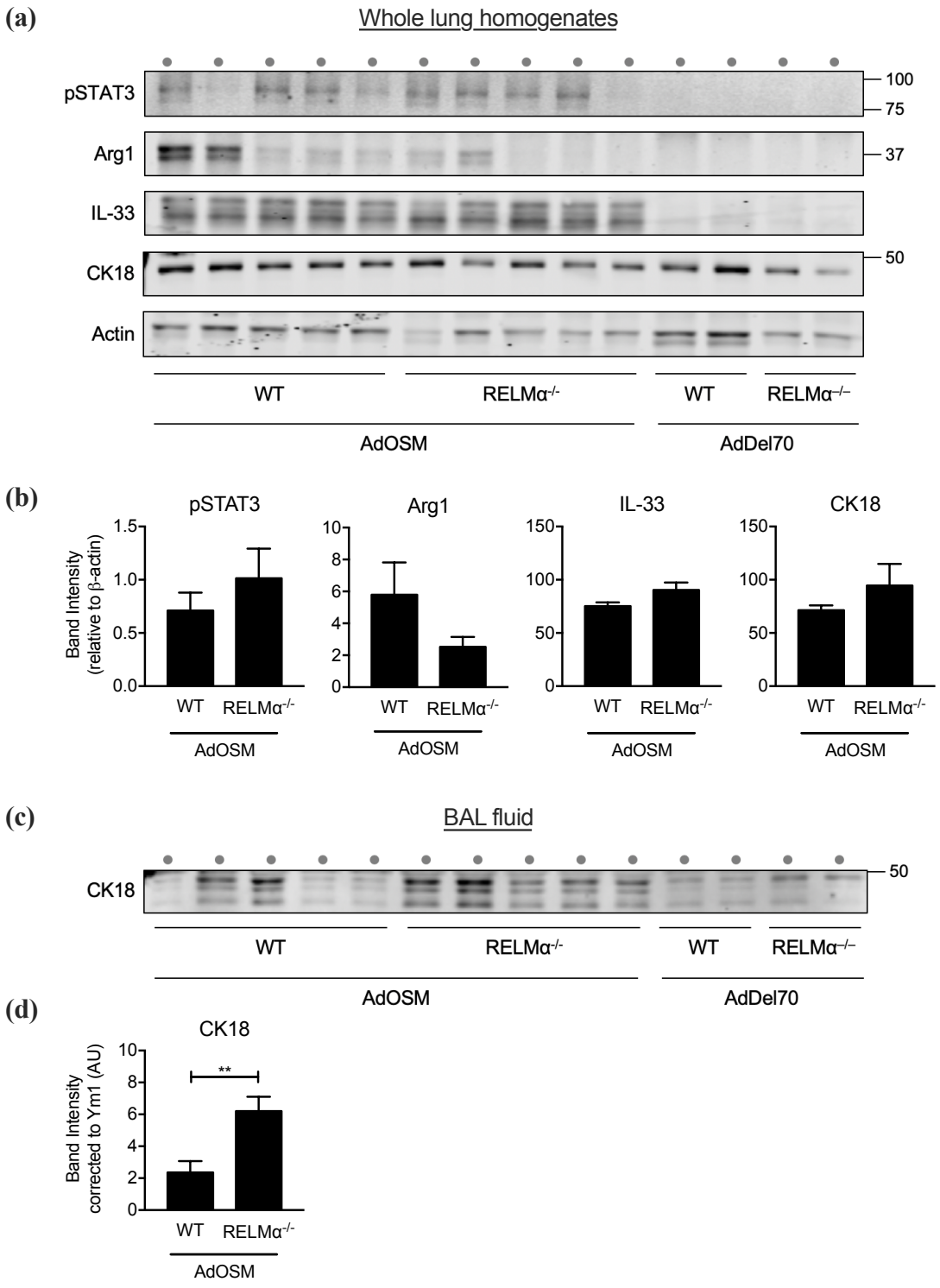
(a)
Whole lung homogenates
pSTAT3
Arg1
IL-33
CK18
Actin
100
75
37
50
WT
RELMα-/-
WT
RELMα-/-
AdOSM
AdDel70
(b)
pSTAT3
Arg1
IL-33
CK18
Band Intensity (relative to β-actin)
WT
RELMα-/-
AdOSM
(c)
BAL fluid
CK18
50
WT
RELMα-/-
WT
RELMα-/-
AdOSM
AdDel70
(d)
CK18
Band Intensity corrected to Ym1 (AU)
**
WT
RELMα-/-
AdOSM

Figure 22. Ym1, eotaxin-2, and IL-5 protein in BAL fluid. BAL fluid from naïve, AdDel70- and AdOSM-treated wildtype and RELMα$^{-/-}$ mice were analyzed by ELISA for the alternatively activated/M2 marker Ym1 and Th2-associated mediators eotaxin-2 and IL-5. Data are expressed as mean ± SEM (n = 5 mice/group). Statistical significance was determined by two-way ANOVA with Tukey's post hoc test ($^{*}P < 0.05$, $^{**}P < 0.01$, $^{***}P < 0.001$, $^{****}P < 0.0001$ between indicated groups). *(Ym1 ELISA submitted to Journal of Leukocyte Biology in the manuscript entitled "RELMα is induced by Oncostatin M in vivo and modulates extracellular matrix and cytoprotection in mouse lung inflammation.")*

Figure 22

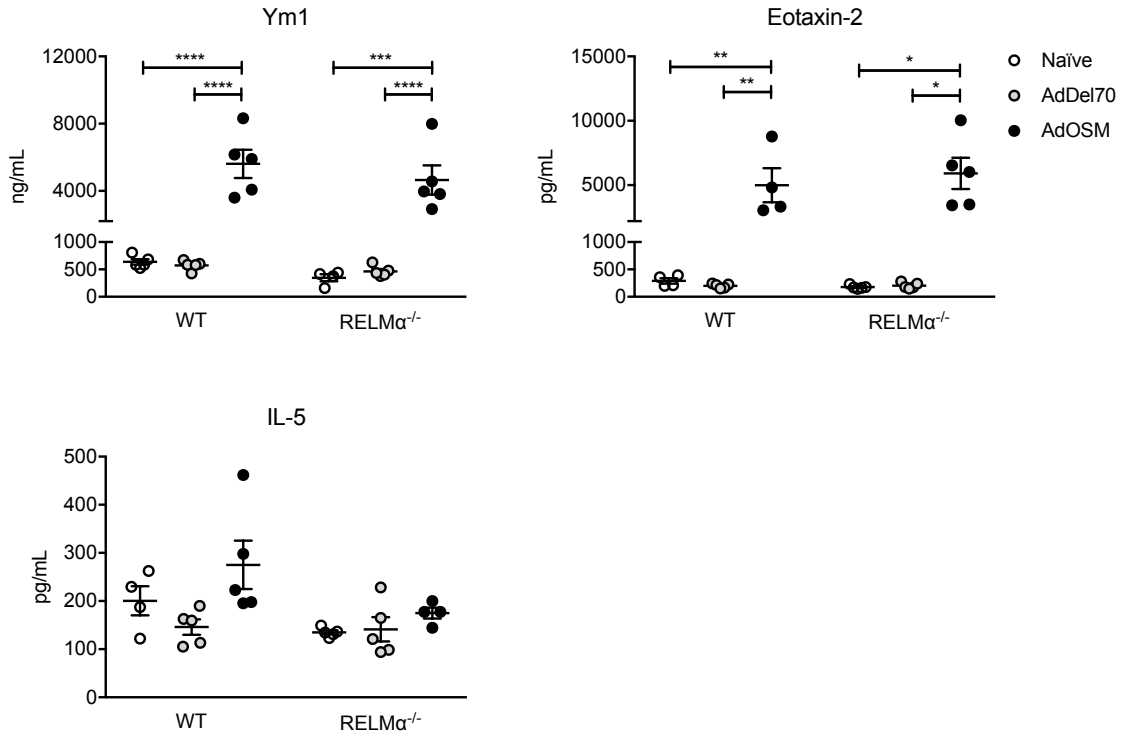
Ym1
ng/mL
12000
8000
4000
1000
500
0
****
****
***
****
WT
RELMα-/-
Eotaxin-2
pg/mL
15000
10000
5000
1000
500
0
**
**
*
*
WT
RELMα-/-
Naïve
AdDel70
AdOSM
IL-5
pg/mL
500
400
300
200
100
0
WT
RELMα-/-

Figure 23. Histological analyses of formalin-fixed, paraffin-embedded lung tissue from AdDel70- and AdOSM-treated wildtype and RELMα$^{-/-}$ mice. Lung sections were prepared from AdDel70- or AdOSM-treated wildtype or RELMα$^{-/-}$ mice as indicated. Representative images of lung tissue sections stained with **(a)** H&E, **(b)** Ki67 for proliferating cells, **(c)** PAS for mucous-producing goblet cells, and **(d)** αSMA. Scale bars, 100 μm. **(e)** Quantification of % Ki67^{+} cells in the epithelium and parenchyma. **(f)** Quantification of % αSMA staining in the parenchyma per lung tissue section. Three sections were analyzed per mouse, excluding major airways and blood vessels. Data are expressed as mean ± SEM (n = 3-5 mice/group). Statistical significance was determined by two-way ANOVA with Tukey's post hoc test ($^{\#}P < 0.001$ relative to controls, $^{****}P < 0.0001$ between indicated groups). *(Submitted to Journal of Leukocyte Biology in the manuscript entitled "RELMα is induced by Oncostatin M in vivo and modulates extracellular matrix and cytoprotection in mouse lung inflammation.")*

Figure 23

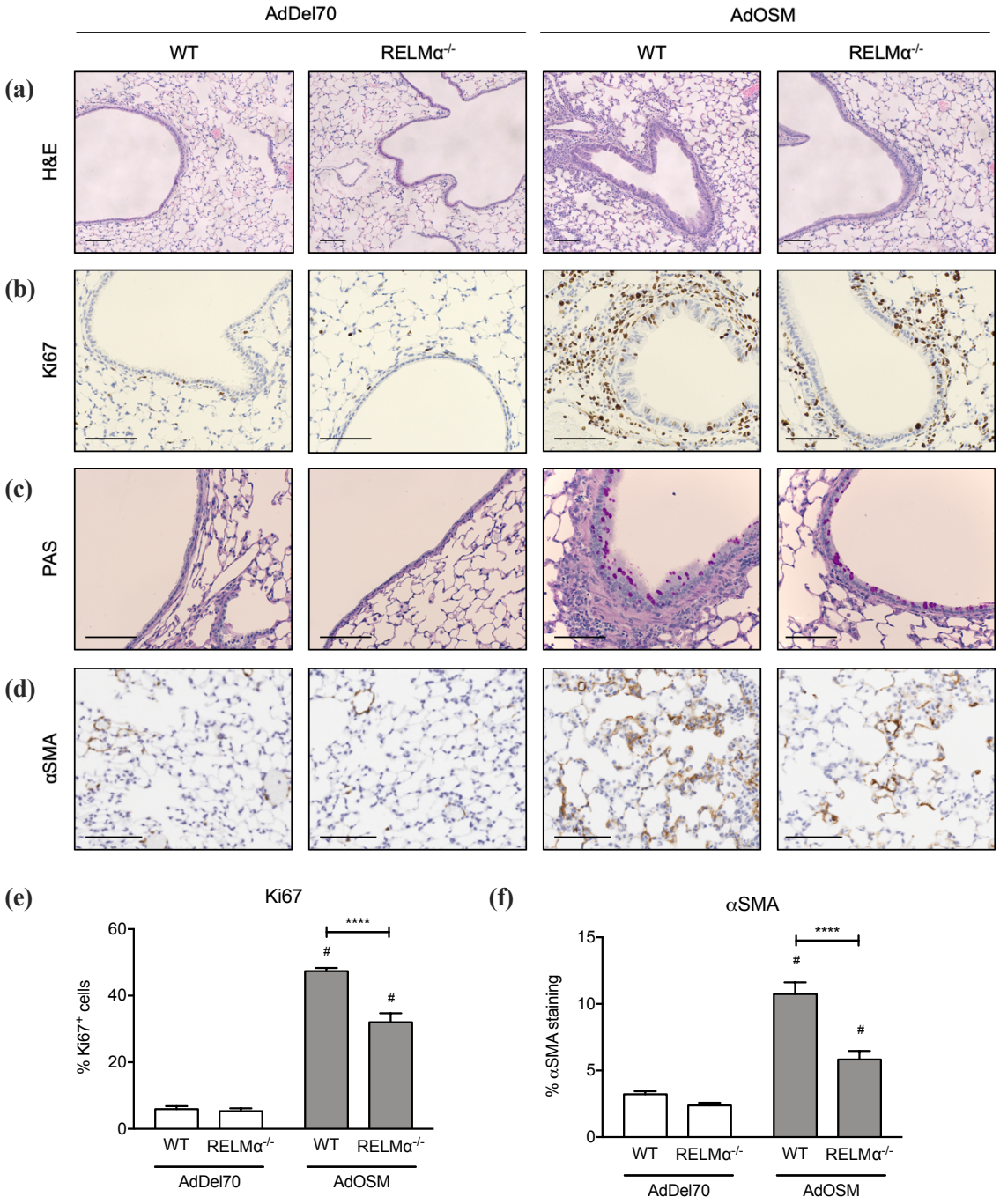
AdDel70
AdOSM
WT
RELMα-/-
WT
RELMα-/-
(a)
H&E
(b)
Ki67
(c)
PAS
(d)
αSMA
(e)
Ki67
% Ki67+ cells
60
40
20
0
****
#
#
WT
RELMα-/-
WT
RELMα-/-
AdDel70
AdOSM
(f)
αSMA
% αSMA staining
15
10
5
0
****
#
#
WT
RELMα-/-
WT
RELMα-/-
AdDel70
AdOSM

Figure 24. Representative images of H&E, αSMA, and PSR-stained lung tissue sections of AdOSM-treated animals. (a) High magnification images of H&E stained lung tissue sections from AdOSM-treated wildtype and RELMα$^{-/-}$ mice, showing thickening of the airway epithelium in wildtype but not in RELMα$^{-/-}$ mouse lungs. Scale bars, 50 μm. **(b)** Representative images of entire lung sections from AdOSM-treated wildtype and RELMα$^{-/-}$ mice stained with αSMA. Wildtype sections have a higher proportion of positive staining (brown). Scale bars, 1 mm. **(c)** Representative images of lung parenchyma stained with PSR, captured under polarized light, to show collagen accumulation in AdDel70- and AdOSM-treated wildtype and RELMα$^{-/-}$ mice. Scale bars, 200 μm. (n = 5 mice/group).

Figure 24

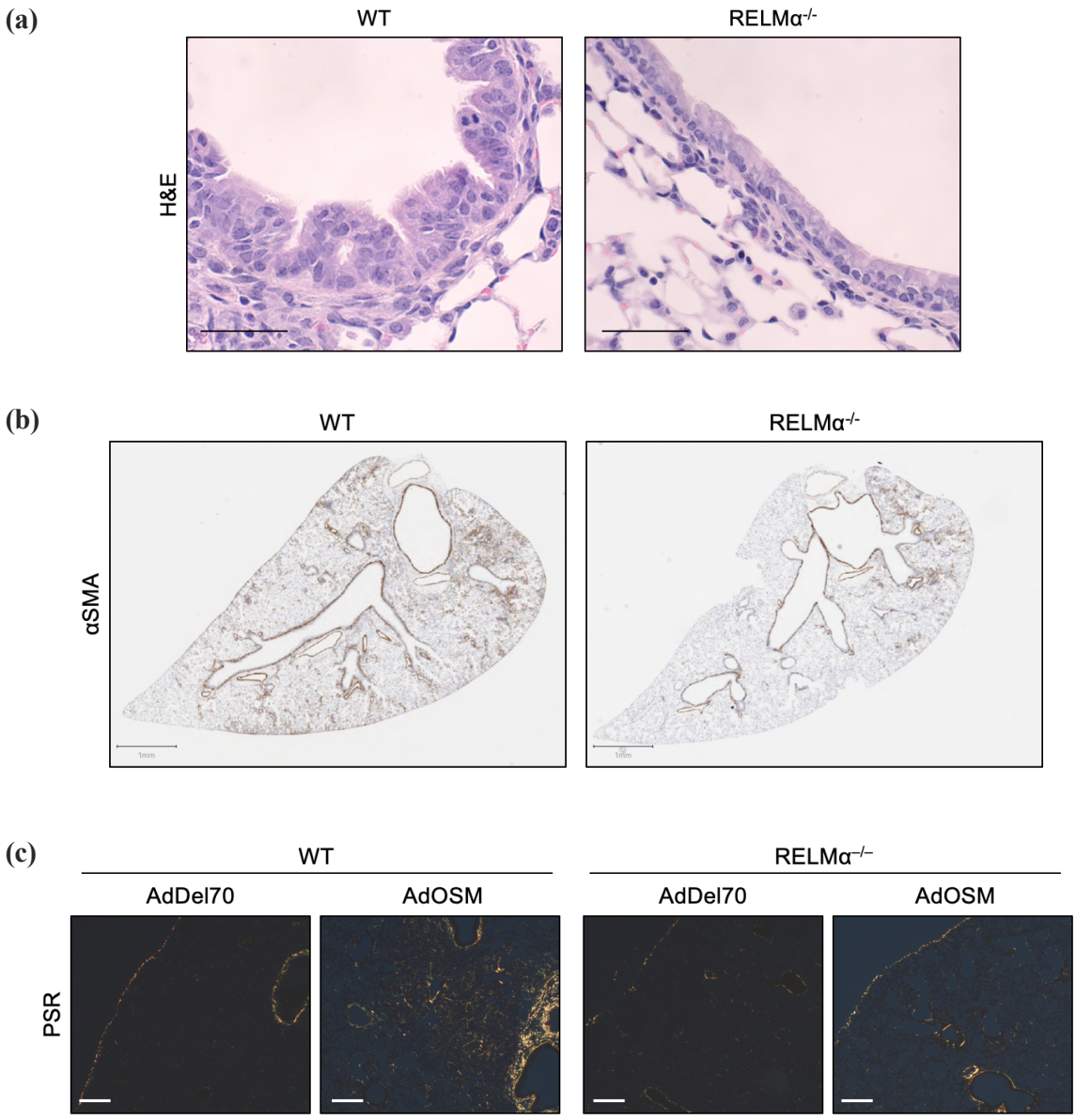
(a)
WT
RELMα-/-
H&E
(b)
WT
RELMα-/-
αSMA
(c)
WT
RELMα−/−
AdDel70
AdOSM
AdDel70
AdOSM
PSR

Figure 25. RELMα is capable of forming higher-order oligomers in BAL fluid, but not in whole lung. BAL fluid and whole lung homogenates from AdDel70- and AdOSM-treated wildtype mice and AdOSM-treated RELMα$^{-/-}$ mice were analyzed by Western blot under reducing and non-reducing conditions and probed for RELMα. Under reducing conditions, RELMα can be found as a monomer (~9.4 kDa) in BAL fluid (green arrowheads) and whole lung extracts. Under non-reducing conditions, we observed multiple bands (red arrowheads) in BAL fluid of AdOSM-treated wildtype mice, suggesting that RELMα is capable of forming higher-order oligomers in BAL fluid but much less so in whole lung tissue.

Figure 25

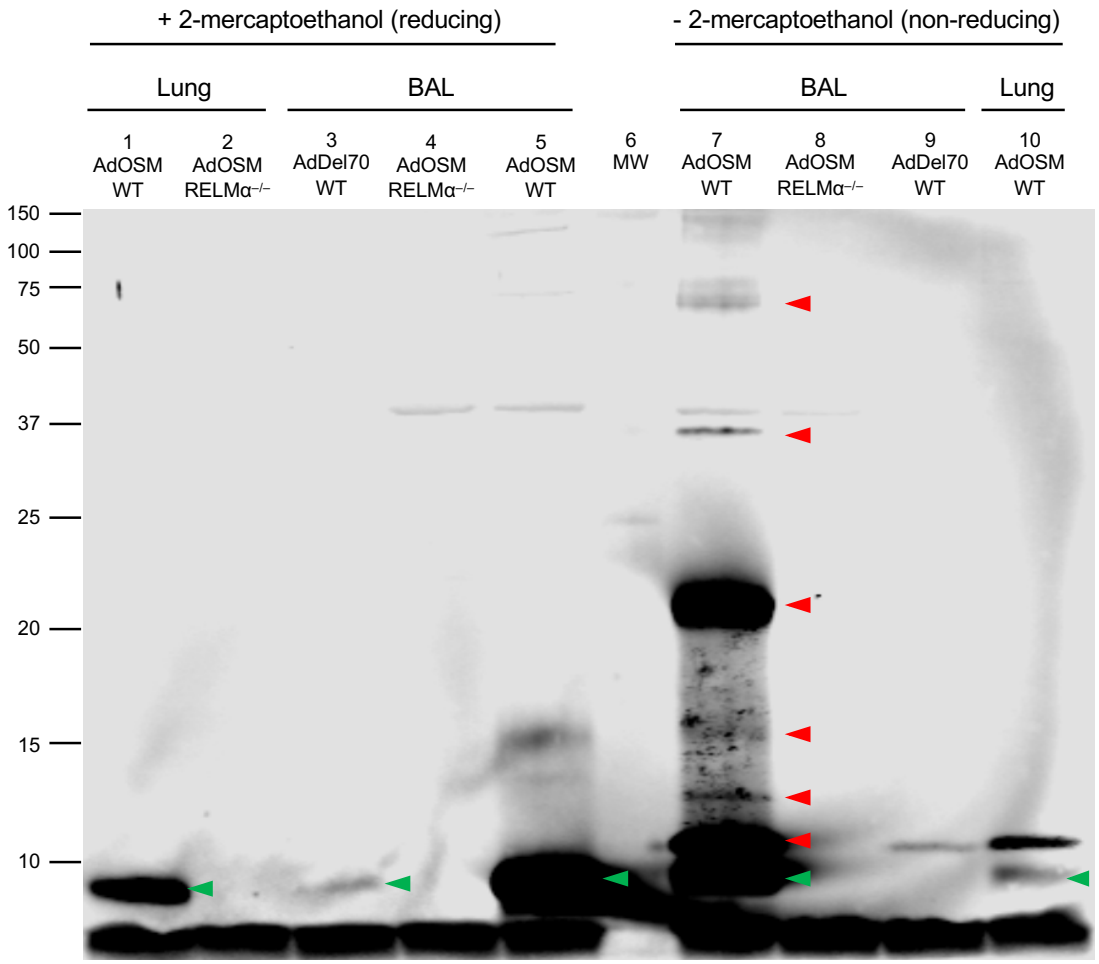
+ 2-mercaptoethanol (reducing)
- 2-mercaptoethanol (non-reducing)
Lung
BAL
BAL
Lung
1 AdOSM WT
2 AdOSM RELMα−/−
3 AdDel70 WT
4 AdOSM RELMα−/−
5 AdOSM WT
6 MW
7 AdOSM WT
8 AdOSM RELMα−/−
9 AdDel70 WT
10 AdOSM WT
150
100
75
50
37
25
20
15
10

Supplementary Figure 1. Gene expression of IFNβ, IFNγ, IFNAR, IFIT1, and IL-4Rα in wildtype and RELMα$^{-/-}$ mice. Total lung mRNA expression analyzed by NanoString Technologies 7 days post-infection. Gene expression levels are represented as NanoString counts and are normalized to housekeeping genes ACTB and PGK1. Data are expressed as mean ± SEM (n = 5 mice/group). Statistical significance was determined by two-way ANOVA with Tukey's post hoc test ($^{*}P < 0.05$, $^{**}P < 0.01$, $^{****}P < 0.0001$ between indicated groups). *(IFNγ gene expression submitted to Journal of Leukocyte Biology in the manuscript entitled "RELMα is induced by Oncostatin M in vivo and modulates extracellular matrix and cytoprotection in mouse lung inflammation.")*

Supplementary Figure 1

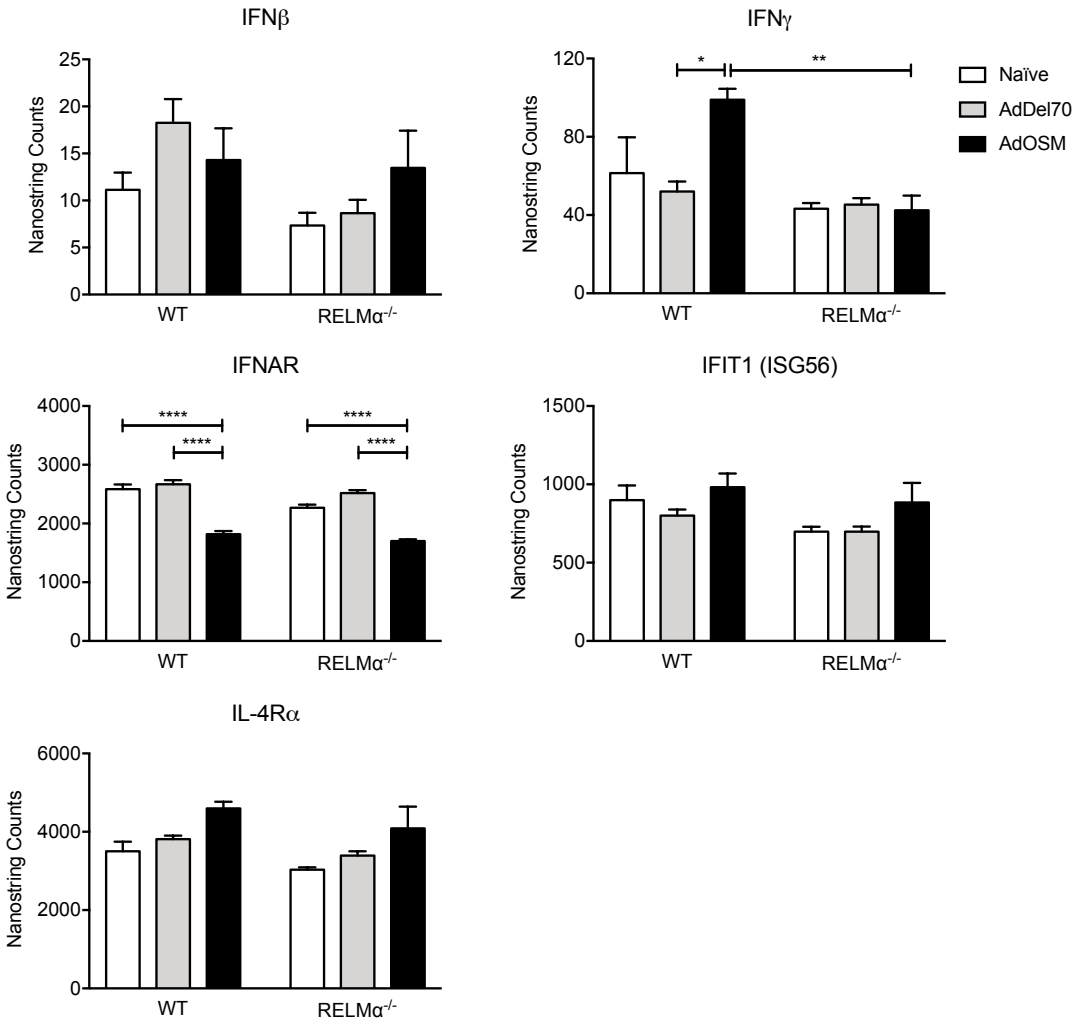

Supplementary Figure 2. Regulation of RELMβ by RELMα and IL-33 in C57Bl/6 and BALB/c mice. (a) Wildtype and IL-33$^{-/-}$ C57Bl/6 (left panel) and BALB/c mice (right panel) were endotracheally administered AdDel70 or AdOSM. RELMβ mRNA expression in total lung homogenates 7 days post-infection, analyzed by RT-PCR. Expression levels are relative to 18S ribosomal RNA. **(b)** Whole lung RELMβ mRNA expression in wildtype and RELMα$^{-/-}$ C57Bl/6 mice 7 days post-infection, analyzed by NanoString Technologies. Data are expressed as mean ± SEM (n = 4-6 mice/group). Statistical significance determined by two-way ANOVA with Tukey's post hoc test ($^{*}P < 0.05$, $^{**}P < 0.01$, $^{****}P < 0.0001$ between indicated groups). **(c)** Representative images of CISH for OSM (red) and RELMβ (turquoise) in formalin-fixed, paraffin-embedded lung tissue sections from AdDel70- and AdOSM-treated wildtype and RELMα$^{-/-}$ C57Bl/6 mice at day 7. Scale bars, 50 μm.

Supplementary Figure 2

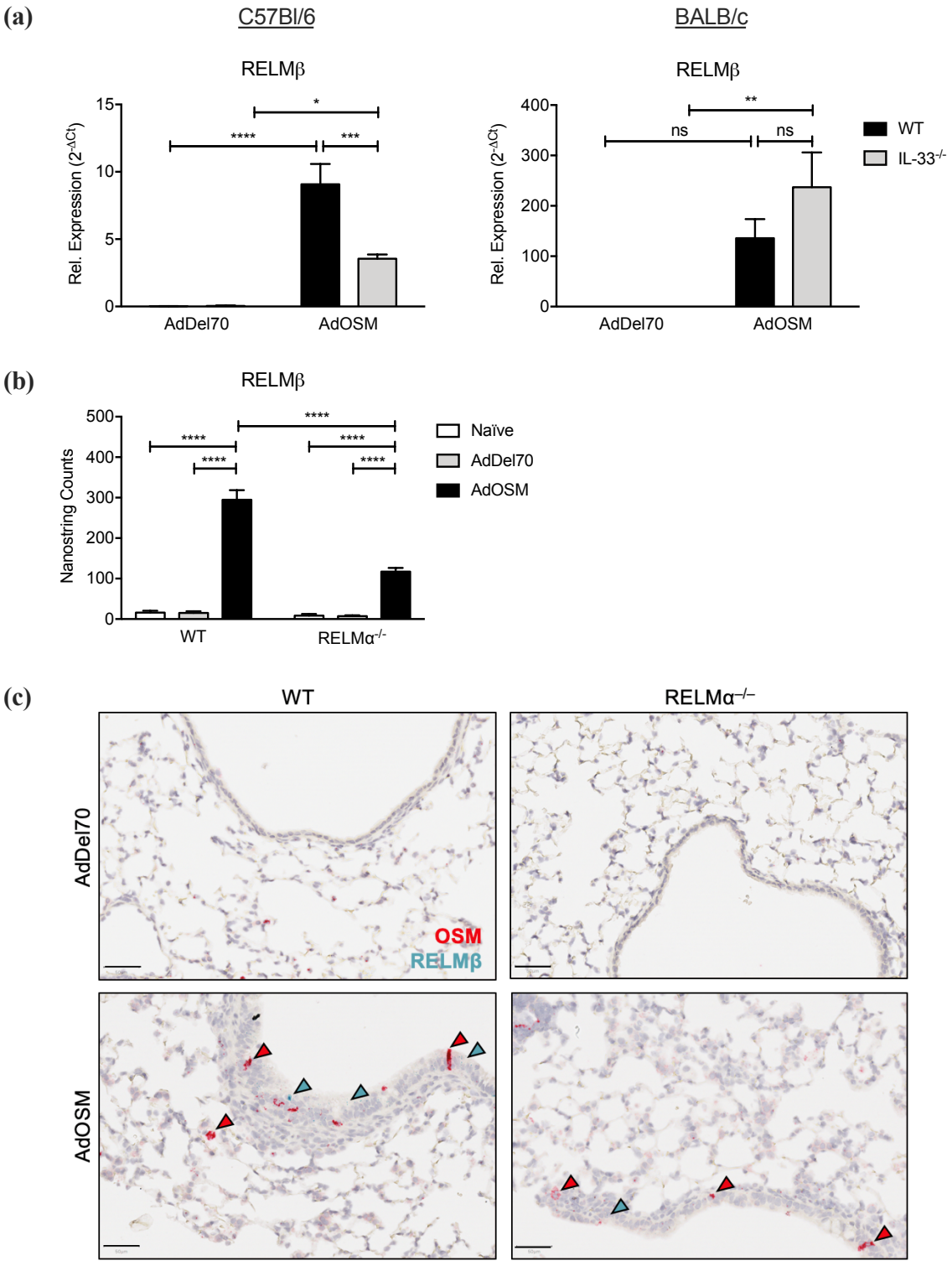

CHAPTER 6: DISCUSSION

6.1 Summary of findings

In vivo experiments using a mouse model of OSM-induced lung inflammation demonstrated that overexpression of OSM in mouse lungs strongly induces mRNA expression of RELMα in columnar airway epithelial cells (**Figure 4**) and RELMα protein detected in BAL fluid in both C57Bl/6 and BALB/c strains of mice after 7 and 14 days (**Figure 3**). Similar trends were observed with overexpression of IL-6 in C57Bl/6 and BALB/c mouse lungs at day 7 (**Figure 5a**), although RELMα protein levels in BAL fluid were much lower than induced by AdOSM (**Figure 5b**). Maximal induction of RELMα protein by AdOSM in C57Bl/6 mice required IL-6, as demonstrated using IL-$6^{-/-}$ and IL-$33^{-/-}$ mice (**Figure 5c**). As observed in lung tissue sections stained by CISH, RELMα mRNA expression was primarily localized to columnar airway epithelial cells, with some RELMα^{+} mononuclear cells in the lung parenchyma.

Given that both IL-6 and IL-33 can regulate RELMα expression *in vivo*, RELMα production by macrophages was assessed *in vitro*. Unstimulated, CA/M1-polarized BMDMs, and those stimulated with IL-6 or IL-33 alone did not produce RELMα after 24 and 48 hours. AA/M2-polarized BMDMs secreted RELMα into culture supernatants and when co-stimulated with IL-6, induction of RELMα was further elevated, assessed by Western blot and ELISA (**Figure 9b**). However, when AA/M2-polarized BMDMs were co-stimulated with IL-33, RELMα protein levels were not further elevated (**Figure 9c**). To

address other possible cell sources of RELMα, C10 and LA4 alveolar epithelial cell lines were stimulated with LPS/IFNγ (CA/M1 stimulus) or IL-4/IL-13 (AA/M2 stimulus), alone or in combination with IL-6 or OSM for 24 hours. Although these cells responded to the stimuli with MCP-1 production, RELMα could not be detected in culture supernatants by ELISA (**Figure 10**).

To investigate the functions of RELMα in OSM-mediated lung inflammatory responses, wildtype and RELMα$^{-/-}$ C57Bl/6 mice were compared. RELMα mRNA and protein in whole lung homogenates, and RELMα protein in BAL fluid and serum were detectable in naïve and AdDel70-treated wildtype mice and were significantly upregulated upon AdOSM infection (**Figure 11**). RELMα mRNA and protein were not detectable in RELMα$^{-/-}$ mice. RELMα-deficiency in C57Bl/6 mice did not affect the mRNA and protein expression of adenovirus-encoded OSM in lung tissue and BAL fluid, respectively, nor of mRNA expression of OSMRβ in lung tissue (**Figure 12**), nor of OSM-induced accumulation of immune cell infiltrates in BAL fluid (including eosinophils, neutrophils and lymphocytes). Interestingly, quantification of damaged/dead cells in BAL fluid of AdOSM-treated RELMα$^{-/-}$ mice were present at significantly high numbers in comparison to other treatment groups (**Figure 14**). This correlated with increased LDH and increased CK18 in RELMα$^{-/-}$ mice, indicative of cell death.

Although RELMα-deficiencies did not affect mRNA expression of Th2-associated mediators including IL-4, IL-5, IL-6 and eotaxin-2 (**Figure 19**), the absence of RELMα

resulted in less accumulation of AA/M2 macrophages (**Figure 17**) and Th1 cells (**Figure 18**), less upregulation of ECM remodeling genes (**Figure 20**) and less parenchymal αSMA$^+$ staining in RELMα$^{-/-}$ mice treated with AdOSM (**Figure 23d, f**), characteristics of altered tissue repair and wound healing phenotypes.

Together, these results indicate that RELMα is induced downstream of OSM, IL-6 and IL-33 in C57Bl/6 mice, and suggest that OSM-induced RELMα increases matrix deposition and protects against epithelial cell damage in mouse lung tissue.

6.2 OSM and IL-6 regulate RELMα in C57Bl/6 and BALB/c mice

There were significantly higher levels of RELMα protein present in the BAL fluid of C57Bl/6 mice in response to AdOSM compared to BALB/c mice (**Figure 3b**). We have previously shown that in BAL fluid of AdOSM-treated C57Bl/6 mice, there was marked elevation of Th2 inflammatory mediators and eosinophilia which were absent in the BALB/c strain [14]. Since RELMα can be regulated by Th2 cytokines [64,87], the absence of a Th2-skewed cytokine environment in BALB/c mice correlates with lower levels of RELMα found in BAL fluid of these mice. In addition, RELMα expression could be seen in mononuclear cells throughout the lung parenchyma of C57Bl/6 mice by chromogenic *in situ* hybridization (**Figure 4**), whereas in BALB/c mouse lung parenchymal cells, RELMα$^+$ cells were much less frequent, a likely reason for lower protein levels in BAL fluid in BALB/c mice.

We also show that in wildtype mice treated with AdOSM, there was accumulation of RELMα^{+} CD68^{+} macrophages by CISH colocalization (**Figure 15b, left panel**). Cells that stained positive for CD68 but not RELMα likely reflect non-activated or CA/M1 macrophages. In this model of lung inflammation, we postulate that a major source of RELMα are the columnar airway epithelial cells, and that lung AA/M2 macrophages also contribute to RELMα levels in C57Bl/6 mice.

Among the gp130 cytokines, the receptor chains for OSM, OSMRβ and gp130, are widely expressed on connective tissue cells, and for this reason OSM is able to activate several signaling pathways including JAK/STAT, MAPK, and PI3K/Akt [17,27]. Based on *in vitro* studies [28,88], OSM is more active than other gp130 cytokines, such as IL-6, LIF or IL-31, and robustly regulates expression of signaling intermediates including STAT3 and STAT1, as well as genes including of IL-4Rα, IL-6, and ECM genes MMP1 and TIMP1 in connective tissue cells. A similar trend was also observed *in vivo* in both C57Bl/6 and BALB/c strains of mice, where overexpression of AdOSM in mouse lung was able to induce RELMα protein expression more robustly than AdIL-6 at days 2 and 7 post-infection (**Figure 5a, b**). Using IL-6-deficient C57Bl/6 mice, we also show that maximal RELMα expression induced by AdOSM is mediated in part through IL-6 (**Figure 5c**). We have previously demonstrated that IL-6 was able to activate STAT3 and STAT6, and further enhance STAT6 signaling in AA/M2-polarized macrophages, and that IL-6 is required for OSM-induced M2 macrophage accumulation in mouse lung [40]. Similarly, using BMDMs we demonstrate that IL-6 can further upregulate RELMα protein expression

in AA/M2-polarized macrophages (**Figure 9b**), consistent with other studies showing that IL-6 can "hyperpolarize" AA/M2 macrophage phenotype [39,40]. We speculate that *in vivo*, OSM acts on lung epithelial/stromal cells whereas IL-6 acts on AA/M2-polarized macrophages to maximally induce expression of RELMα directly, and to maximize accumulation of AA/M2-polarized cells in the lung.

6.3 IL-33 regulates RELMα in C57Bl/6 mice, but not in BALB/c mice

IL-33 has been implicated in models of allergic airway disease and in asthma, where it can amplify Th2-skewed responses upon engagement with its receptor, ST2, which is widely expressed on Th2 cells [42,43]. Previous work has shown that overexpression of AdOSM for 7 days highly induces IL-33 mRNA and protein expression in lungs of both C57Bl/6 and BALB/c mice [28]. In correlation with induced IL-33 expression in AdOSM-treated C57Bl/6 mice, Th2-associated mediators including IL-4, IL-5, and eotaxin-2 were also elevated [14]. Although IL-33 was also induced in AdOSM-treated BALB/c mice [28], Th2 cytokines were not elevated [14], and thus knocking out IL-33 would have no effect on the Th2-skewed microenvironment or lack thereof, and therefore RELMα expression would not be altered in IL-33$^{-/-}$ BALB/c mice (**Figure 7**). On the other hand, the absence of IL-33 in C57Bl/6 mice would decrease Th2 responses and thus reduce RELMα expression (**Figure 6**).

Similar to a previous study demonstrating that in AdOSM-treated mice, IL-33 was expressed in type II alveolar epithelial cells by immunohistochemistry [28], analysis of

AdOSM-treated wildtype mouse lung sections by CISH also showed IL-33 mRNA expression in cells of the lung parenchyma (**Figure 8**), some of which were also RELMα^{+}. *In vitro* studies in C10 alveolar epithelial cells showed that stimulation with OSM markedly induced IL-33 more robustly than other gp130 cytokines including IL-6, LIF, and IL-31 [28]. However, when the same cell line was stimulated with OSM, RELMα could not be detected in cell culture supernatants (**Figure 10**). Of note, C10 alveolar epithelial cells are derived from a BALB/c background, which may affect RELMα responses compared to cells generated from a C57Bl/6 background. Albeit cell lines *in vitro* are not necessarily representative of the complex microenvironment *in vivo* that could regulate RELMα, we did not observe RELMα mRNA in type II AEC *in vivo*. It is likely that columnar epithelial cells (see CISH images, **Figure 4**), are major sources of RELMα in our system. Whether OSM directly stimulates RELMα in columnar epithelial cells, or indirectly through other mediators is not known.

Since RELMα expression was not altered between wildtype and IL-33$^{-/-}$ BALB/c mice treated with AdOSM but was reduced in IL-33-deficient C57Bl/6 mice, *in vitro* experiments using BMDMs derived from C57Bl/6 mice were examined for the regulation of RELMα by IL-33. Kurowska-Stolarska *et al*. showed that IL-33 released upon epithelial cell injury can synergize with IL-13 and act on alveolar macrophages to induce macrophage polarization into the AA/M2 phenotype, while enhancing expression of Arg1 and Ym1 [46], typical markers of AA/M2 macrophages in addition to RELMα. However, BMDMs co-stimulated with IL-33 and IL-4/IL-13 did not further enhance RELMα secretion in

comparison to those stimulated with IL-4/IL-13 alone (**Figure 9c**). Further testing of BMDMs for expression of ST2 receptors is required to ensure whether these cells respond to IL-33.

6.4 RELMα and Th2 inflammation

RELMα has been implicated in several different murine models of lung inflammation, including parasitic infection and pulmonary fibrosis [52,60]. In a model of pulmonary inflammation, RELMα$^{-/-}$ mice challenged with the parasite *S. mansoni* (*Sm*) eggs presented elevated Th2 cytokine levels including IL-4, IL-5, and IL-13 in comparison to wildtype counterparts [60]. However, in a different model of pulmonary fibrosis where RELMα$^{-/-}$ mice were treated with bleomycin, these mice exhibited decreased IL-4 expression and less fibrosis in comparison to wildtype mice [52]. In our model of Th2-skewed pulmonary inflammation, Th2 cytokines were not differentially expressed between wildtype and knockout mice (**Figure 19**), suggesting the Th2 cell responses were not altered. We did observe lower IFNγ mRNA expression in RELMα$^{-/-}$ mice (**Supplementary Figure 1**), as well as reduced IFNγ-producing CD4^{+} Th1 cells in total lung of knockout mice relative to wildtype mice (**Figure 18**). However, in this and previous studies [40], we cannot detect IFNγ or IL-12 in BAL fluid, and the mRNA for IFNγ is low and minimally induced (2-fold) by AdOSM in total lung. That being noted, it appears that RELMα can regulate activated Th1 cells although it is not clear if this is a direct or indirect action. Taken together, the function of RELMα in regulating Th1 and Th2 responses appears dependent on the specific model of lung inflammation. In a model of type 2 immunity during nematode infection,

studies have shown that Ym1 can induce epithelial cell expression of RELMα [72]. Ym1 is another AA/M2 macrophage-associated protein elevated in Th2 inflammation. Whether OSM induces Ym1 in our model system, and whether OSM induces RELMα in columnar epithelial cells directly or indirectly (or both) through Ym1 requires further study.

6.5 RELMα and ECM accumulation

In our system of OSM-induced lung inflammation, although there were no significant differences in Th2 cytokine expression between wildtype and RELMα$^{-/-}$ mice, we did observe a lower fibrotic response in knockout mice treated with AdOSM. Similar to the bleomycin model of pulmonary fibrosis [52], we observed reduced type I collagen lung mRNA expression (**Figure 20**), correlating with markedly less αSMA^{+} staining in lung tissue of AdOSM-treated RELMα$^{-/-}$ mice relative to wildtype mice (**Figure 23d, f**), suggesting that knockout mice were partially protected from this particular fibrotic phenotype, and that RELMα may participate in myofibroblast accumulation.

Several studies have suggested a role for AA/M2 macrophages in the exacerbation of pulmonary fibrosis and other models of tissue repair and wound healing [39,89]. Here, we show that AdOSM induced the accumulation of CD206^{+} M2 macrophages, whereas in the absence of RELMα there was significantly less accumulation of these macrophages in the lung (**Figure 17**). This trend was also associated with reduced lung mRNA expression of ECM remodeling genes COL1A1, COL3A1, MMP13, and TIMP1 in knockout animals (**Figure 20**). Taken together, RELMα may function to maintain M2 macrophage numbers

in the lung, which may then contribute to myofibroblast differentiation and ultimately lead to matrix deposition and lung fibrosis.

6.6 RELMα and cell death

In addition to the roles of RELMα in lung fibrosis and Th2-mediated lung inflammation, others have also suggesting that RELMα has anti-apoptotic properties. Using explant cultures of embryonic mouse lung, Wagner *et al.* showed that RELMα treatment resulted in reduced numbers of apoptotic cells, suggesting that RELMα impairs apoptosis while regulating maturation in the developing mouse lung [90]. Chung *et al.* demonstrated that mouse lung fibroblasts treated with TNFα and cycloheximide, an antibiotic that disrupts protein synthesis, induced expression of caspase-3 and -8, indicative of programmed cell death [91]. Pre-treatment with RELMα inhibited activation of caspase-3 and -8 by TNFα and cycloheximide, again suggesting an anti-apoptotic role for RELMα in mouse lung cells. In AdOSM-treated RELMα$^{-/-}$ mice a subset of cells, that were not the typical immune cells found in BAL fluid, were observed at a significantly higher frequency than other treatment groups (**Figure 14**). These cells appeared to be damaged/dead cells since there was lack of an intact membrane and nucleus, and may be dead epithelial cells as a result of epithelial injury. An LDH assay also indicated higher cytotoxicity in BAL fluid of AdOSM-treated RELMα$^{-/-}$ mice, in correlation with high numbers of damaged/dead cells. Furthermore, CK18 levels in whole lung tissue were not altered between treatment groups, whereas full-length CK18 released into BAL fluid were higher in RELMα$^{-/-}$ mice than wildtype mice treated with AdOSM (**Figure 21c, d**). As a component of the intermediate filament system,

CK18 is expressed at high levels in epithelial cells, and is used as a marker for distinguishing epithelial cell death modes. Upon cell death by apoptosis, activated caspases cleave CK18 into fragments, whereas in necrosis CK18 is released in its full-length intact form [92,93]. In addition, there was less epithelial cell hyperplasia evident in AdOSM-treated RELMα$^{-/-}$ mice observed in H&E-stained lung tissue sections (**Figure 23a, Figure 24a**). Together, this shows that AdOSM infection in the absence of RELMα led to more epithelial cell death in mouse lung, and supports a cytoprotective role for RELMα.

The mechanism(s) by which RELMα is cytoprotective and modulates ECM remodeling in the AdOSM model is not clear. Although the receptor for RELMα remains to be identified, some have suggested that RELMα could bind to intracellular Bruton's tyrosine kinase (BTK) [60,94]. While the interaction between the two is unclear since RELMα is secreted whereas BTK is cytoplasmic, activation of the BTK pathway can lead to myeloid cell chemotaxis, and in a different study, downregulate Th2 cytokine production in CD4^{+} T cells [60,94]. Others have proposed that RELMα could induce myofibroblast differentiation through the induction of αSMA in fibroblasts [95], however it is unclear how RELMα binds or activates these fibroblasts. RELMα also induces myofibroblast transition in mouse adipocytes and this may play a role in dermal fibrosis [96].

To date, the human homolog for mouse RELMα has yet to be identified, but interestingly, one study demonstrated by immunohistochemistry that human RELMβ was present in epithelial cells and alveolar macrophages of human lung tissue from IPF patients [78],

consistent with murine models showing RELMα expression in the same cell types [63]. In another study, RELMβ was found at significantly higher levels in bronchial biopsies of patients with asthma compared to healthy individuals [76]. Using primary human lung fibroblasts, Fang *et al.* also demonstrated that stimulation with RELMβ increased ECM deposition, including type I collagen and αSMA protein expression, suggesting that RELMβ may play a significant role in airway remodeling mechanisms in human asthma [76]. Further investigation is required to determine whether murine RELMα and human RELMβ function similarly in animal models of lung inflammation and in human pulmonary fibrosis patients.

6.7 RELMα and homeostasis

In both strains, RELMα protein was present in serum of naïve mice at approximately 200 ng/mL (**Figure 3c**), however it is unclear whether RELMα plays a role in systemic circulation in this model. Since the levels of RELMα in BAL fluid can be induced to as high as 12 μg/mL, it is unlikely that the source of RELMα in mouse lung comes from circulating immune cells, but rather the increase in RELMα levels in serum of AdOSM-treated C57Bl/6 mice is due to spillover or absorption from BAL fluid. Interestingly, in naïve mice RELMα was present at lower levels in BAL fluid than in serum, suggesting different sources of RELMα in these compartments and implying that RELMα derived from different cell sources may play different roles in the lung than in circulation. Recently, RELMα has been shown to play an important role in whole-body metabolism *in vivo*. Kumamoto *et al.* demonstrated that $CD301b^{+}$ mononuclear phagocytes (MNP) in white

adipose tissue were a major source of RELMα [62]. Depletion of these cells disrupted metabolic homeostasis, resulting in significant weight loss and reduced blood glucose levels. These mice also showed decreased levels of RELMα in serum, and reconstitution of RELMα by intraperitoneal administration was able to reestablish homeostasis, revealing a role of systemic RELMα in glucose metabolism. Whether the increases of serum RELMα in our system of AdOSM overexpression in C57Bl/6 mice has effects on glucose homeostasis would require further study.

CHAPTER 7: CONCLUSION

In this thesis, the role of RELMα in OSM-induced lung inflammation and ECM accumulation were examined. In both C57Bl/6 and BALB/c mice, RELMα was significantly induced by AdOSM after 7 and 14 days at the mRNA level in whole lung tissue and at the protein level in BAL fluid. However, CISH staining of lung tissue sections revealed that in addition to columnar airway epithelial cells, mononuclear cells in the lung parenchyma of C57Bl/6 but not BALB/c mice also expressed RELMα. In IL-$6^{-/-}$ and IL-$33^{-/-}$ mice on C57Bl/6 background, induction of RELMα by AdOSM was significantly reduced, demonstrating that maximal induction of RELMα is dependent on IL-6 and IL-33. Based on *in vitro* experiments and literature, one possible pathway by which IL-6 induces RELMα is through AA/M2-polarized macrophages, whereas IL-33 amplifies the Th2-skewed cytokine response to induce RELMα expression.

The roles of RELMα have been studied in context of different models of inflammatory diseases and metabolic dysfunction. In models of lung injury and allergic airway inflammation, RELMα promotes chemotaxis for anti-inflammatory macrophages and dendritic cells and induces myofibroblast differentiation and ECM deposition. In adipose tissue and liver, RELMα functions to increase glucose tolerance. In this model of OSM-induced lung inflammation, the absence of RELMα led to less accumulation of AA/M2 macrophages and Th1 cells in the lung and less upregulation of ECM genes. Strikingly,

RELMα-deficiency led to increased epithelial cell damage/death, supporting a cytoprotective role for RELMα.

Taken together, this data suggests that OSM-induced RELMα increases ECM deposition and protects against epithelial cell damage/death, though further investigation is required to determine clinical significance. Although RELMα has yet to be identified in humans and its receptor(s) is not well characterized, the closest human homolog, RELMβ, has been found in patients with asthma and others have shown that human RELMβ shares similar functions as mouse RELMα in airway remodeling mechanisms, where both can induce expression of type I collagen and αSMA. Given that both human RELMβ and mouse RELMα are expressed in the same cell types in lungs of asthma/IPF patients and in murine models of asthma and Th2-skewed lung inflammation, RELMα may be a more closely related functional homolog to human RELMβ than its structural homolog, mouse RELMβ. Whether mouse RELMα and human RELMβ function similarly in tissue repair and fibrosis requires further study. Thus, studying RELMα, the functional homolog of human RELMβ, in OSM-mediated lung inflammation may serve as a model of human chronic respiratory diseases and help to identify alternative mechanisms of pathogenesis.

CHAPTER 8: REFERENCES

[1] Burgess JK, Mauad T, Tjin G, et al. The extracellular matrix – the under-recognized element in lung disease? *J Pathol*. 2016;240:397–409

[2] Hogg JC, Timens W. The Pathology of Chronic Obstructive Pulmonary Disease. *Annu Rev Pathol Mech Dis*. 2009;4:435–459

[3] Mauad T, Bel EH, Sterk PJ. Asthma therapy and airway remodeling. *J Allergy Clin Immunol*. 2007;120:997–1009

[4] American Thoracic Society (ATS), European Respiratory Society (ERS). Idiopathic Pulmonary Fibrosis: diagnosis and treatment. *Am J Respir Crit Care Med*. 2000;161:646–664

[5] Bonella F, Stowasser S, Wollin L. Idiopathic pulmonary fibrosis: current treatment options and critical appraisal of nintedanib. *Drug Des Devel Ther*. 2015;9:6407–6419

[6] Lo Re S, Lison D, Huaux F. CD4+ T lymphocytes in lung fibrosis: diverse subsets, diverse functions. *J Leukoc Biol*. 2013;93:499–510

[7] Wynn TA, Vannella KM. Macrophages in Tissue Repair, Regeneration, and Fibrosis. *Immunity*. 2016;44:450–462

[8] Bonniaud P, Kolb M, Galt T, et al. Smad3 Null Mice Develop Airspace Enlargement and Are Resistant to TGF-β-Mediated Pulmonary Fibrosis. *J Immunol*. 2014;173:2099–2108

[9] Migliaccio CT, Buford MC, Jessop F, et al. The IL-4Rα pathway in macrophages

and its potential role in silica-induced pulmonary fibrosis. *J Leukoc Biol*. 2008;83:630–639

[10] Todd NW, Luzina IG, Atamas SP, et al. Molecular and cellular mechanisms of pulmonary fibrosis. *Fibrogenesis Tissue Repair*. 2012;5:11

[11] Richards CD. The Enigmatic Cytokine Oncostatin M and Roles in Disease. *ISRN Inflamm*. 2013;2013:1–23

[12] Mozaffarian A, Brewer AW, Trueblood ES, et al. Mechanisms of Oncostatin M-Induced Pulmonary Inflammation and Fibrosis. *J Immunol*. 2008;181:7243–7253

[13] Tanaka M, Miyahima A. Onconstatin M, a multifunctional cytokine. *Rev Physiol Biochem Pharmacol*. 2003;149:39–52

[14] Wong S, Botelho FM, Rodrigues RM, et al. Oncostatin M overexpression induces matrix deposition, STAT3 activation, and SMAD1 Dysregulation in lungs of fibrosis-resistant BALB/c mice. *Lab Investig*. 2014;94:1003–1016

[15] O'Donoghue RJJ, Knight DA, Richards CD, et al. Genetic partitioning of interleukin-6 signalling in mice dissociates Stat3 from Smad3-mediated lung fibrosis. *EMBO Mol Med*. 2012;4:939–951

[16] West NR, Owens BMJ, Hegazy AN. The oncostatin M - stromal cell axis in health and disease. 2018;1–18

[17] Hermanns HM. Oncostatin M and interleukin-31: Cytokines, receptors, signal transduction and physiology. *Cytokine Growth Factor Rev*. 2015;26:545–558

[18] West NR, Owens BMJ, Hegazy AN. The oncostatin M-stromal cell axis in health and disease. *Scand J Immunol*. 2018;88:1–18

[19] Schindeler A, McDonald MM, Bokko P, et al. Bone remodeling during fracture repair: The cellular picture. *Semin Cell Dev Biol*. 2008;19:459–466

[20] Richards CD, Langdon C, Deschamps P, et al. Stimulation of osteoclast differentiation in vitro by mouse oncostatin M, leukaemia inhibitory factor, cardiotrophin-1 and interleukin 6: Synergy with dexamethasone. *Cytokine*. 2000;12:613–621

[21] Guihard P, Boutet MA, Brounais-Le Royer B, et al. Oncostatin M, an inflammatory cytokine produced by macrophages, supports intramembranous bone healing in a mouse model of tibia injury. *Am J Pathol*. 2015;185:765–775

[22] Langdon C, Leith J, Smith F, et al. Oncostatin M stimulates monocyte chemoattractant protein-1- and interleukin-1-induced matrix metalloproteinase-1 production by human synovial fibroblasts in vitro. *Arthritis Rheum*. 1997;40:2139–2146

[23] Song HY, Kim MR, Lee MJ, et al. Oncostatin M decreases adiponectin expression and induces dedifferentiation of adipocytes by JAK3- and MEK-dependent pathways. *Int J Biochem Cell Biol*. 2007;39:439–449

[24] Sanchez-Infantes D, White UA, Elks CM, et al. Oncostatin M is produced in adipose tissue and is regulated in conditions of obesity and type 2 diabetes. *J Clin Endocrinol Metab*. 2014;99:217–225

[25] Albasanz-Puig A, Murray J, Preusch M, et al. Oncostatin M is expressed in atherosclerotic lesions: A role for Oncostatin M in the pathogenesis of atherosclerosis. *Atherosclerosis*. 2011;216:292–298

[26] Kubin T, Pöling J, Kostin S, et al. Oncostatin M is a major mediator of cardiomyocyte dedifferentiation and remodeling. *Cell Stem Cell*. 2011;9:420–432

[27] West NR. Coordination of Immune-Stroma Crosstalk by IL-6 Family Cytokines. *Front Immunol*. 2019;10:1–16

[28] Richards CD, Izakelian L, Dubey A, et al. Regulation of IL-33 by Oncostatin M in Mouse Lung Epithelial Cells. *Mediators Inflamm*;2016 . Epub ahead of print 2016. DOI: 10.1155/2016/9858374

[29] Simpson JL, Baines KJ, Boyle MJ, et al. Oncostatin m (OSM) is increased in asthma with incompletely reversible airflow obstruction. *Exp Lung Res*. 2009;35:781–794

[30] Baines KJ, Simpson JL, Gibson PG. Innate Immune Responses Are Increased in Chronic Obstructive Pulmonary Disease. *PLoS One*. 2011;6:1–7

[31] Pothoven KL, Norton JE, Hulse KE, et al. Oncostatin M promotes mucosal epithelial barrier dysfunction, and its expression is increased in patients with eosinophilic mucosal disease. *J Allergy Clin Immunol*. 2015;136:737-746.e4

[32] Fritz DK, Kerr C, Fattouh R, et al. A Mouse Model of Airway Disease: Oncostatin M-Induced Pulmonary Eosinophilia, Goblet Cell Hyperplasia, and Airway Hyperresponsiveness Are STAT6 Dependent, and Interstitial Pulmonary Fibrosis Is STAT6 Independent. *J Immunol*. 2011;186:1107–1118

[33] Botelho FM, Rangel-Moreno J, Fritz D, et al. Pulmonary Expression of Oncostatin M (OSM) Promotes Inducible BALT Formation Independently of IL-6, Despite a Role for IL-6 in OSM-Driven Pulmonary Inflammation. *J Immunol*. 2013;191:1453–1464

[34] Dubey A, Izakelian L, Ayaub EA, et al. Separate roles of IL-6 and oncostatin M in mouse macrophage polarization in vitro and in vivo. *Immunol Cell Biol*. 2018;96:257–272

[35] Jones SA, Jenkins BJ. Recent insights into targeting the IL-6 cytokine family in inflammatory diseases and cancer. *Nat Rev Immunol*;130 . Epub ahead of print 2018. DOI: 10.1038/s41577-018-0066-7

[36] Le T-TT, Karmouty-Quintana H, Melicoff E, et al. Blockade of IL-6 Trans Signaling Attenuates Pulmonary Fibrosis . *J Immunol*. 2014;193:3755–3768

[37] Scheller J, Chalaris A, Schmidt-Arras D, et al. The pro- and anti-inflammatory properties of the cytokine interleukin-6. *Biochim Biophys Acta - Mol Cell Res*. 2011;1813:878–888

[38] Zhou Y, Murthy JN, Zeng D, et al. Alterations in adenosine metabolism and signaling in patients with chronic obstructive pulmonary disease and idiopathic pulmonary fibrosis. *PLoS One*;5 . Epub ahead of print 2010. DOI: 10.1371/journal.pone.0009224

[39] Ayaub EA, Dubey A, Imani J, et al. Overexpression of OSM and IL-6 impacts the polarization of pro-fibrotic macrophages and the development of bleomycin-induced lung fibrosis. *Sci Rep*. 2017;7:13281

[40] Dubey A, Izakelian L, Ayaub EA, et al. Separate roles of IL-6 and oncostatin M in mouse macrophage polarization in vitro and in vivo. *Immunol Cell Biol*. 2018;96:257–272

[41] Ayaub EA, Kolb PS, Mohammed-ali Z, et al. GRP78 and CHOP modulate

macrophage apoptosis and the development of bleomycin-induced pulmonary fibrosis. *J Pathol*. 2016;153:411–425

[42] Miller AM. Role of IL-33 in inflammation and disease. *J Inflamm*. 2011;8:1–12

[43] Molofsky AB, Savage AK, Locksley RM. Interleukin-33 in Tissue Homeostasis, Injury, and Inflammation. *Immunity*. 2015;42:1005–1019

[44] Lüthi AU, Cullen SP, McNeela EA, et al. Suppression of Interleukin-33 Bioactivity through Proteolysis by Apoptotic Caspases. *Immunity*. 2009;31:84–98

[45] Cayrol C, Girard J-P. The IL-1-like cytokine IL-33 is inactivated after maturation by caspase-1. *Proc Natl Acad Sci*. 2009;106:9021–9026

[46] Kurowska-Stolarska M, Stolarski B, Kewin P, et al. IL-33 Amplifies the Polarization of Alternatively Activated Macrophages That Contribute to Airway Inflammation. *J Immunol*. 2009;183:6469–6477

[47] Byers DE, Alexander-Brett J, Patel AC, et al. Long-term IL-33-producing epithelial progenitor cells in chronic obstructive lung disease. *J Clin Invest*. 2013;123:3967–3982

[48] Stolarski B, Kurowska-Stolarska M, Kewin P, et al. IL-33 Exacerbates Eosinophil-Mediated Airway Inflammation. *J Immunol*. 2010;185:3472–3480

[49] Willebrand R, Voehringer D. IL-33-Induced cytokine secretion and survival of mouse eosinophils is promoted by autocrine GM-CSF. *PLoS One*. 2016;11:1–14

[50] Bouffi C, Rochman M, Zust CB, et al. IL-33 Markedly Activates Murine Eosinophils by an NF-κB–Dependent Mechanism Differentially Dependent upon an IL-4–Driven Autoinflammatory Loop. *J Immunol*. 2013;191:4317–4325

[51] Pine GM, Batugedara HM, Nair MG. Here, there and everywhere: Resistin-like molecules in infection, inflammation, and metabolic disorders. *Cytokine*. 2018;110:442–451

[52] Liu T, Yu H, Ullenbruch M, et al. The in vivo fibrotic role of FIZZ1 in pulmonary fibrosis. *PLoS One*. 2014;9:1–11

[53] Kim K-H, Zhao L, Moon Y, et al. Dominant inhibitory adipocyte-specific secretory factor (ADSF)/resistin enhances adipogenesis and improves insulin sensitivity. *Proc Natl Acad Sci*. 2004;101:6780–6785

[54] Kim KH, Lee K, Moon YS, et al. A Cysteine-rich Adipose Tissue-specific Secretory Factor Inhibits Adipocyte Differentiation. *J Biol Chem*. 2001;276:11252–11256

[55] Steppan CM, Patel HR, Banerjee RR, et al. The hormone resistin links obesity to diabetes. *Nature*. 2002;409:307–312

[56] Blagoev B, Kratchmarova I, Nielsen MM, et al. Inhibition of Adipocyte Differentiation by Resistin-like Molecule α. *J Biol Chem*. 2002;277:42011–42016

[57] Daquinag AC, Zhang Y, Amaya-Manzanares F, et al. An Isoform of Decorin Is a Resistin Receptor on the Surface of Adipose Progenitor Cells. *Cell Stem Cell*. 2011;9:74–86

[58] Jang JC, Li J, Gambini L, et al. Human resistin protects against endotoxic shock by blocking LPS–TLR4 interaction. *Proc Natl Acad Sci*. 2017;114:E10399–E10408

[59] Munitz A, Waddell A, Seidu L, et al. Resistin-like molecule α enhances myeloid cell activation and promotes colitis. *J Allergy Clin Immunol*. 2008;122:1200–1208

[60] Nair MG, Du Y, Perrigoue JG, et al. Alternatively activated macrophage-derived

RELM-α is a negative regulator of type 2 inflammation in the lung. *J Exp Med*. 2009;206:937–952

[61] Chen F, Wu W, Jin L, et al. B Cells Produce the Tissue-Protective Protein RELMα during Helminth Infection, which Inhibits IL-17 Expression and Limits Emphysema. *Cell Rep*. 2018;25:2775–2783

[62] Kumamoto Y, Camporez JPG, Jurczak MJ, et al. CD301b+ Mononuclear Phagocytes Maintain Positive Energy Balance through Secretion of Resistin-like Molecule Alpha. *Immunity*. 2016;45:583–596

[63] Holcomb IN, Kabakoff RC, Chan B, et al. FIZZ1, a novel cysteine-rich secreted protein associated with pulmonary inflammation, defines a new gene family. *EMBO J*. 2000;19:4046–4055

[64] Liu T, Jin H, Ullenbruch M, et al. Regulation of Found in Inflammatory Zone 1 Expression in Bleomycin-Induced Lung Fibrosis: Role of IL-4/IL-13 and Mediation via STAT-6. *J Immunol*. 2004;173:3425–3431

[65] Nair MG, Cochrane DW, Allen JE. Macrophages in chronic type 2 inflammation have a novel phenotype characterized by the abundant expression of Ym1 and Fizz1 that can be partly replicated in vitro. *Immunol Lett*. 2003;85:173–180

[66] Banerjee RR, Lazar MA. Dimerization of Resistin and Resistin-like Molecules Is Determined by a Single Cysteine. *J Biol Chem*. 2001;276:25970–25973

[67] Chen J, Wang L, Boeg YS, et al. Differential dimerization and association among resistin family proteins with implications for functional specificity. *J Endocrinol*. 2002;175:499–504

[68] Doherty TA, Khorram N, Sugimoto K, et al. Alternaria Induces STAT6-Dependent Acute Airway Eosinophilia and Epithelial FIZZ1 Expression That Promotes Airway Fibrosis and Epithelial Thickness. *J Immunol*. 2012;188:2622–2629

[69] Lee M, Shim D, Yoon J, et al. Retnla Overexpression Attenuates Allergic Inflammation of the Airway. *PLoS One*. 2014;9:1–19

[70] Knipper JA, Willenborg S, Brinckmann J, et al. Interleukin-4 Receptor α Signaling in Myeloid Cells Controls Collagen Fibril Assembly in Skin Repair. *Immunity*. 2015;43:803–816

[71] Chen G, Wang SH, Jang JC, et al. Comparison of RELMα and RELMβ single- and double-gene-deficient mice reveals that RELMα expression dictates inflammation and worm expulsion in hookworm infection. *Infect Immun*. 2016;84:1100–1111

[72] Sutherland TE, Rückerl D, Logan N, et al. Ym1 induces RELMα and rescues IL-4Rα deficiency in lung repair during nematode infection. *PLoS Pathog*. 2018;14:1–27

[73] Steppan CM, Brown EJ, Wright CM, et al. A family of tissue-specific resistin-like molecules. *Proc Natl Acad Sci U S A*. 2001;98:502–506

[74] Mishra A, Wang M, Schlotman J, et al. Resistin-like molecule-β is an allergen-induced cytokine with inflammatory and remodeling activity in the murine lung. *Am J Physiol*. 2012;293:305–313

[75] Lemessurier KS, Palipane M, Tiwary M, et al. Chronic features of allergic asthma are enhanced in the absence of resistin-like molecule-beta. *Sci Rep*. 2018;1–13

[76] Fang CL, Yin LJ, Sharma S, et al. Resistin-like molecule-β (RELM-β) targets

airways fibroblasts to effect remodelling in asthma: From mouse to man. *Clin Exp Allergy*. 2015;45:940–952

[77] Fang C, Meng Q, Wu H, et al. Resistin-like molecule-β is a human airway remodelling mediator. *Eur Respir J*. 2012;39:458–466

[78] Liu T, Baek HA, Yu H, et al. FIZZ2/RELM-β Induction and Role in Pulmonary Fibrosis. *J Immunol*. 2011;187:450–461

[79] Gerstmayer B, Küsters D, Gebel S, et al. Identification of RELMγ, a novel resistin-like molecule with a distinct expression pattern. *Genomics*. 2003;81:588–595

[80] Schinke T, Haberland M, Jamshidi A, et al. Cloning and functional characterization of resistin-like molecule γ. *Biochem Biophys Res Commun*. 2004;314:356–362

[81] Braciak TA, Graham FL, Richards CD, et al. Construction of recombinant human type 5 adenoviruses expressing rodent IL-6 genes: An approach to investigate in vivo cytokine function. *J Immunol*. 1993;151:5145–5153

[82] Richards CD, Kerr C, Tong L, et al. Modulation of extracellular matrix using adenovirus vectors. *Biochem Soc Trans*. 2002;30:107–111

[83] Langdon C, Kerr C, Hassen M, et al. Murine oncostatin M stimulates mouse synovial fibroblasts in vitro and induces inflammation and destruction in mouse joints in vivo. *Am J Pathol*. 2000;157:1187–1196

[84] Kerr C, Langdon C, Graham F, et al. Adenovirus Vector Expressing Mouse Oncostatin M Induces Acute-Phase Proteins and TIMP-1 Expression In Vivo in Mice. *J Interf Cytokine Res*. 1999;19:1195–1205

[85] Munitz A, Cole ET, Karo-atar D, et al. Resistin-Like Molecule–α Regulates IL-13–

Induced Chemokine Production but Not Allergen-Induced Airway Responses. *Am J Respir Cell Mol Biol*. 2012;46:703–713

[86] Patel SD, Rajala MW, Rossetti L. Disulfide-Dependent Multimeric Assembly of Resistin Family Hormones. *Science (80-)*. 2004;304:1154–1159

[87] Stutz AM, Pickart LA, Trifilieff A, et al. The Th2 Cell Cytokines IL-4 and IL-13 Regulate Found in Inflammatory Zone 1/Resistin-Like Molecule Gene Expression by a STAT6 and CCAAT/Enhancer-Binding Protein-Dependent Mechanism. *J Immunol*. 2003;170:1789–1796

[88] Fritz DK, Kerr C, Botelho F, et al. Oncostatin M (OSM) primes IL-13- and IL-4-induced eotaxin responses in fibroblasts: Regulation of the type-II IL-4 receptor chains IL-4Rα and IL-13Rα1. *Exp Cell Res*. 2009;315:3486–3499

[89] Gibbons MA, MacKinnon AC, Ramachandran P, et al. Ly6C hi monocytes direct alternatively activated profibrotic macrophage regulation of lung fibrosis. *Am J Respir Crit Care Med*. 2011;184:569–581

[90] Wagner K, Hellberg AK, Balenger S, et al. Hypoxia-Induced mitogenic factor has antiapoptotic action and is upregulated in the developing lung. *Am J Respir Cell Mol Biol*. 2004;31:276–282

[91] Chung MJ, Liu T, Ullenbruch M, et al. Antiapoptotic effect of found in inflammatory zone (FIZZ)1 on mouse lung fibroblasts. *J Pathol*. 2007;212:180–187

[92] Ueno T, Toi M, Linder S. Detection of epithelial cell death in the body by cytokeratin 18 measurement. *Biomed Pharmacother*. 2005;59:S359–S362

[93] Kramer G, Mauermann J, Steiner G, et al. Differentiation between Cell Death Modes

Using Measurements of Different Soluble Forms of Extracellular Cytokeratin 18. *Cancer Res*. 2004;64:1751–1756

[94] Su Q, Zhou Y, Johns RA. Bruton's tyrosine kinase (BTK) is a binding partner for hypoxia induced mitogenic factor (HIMF/FIZZ1) and mediates myeloid cell chemotaxis. *FASEB J*. 2007;21:1376–1382

[95] Liu T, Hu B, Choi YY, et al. Notch1 signaling in FIZZ1 induction of myofibroblast differentiation. *Am J Pathol*. 2009;174:1745–55

[96] Martins V, Santos FGDL, Wu Z, et al. FIZZ1-Induced Myofibroblast Transdifferentiation from Adipocytes and Its Potential Role in Dermal Fibrosis and Lipoatrophy. *Am J Pathol*. 2015;185:2768–2776